
Biological role and genetic redundancy within the Ebf gene family

Jeehee Kim

**A thesis
submitted for the Degree of Doctor of Natural Sciences
(Dr. rer. nat.)
at the Faculty of Biology,
Ludwig-Maximilians-University of Munich**



Munich 2014

Biological role and genetic redundancy within the Ebf gene family

Dissertation zur Erlangung des Doktorgrades der
Naturwissenschaften (Dr. rer. nat.) der Fakultät für Biologie der
Ludwig-Maximilians-Universität München

vorgelegt von
Jeehee Kim

angefertigt am
Helmholtz Zentrum für Gesundheit und Umwelt
München

München, den 30.09.2014

Erstgutachter: Prof. Dr. Barbara Conradt

Zweitgutachter: Prof. Dr. Bettina Kempkes

Tag der mündlichen Prüfung: 10.03.2015

Contents

1. List of Publications	1
2. Declaration	2
3. Summary	3
Zusammenfassung	4
4. Aims of the thesis	5
5. Introduction	6
5.1. Early B cell factor	6
5.1.1. The structure of early B cell factors family	6
5.1.2. The biological function of <i>Ebf</i> gene family.....	8
5.1.2.1. <i>Ebf1</i>	8
5.1.2.2. <i>Ebf2</i>	9
5.1.2.3. <i>Ebf3</i>	10
5.1.2.4. <i>Ebf4</i>	11
5.1.2.5. <i>Ebf</i> genes in invertebrates	11
5.2. Genetic redundancy.....	12
5.3. <i>Ebf3</i> and muscle development.....	13
5.3.1. Muscle development	13
5.3.2. Diaphragm.....	15
5.3.3. Muscle function of diaphragm	16
5.4. RNA interference	18
5.4.1. MicroRNA.....	18
5.4.2. RNA interference process	19
6. Publications	21
6.1. Contributions	21
6.2. Publication I : An RNAi-based approach to down-regulate a gene family <i>in vivo</i>	22
6.3. Publication II : Ebf factors and MyoD cooperate to regulate muscle relaxation via <i>Atp2a1</i>	41
7. Discussion	67
7.1. Generation of <i>EbfmiRNA</i> mouse line	67
7.2. RNAi and RNA polymerase II driven shRNA	69

7.3. RNAi expression <i>in vivo</i>	70
7.4. <i>Ebf3</i> in muscle function	72
7.5. Biochemical mechanisms of muscle function.....	73
8. Outlook	76
9. References.....	78
10. Acknowledgement	86
11. Curriculum Vitae	87

1. List of Publications

Publication I.

“An RNAi-based approach to down-regulate a gene family in vivo.”

Jeehee Kim, Aurora Badaloni, Torsten Willert, Ursula Zimmer-Strobl, Ralf Kühn, Wolfgang Wurst, Matthias Kieslinger

PLoS ONE 2013; 8(11): e80312.

Publication II.

“Ebf Factors and MyoD Cooperate to Regulate Muscle Relaxation via Atp2a1.”

Saihong Jin, Jeehee Kim, Torsten Willert, Tanja Klein-Rodewald, Mario Garcia-Dominguez, Matias Mosqueira, Rainer Fink, Irene Esposito, Lorenz C. Hofbauer, Patrick Charnay & Matthias Kieslinger

Nature Communications 2014; 5:3793

2. Declaration

Eidesstattliche Erklärung

Ich versichere hiermit an Eides statt, dass die von mir vorgelegte Dissertation von mir selbstständig und ohne unerlaubte Hilfe angefertigt ist.

München, den 30. 9. 2014

Jeehee Kim

Erklärung

Hiermit erkläre ich, dass die Dissertation nicht ganz oder in wesentlichen Teilen einer anderen Prüfungskommission vorgelegt worden ist, und dass ich mich anderweitig einer Doktorprüfung ohne Erfolg nicht unterzogen habe.

München, den 30. 9. 2014

Jeehee Kim

3. Summary

The early B cell factor (*Ebf*) gene family encodes for a group of highly homologous transcription factors. Invertebrates, four *Ebf* family members (*Ebf1*, *Ebf2*, *Ebf3* and *Ebf4*) have been identified. The expression of individual *Ebf* family members is largely overlapping and all *Ebf* transcription factors bind to the same DNA sequence. Consequently, their biological roles are often masked by genetic redundancy.

To overcome this redundancy, a new RNAi construct was established that shows a high efficiency to down regulate *Ebf* family members (*Ebf1*, *Ebf2* and *Ebf3*) simultaneously in cultured cells. RNAi has been developed as a powerful tool to silence the expression of target genes facilitating the study of specific gene function. A new transgenic mouse line has been generated that allows the tissue-specific expression of this new RNAi construct together with the marker gene *Gfp*. However, the data presented here shows no phenotypic changes in B cell development or neuronal differentiation of the cerebellum in the transgenic mice upon tissue-specific induction of the polycistronic mir155-based RNAi construct.

Compared to *Ebf1* and *Ebf2*, the biological role of *Ebf3* and *Ebf4* are poorly characterized. To determine the function of *Ebf3*, I contributed to the analysis of *Ebf3*-deficient mice. *Ebf3* is significantly expressed in diaphragm, skeletal muscle and bone marrow, but not in lung and heart. Interestingly, all *Ebf3* knock-out mice display respiratory failure, leading to their perinatal death. *Ebf3*-deficient mice display a functional defect of their diaphragm, resulting from impaired muscle relaxation.

The SERCA1 protein, which is encoded by the *Atp2a1* gene, is an ATP-dependent Ca^{2+} ion pump, which is important for the regulation muscle relaxation by transporting calcium ion into the sarcoplasmic reticulum. In absence of *Ebf3*, the expression of *Atp2a1* is strongly down-regulated, causing the respiratory failure. *Atp2a1* is a direct target gene of *Ebf3*, which cooperates with MyoD to induce *Atp2a1* gene expression.

Taken together, this work contributes to a better understanding of Ebf transcription factors by describing a new role for *Ebf3* in muscle biology and developing a new approach to address the genetic redundancy within this gene family.

Zusammenfassung

Die "Early B cell factor" (*Ebf*) Genfamilie kodiert für eine Gruppe hoch homologer Transkriptionsfaktoren, von denen in Wirbeltieren vier Familienmitglieder (*Ebf1*, *Ebf2*, *Ebf3* und *Ebf4*) identifiziert wurden. Die Expression der einzelner Familienmitglieder ist großteils überlappend und alle Ebf Transkriptionsfaktoren binden an die gleiche DNA Bindungsstelle. Daraus ergibt sich, daß ihre biologischen Funktionen häufig durch genetische Redundanz kompensiert werden.

Um diese Redundanz zu überwinden, wurde ein RNAi Konstrukt neu entwickelt, welches eine hohe Effizienz besitzt, die Expression mehrerer *Ebf* Familienmitglieder (*Ebf1*, *Ebf2* und *Ebf3*) in Zellkulturen herunterzuregulieren. RNAi hat sich zu einem mächtigen Werkzeug entwickelt, um die Expression bestimmter Gene zu inhibieren und die Funktion spezifischer Gene zu untersuchen. Des Weiteren wurde eine neue transgene Mauslinie entwickelt, welche die gewebs-spezifische Expression des RNAi-Konstrukts erlaubt. In der transgenen Mauslinie konnten jedoch nach Induktion des polycistronischen miR155-basierten Konstrukts keine phänotypischen Veränderungen in der B-Zellentwicklung oder in der neuronalen Differenzierung des Cerebellums beobachtet werden.

Verglichen mit *Ebf1* und *Ebf2* sind die biologischen Rollen von *Ebf3* und *Ebf4* kaum charakterisiert. Um daher die Funktion von *Ebf3* zu analysieren, untersuchten trug ich zur Untersuchung *Ebf3*-defizienter Mäuse bei. *Ebf3* ist stark exprimiert in Skelettmuskeln, Zwerchfell und Knochenmark, jedoch nicht in Lunge und Herz. Interessanterweise zeigen alle *Ebf3* knock-out Mäuse ein Versagen der Atmung, was zu ihrem Tod kurz nach der Geburt führt. Wir entdeckten, daß *Ebf3*-defiziente Mäuse an einem funktionalen Defekt des Zwerchfells litten, welcher aus einer defekten Muskelentspannung resultiert. Das Protein *Serca1*, welches eine ATP-abhängige Pumpe für Ca^{2+} -Ionen darstellt und essentiell ist für die Muskelentspannung, weist in Abwesenheit von *Ebf3* eine stark verminderte Expression auf. *Atp2a1*, das Gen welches für *Serca1* kodiert, ist ein direktes Zielgen von Ebf3, das gemeinsam mit MyoD die Expression von *Atp2a1* induziert.

Zusammenfassend trägt diese Arbeit zu einem besseren Verständnis der Ebf Transkriptionsfaktoren bei, indem sie eine neue Rolle für *Ebf3* in der Muskelfunktion beschreibt und ein neues Systems zur Analyse genetischer Redundanz innerhalb dieser Genfamilie weiter entwickelt.

4. Aims of the thesis

I. Down-regulation of several genes simultaneously by RNAi *in vivo*

In vertebrates, four of highly conserved *Ebf* family members have been identified. The overlapping expression pattern of *Ebf* genes masks the contribution of biological function of individual *Ebf* members by genetic redundancy. To study the biological role of the *Ebf* gene family, an RNAi-based system has been developed allowing the down-regulation of *Ebf* genes simultaneously *in vitro*.

Since this system has been further developed for use in transgenic mice, the first aim is to analyze this new *EbfmiRNA* mouse line at the cellular and molecular level for efficiency and specificity in down-regulating *Ebf* genes *in vivo*.

II. The biological role of *Ebf3*

Ebf3 was identified as an important regulatory factor in neuronal differentiation. However, its biological role outside of the nervous system is unclear. . Therefore, the second aim is to gain a better understanding of the function of *Ebf3* by analyzing *Ebf3*-deficient mice in non-neural tissues.

Ebf3-deficient mice show respiratory failure caused malfunction of the diaphragm resulting in their perinatal death. Thus, the biochemical mechanisms of muscle function of diaphragm and the involvement of *Ebf3* needed a detailed molecular analysis.

5. Introduction

5.1. Early B cell factor

5.1.1. The structure of the Ebf protein family

The early B cell factor (Ebf) gene family encodes for a group of transcription factors that contain highly conserved domains including a DNA-binding domain (DBD), a transcription factor Ig-like or immunoglobulin-plexin transcription factor (TIG/IPT) domain and a helix-loop-helix (HLH) domain. Additionally, the Ebf family members contain a transcriptional-activation domain (TAD) at the carboxyl-terminus.

In vertebrates, four members of the *Ebf* gene family (*Ebf1*, *Ebf2*, *Ebf3* and *Ebf4*) have been identified based on the high sequence similarity of the structured domains (Travis et al., 1993; Hagman et al., 1995; Dubois & Vincent, 2001; Liberg et al., 2002; Lukin et al., 2008; Fig. 1A). Among the mouse *Ebf* proteins, *Ebf1* and *Ebf3* show the highest homology with *Ebf2* and *Ebf4* being slightly more distant (Wang et al., 1997; Dubois & Vincent, 2001; Liao, 2009).

The DBD resides at the amino-terminus, from amino acid 50 to 251 (Liao, 2009; Fig. 1A). The DBD includes the zinc-coordination motif (H-X₃-C-X₂-C-X₅-C) consisting of 14 amino acids, termed zinc knuckle (Lukin et al., 2008; Fig. 1B). This zinc knuckle is a particular feature of the Ebf DNA-binding domain that is crucial for DNA sequence recognition and binding. The DBD in total extends far beyond the zinc knuckle, and establishes one of the largest surfaces of interaction between a transcription factor and DNA currently known (Hagman et al., 1993; Fields et al., 2008; Siponen et al., 2010; Treiber et al., 2010). Due to the high homology, all *Ebf* family members bind as dimers to the same DNA sequences that are variations of the palindromic sequence, 5'-ATTCCCNNGGGAAT-3' (Hagman et al., 1993; 1995).

The DBD is followed by the TIG/IPT and the HLH domain. Although the main function of the TIG/IPT domain is still unclear, it presumably has a role in protein dimerization or protein-protein interactions. In Rel family proteins, for example, the main function of the TIG domain is to establish protein dimerization. However, in Ebf proteins, the TIG domain alone is not sufficient for dimerization (Aravind & Koonin, 1999; Siponen et al., 2010; Treiber et al., 2010).

The HLH domain is the main mediator of dimerization, which is a prerequisite for DNA binding (Hagman et al., 1993; Wang & Reed, 1993). In vertebrates, all Ebf family members possess a duplication of helix 2, helix 2' (Fig. 1A), whereas invertebrates have only helix 1 and helix 2 without helix 2'. The interaction of helix 2' with its counterpart is weaker than the interaction of the two first helices with their counterparts, and helix 2' is not required for dimerization (Hagman et al., 1993; Crozatier et al., 1996; Siponen et al., 2010). Therefore, the exact function of the duplicated helix remains unclear.

At the carboxyl-terminus, the TAD shows some variation in the number of amino acid and the lowest sequence homology between individual *Ebf* genes (Hagman et al., 1995; Dubois & Vincent, 2001; Fig. 1A). Although the TAD is necessary for the transcription of most Ebf target genes, some gene promoters like *mb-1* or *Vpreb1* do not require the TAD for transactivation (Fields et al., 2008). The exact mechanisms of transactivation and interacting proteins have not been identified yet.

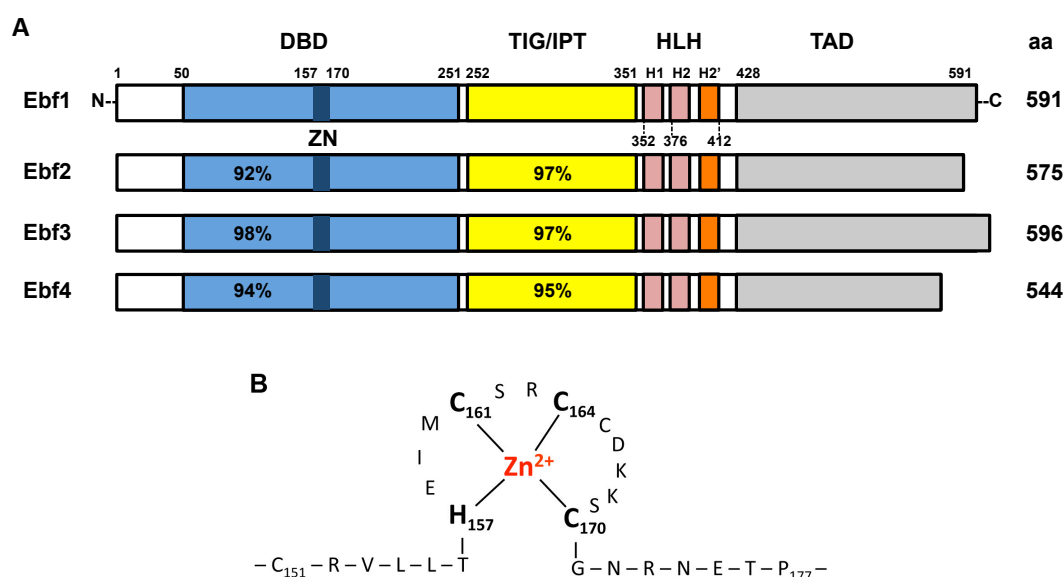


Figure 1. Schematic overview of conserved domains of the Ebf protein family.

(A) Structural features of the conserved domains in Ebf proteins. All members of the Ebf protein family show four structured domains, which are the DBD, TIG/IPT, HLH domain and TAD. The DBD contains a unique zinc binding structure, termed zinc knuckle (ZN, dark blue box). The percentages of the sequence similarities in the DBD and TIG/IPT domain are given between Ebf1 and the other family members. In the HLH domain, two pink boxes indicate helix 1 (H1) and helix 2 (H2), and the duplication of helix 2 (H2') is indicated as an orange box. At the C-terminus, the TAD shows a lower sequence homology (figure modified from Dubois & Vincent, 2001; Liao, 2009). (B) The structure of the zinc knuckle. The atypical Zn^{2+} -coordination motif consists of 14 amino acids including H157, C161, C164 and C170 (figure modified from Hagman et al., 1995).

Homologues of *Ebf* genes also exist in invertebrates and the best characterized examples are *uncoordinated-3 (unc-3)* in *Caenorhabditis elegans* and *collier (Col)* in *Drosophila melanogaster*. Both *Unc-3* and *Collier* show a similar domain organization and extensive sequence conservation in the DBD, TIG/IPT and HLH domains (Fig. 2). However, in the HLH domain, the duplication of helix 2 is absent (Crozatier et al., 1996; Prasad et al., 1998; Dubois & Vincent, 2001).

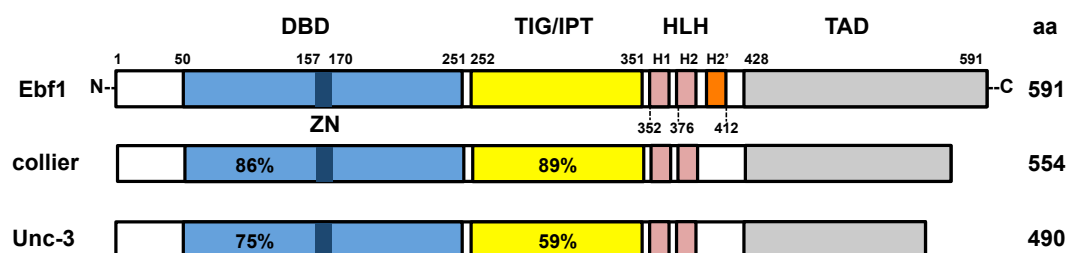


Figure 2. Evolutionary comparison of conserved domains in Ebf proteins.

C.elegans *Unc-3* and *Drosophila* *Collier* display highly conserved domains including DBD and TIG/IPT domain. The percentages of identity are given between Ebf1 and its homologs. The DBD contains a zinc knuckle (ZN). In the HLH domain of both *Unc-3* and *Collier*, helix 1 and 2 are conserved, but they lack helix 2' (figure modified from Dubois & Vincent, 2001; Liao, 2009).

5.1.2. The biological function of the *Ebf* gene family

5.1.2.1. *Ebf1*

Ebf1 is strongly expressed in immature olfactory neuronal precursors, mature neurons of the olfactory epithelium and early post-mitotic neurons. This expression pattern indicates a potential function of *Ebf1* in the development and function of the nervous system, particularly with respect to olfactory receptors (Wang & Reed, 1993; Garel et al., 1997, 2000). However, *Ebf1*-deficient embryos have no functional defects in development and function of the olfactory epithelium or early post-mitotic neuronal differentiation. This is likely due to the co-expression of other *Ebf* members, *Ebf2* and *Ebf3*, which compensate for the loss of *Ebf1* (Garel et al., 1997; Wang et al., 2004).

Interestingly, however, *Ebf1* is the only *Ebf* gene expressed in the developing striatum (Garel et al., 1997). *Ebf1*^{-/-} mice show a significant reduction in size and an abnormal shape of the postnatal striatum due to atrophy, indicating an essential role of *Ebf1* in the development of the striatum (Garel et al., 1999).

Additionally, *Ebf1* is the only *Ebf* family member which expressed in hematopoietic cells, specifically in B cells. *Ebf1*-deficient mice have a complete block in B cell development at the pro-B cell stage. Accordingly, *Ebf1* is also identified as an essential regulator for the differentiation of early B-lymphocytes (Hardy et al., 1995; Lin & Grosschedl 1995).

Taken together, the results from B-lymphocytes and the striatum indicate critical roles for single *Ebf* genes only when no other family member is co-expressed.

5.1.2.2. *Ebf2*

Another member of the *Ebf* gene family, *Ebf2*, is required for neuronal development. In *Ebf2*-deficient mice, the neuroendocrine axis is impaired causing a defect in pubertal development, which leads to hypogonadism. In addition, *Ebf2*^{-/-} mice show a significantly decreased velocity of motor nerve conduction resulting in peripheral neuropathy (Corradi et al., 2003).

Besides its role in neuronal development, *Ebf2* is also important for normal hematopoiesis. *Ebf2* is abundantly expressed in immature osteoblastic cells, adipocytes, and differentiating mesenchymal stem cells. Specifically, osteoblasts have been implicated in the support of haematopoietic stem cells (HSC) as their microenvironment, termed niches, but the exact nature of these cells is unclear (Calvi et al., 2003; Zhang et al., 2003; Kieslinger et al., 2010; Fig. 3).

Ebf2^{-/-} embryos succeed to complete embryonic development normally, but *Ebf2*-null mice show a decreasing number of adult HSC and common lymphoid progenitors. Interestingly, *Ebf2*-expressing osteoblastic cells and HSC are in cell-cell contact at the bone surface. In addition, osteoblastic cells from *Ebf2* knock-out mice have a reduced ability to maintain HSC in cell culture, demonstrating the importance of *Ebf2* for the support of HSC (Kieslinger et al., 2010).

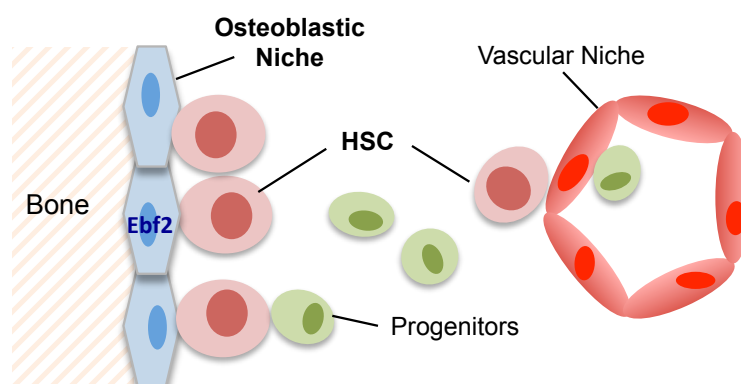


Figure 3. Schematic overview of HSC and niches in the bone marrow.

Two different niches for HSC are currently proposed, an osteoblastic niche at the bone surface consisting mainly but not exclusively of osteoblasts and a vascular niche at blood vessels consisting mainly of perivascular cells. Both niches regulate HSC fates like proliferation and differentiation. Osteoblastic niche cells express *Ebf2* for maintaining the quiescent state of HSCs, while the vascular niche cells support activated states of HSC (figure modified from Moore & Lemischka, 2006).

5.1.2.3. *Ebf3*

Ebf3 was initially identified due to its expression during neuronal differentiation (Garel et al., 1997; Wang et al., 1997). Specifically, *Ebf3* is an important factor which mediates cell migration in the developing cortex and in the projection of olfactory neurons (Wang et al., 2004; Chiara et al., 2012). Furthermore, *Ebf3* can mediate the inhibition of cell proliferation (Liao, 2009). The deletion of the *Ebf3* in gastric cancer cell lines activates cell cycle arrest and apoptosis, and human EBF3 was identified as a tumor suppressor in gastric carcinoma (Kim et al., 2012).

In *Xenopus laevis*, two Ebf family members, *Xebf2* and *Xebf3*, were identified and *Xebf3* was defined as an important regulator of neuronal differentiation (Bally-Cuif et al., 1998; Pozzoli et al., 2001). Moreover, both *Xebf2* and *Xebf3* are strongly expressed in developing muscle tissue in *Xenopus*. Overexpression of *Xebf2* and *Xebf3* leads to an up-regulation of myogenic regulatory factors including *MyoD* and *Myf5*, which are required for skeletal muscle development (Green & Vetter, 2011).

The function of *Ebf3* outside of the neuronal system, however, was poorly explored so far. Here, in the second publication (*Nature Comm.*, 2014), the results show that mammalian skeletal muscle cells express *Ebf3*, and *Ebf3*-deficient mice have a defect in muscle function of the diaphragm resulting in respiratory failure.

5.1.2.4. *Ebf4*

As the most recently identified *Ebf* transcription factor in vertebrates, *Ebf4* was cloned by degenerative PCR based on its high sequence similarity with other *Ebf* family factors (Wang et al., 2002). Like other *Ebf* family members, *Ebf4* is also expressed in the olfactory epithelium and neuronal tissues (Wang et al., 2002).

Ebf4 presumably has a role regulating gene expression in olfactory sensory neurons as a co-regulator with other *Ebf* family members. However, the precise biological function of *Ebf4* remains completely unknown (Wang et al., 2002; Lio, 2009).

5.1.2.5. *Ebf* genes in invertebrates

As mentioned already, homologues of *Ebf* genes also exist in invertebrates, such as *Unc-3* in *C.elegans* and *Collier* in *Drosophila melanogaster* (Crozatier et al., 1996). *Unc-3* is required for controlling the differentiation of both motor neurons and sensory neurons, leading to defect in normal motor neuron formation and correct axonal pathfinding in its absence, resulting in uncoordinated movement (Chalfie & Jorgensen, 1998; Prasad et al., 1998).

Collier (*Col*) was initially identified at the blastoderm stage for regulating the differentiation of a specific head segment (Crozatier et al., 1996). *Col* is also expressed in specific subsets of post-mitotic neurons, both in the CNS (central nervous system) and in the PNS (peripheral nervous system) during development of *Drosophila* embryos (Crozatier et al., 1996). However, the biological role of this expression pattern is not defined. Moreover, *Col* is also required for the formation of a specific embryonic somatic muscle (Crozatier & Vincent, 1999) and the correct adult wing pattern (Vervoort et al., 1999).

Combining the role of *Ebf* factors in different organisms, a contribution to the function of the nervous system emerges as a unifying theme and potentially the evolutionary oldest role of the *Ebf* gene family (Crozatier et al., 1996; Dubois & Vincent, 2001). Other functions such as muscle development and lymphopoiesis have likely been acquired later on.

5.2. Genetic redundancy

Genetic redundancy means that deleting or inactivating a gene has little or no effect on the biological phenotype of the organism because of functional compensation by duplicated or highly homologous genes (Nowak et al., 1997; Cooke et al., 1997; Kafri et al., 2009). Multiple gene families of the mouse genome seem to originate from gene duplication and display a high level of sequence conservation. Therefore it is likely that two or more genes after duplication can be redundant. Interestingly, it is estimated that 10-15% of knock-out mice show no obvious phenotype or change of fitness, and genetic redundancy has already been demonstrated in several cases (Wang et al., 1996; Wang et al., 2004; Barbaric et al., 2007).

A good example of this functional redundancy is the highly homologous family of *Ebf* transcription factors. The high sequence similarity and overlapping expression pattern of *Ebf* members lead to a lack of specific phenotypes upon deletion of single *Ebf* genes (Wang et al., 2004; Liao, 2009). Therefore, genetic redundancy between *Ebf* members has to be considered as an important influence when characterizing the biological roles of single *Ebf* genes.

For example, the expression pattern of *Ebf1*, *Ebf2* and *Ebf3* is largely overlapping in mouse olfactory epithelium. *Ebf1*, *Ebf2* and *Ebf3* knock-out mice have a normal development of the olfactory neuronal system due to complementary function of other *Ebf* family members (Garel et al., 1999; Liberg et al., 2002). However, combined deletion of *Ebf2* and *Ebf3* results in defects in the projection of olfactory neurons (Wang et al., 2004).

Furthermore, three *Ebf* proteins, *Ebf1*, *Ebf2* and *Ebf3*, are also expressed during osteoblastic differentiation (Kieslinger et al., 2005, 2010). In *Ebf2*^{-/-} mice, osteoblastic niche cells have a reduced ability to support HSC. Interestingly, down-regulation of three *Ebf* factors (*Ebf1*, *Ebf2* and *Ebf3*) simultaneously leads to a stronger

impairment of the osteoblastic support for HSC, suggesting redundancy between *Ebf* proteins (Kieslinger et al., 2010).

Another interesting case of functional redundancy is observed among myogenic regulatory factors (MRFs). This gene family consists of four members, *MyoD*, *Myf5*, *myogenin* and *Mrf4*, which are products of early gene duplication and the MRFs are identified as important regulators for skeletal muscle development (Wang et al., 1996; Biressi et al., 2007; Mok & Sweetman, 2011).

For example, both *MyoD* and *Myf5* are expressed in myogenic precursors during mouse skeletal muscle development. This overlapping expression of two highly homologous genes compensates for the loss of function of one gene (Braun et al., 1992; Rudnicki et al., 1992; Kablar et al., 2003). The deletion of *MyoD* results in a normal progression of skeletal muscle development in mice since it can be compensated for by *Myf5*. The other way around, the presence of a functional *MyoD* gene in *Myf5*-absent mice results in the normal formation of skeletal muscle. However, mice lacking both *MyoD* and *Myf5* have a complete block in skeletal muscle development leading to postnatal death (Rudnicki et al., 1993).

5.3. *Ebf3* and muscle development

5.3.1. Muscle development

In vertebrates, muscle cells initially differentiate from mesenchymal progenitor cells in the cervical somites (Birchmeier & Brohmann, 2000; Buckingham et al., 2009). As the somites dissociate a subpopulation of migrating progenitor cells sequentially starts to express the paired box transcription factors *Pax3* and *Pax7*. This expression induces proliferation and expansion of this cell pool (Sato et al., 2010; Dubinska-Magiera et al., 2013). At the same time these transcription factors are also necessary to induce the expression of the MRF factors *Myf5* and *MyoD*. MRFs, basic helix-loop-helix transcription factors, are the main inducers of skeletal muscle differentiation (Relaix et al., 2005; Mok & Sweetman, 2011; Fig. 4).

In the vertebrate body, the most abundant tissue is skeletal muscle, which is essential for health and survival (Brooks & Myburgh, 2014). For example, the

diaphragm has a critical role for sustaining life as it is required for unfolding of the lung and breathing (Coirault et al., 1999b; Ackerman & Greer, 2007).

MRFs are also important to coordinate the correct myogenesis of the diaphragm. Mice with a deletion of *MyoD* have a thinner diaphragm than normal mice. *Myogenin*-deficient mice have an amuscular diaphragm that leads to a functional impairment of the diaphragm (Kablar et al., 2003). These MRFs are expressed together with additional transcription factors that act as co-activators of muscle-specific gene expression (Berkes & Tapscott 2005). In the second publication (*Nature Comm.*, 2014), the results show that *MyoD* cooperates with *Ebf3* to regulate the function of muscle cells in the diaphragm.

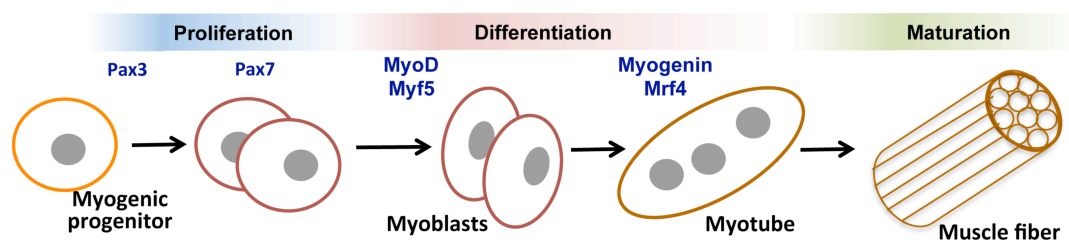


Figure 4. Diagram of mouse skeletal muscle development.

Myogenic progenitors, expressing *Pax3* and *Pax7*, proliferate and expand in cell number. Myogenic differentiation is initiated by the expression of *Myf5* and *MyoD* inducing the fusion of single myoblasts into multinucleated myotubes. Finally, *Myogenin* and *Mrf4* regulate the maturation of myotubes into functional muscle fibers (figure modified from Dubinska-Magiera et al., 2013).

Mammalian skeletal muscle comprises two main types of fibers, which are slow-twitch (type I) and fast-twitch (type II) muscle fibers (Biressi et al., 2007; Schiaffino, 2012). Type I muscle fibers use oxidative metabolism and are adapted for slow muscle contractions, whereas type II fibers mostly utilize glycolytic metabolism for fast-twitch speed and have lower endurance than slow-twitch fibers. Accordingly, type I muscle fibers are rich in mitochondria and have increased vascularization, whereas type II muscle fibers have a variable mitochondrial content and a developed sarcoplasmic reticulum (Schiaffino & Reggiani, 2011; Ehlers et al., 2014). Interestingly, *MyoD*, a critical regulator of myogenesis, is expressed more abundantly

in type II muscle fibers than in type I muscle fibers (Schiaffino & Reggiani, 2011; Schiaffino, 2012; Ehlers et al., 2014).

In addition, the type II fibers are divided into type IIa and type IIb. Type IIa fibers are oxidative metabolic fast-twitch muscle fibers which are fatigue resistant like type I muscle fibers. Type IIb fibers, also known as type IIx, are anaerobic, glycolytic metabolic fast-twitch muscle fibers which produce fast and strong force (Chalmers & Row, 2011; Schiaffino & Reggiani, 2011).

5.3.2. Diaphragm

The diaphragm is a dome-shaped structure formed by skeletal muscles between lung and abdomen. Together with the lung and the rib cage, the diaphragm is the most important structure to control the respiratory system (Merrell & Kardon, 2013). Its ability to contract and relax forces air in and out of the lung, mediating the breathing process (Coirault et al., 1999b; Ackerman & Greer, 2007; Stubbings et al., 2008; Fig. 5).

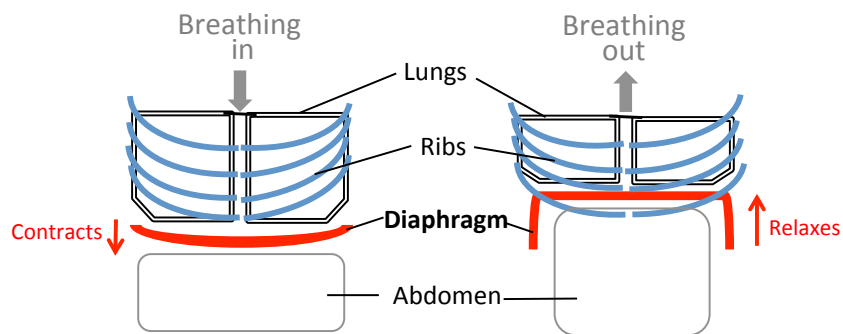


Figure 5. The role of the diaphragm in the respiratory system.

The respiratory system includes lung, diaphragm and rib cage. The contraction and relaxation of the diaphragm forces air in and out of the lungs, delivering oxygen and removing carbon dioxide from the body.

Rapid and complete relaxation of the diaphragm is essential to control breathing frequency and oxygen uptake. Therefore, developmental defects of the diaphragm during embryogenesis lead to respiratory failure, causing postnatal death (Coirault et al., 1999b; Merrell & Kardon, 2013). In addition, impairment of diaphragm relaxation

leads to respiratory problems which can be involved in various diseases, such as fatigue, myopathy, and congestive heart failure (Esau et al., 1983; Coirault et al., 1997; Lecarpentier et al., 1999).

The diaphragm in both human and rodent has a similar morphology. The diaphragm consists of several different tissues including skeletal muscle, connective tissue, mesothelium, blood vessels, and nerves. All of its muscle cells are derived from migratory muscle precursor cells, which come from mesodermal cervical somites (Birchmeier & Brohmann, 2000; Ackerman & Greer, 2007). The boundary of the diaphragm is muscularized, whereas the central region consists of tendon and has a distinct shape. The central tendon is attached to the liver by ligaments. Also, the vena cava inferior and the esophagus, which are surrounded by crural muscle, pass through the central part of diaphragm (Sweeney, 1998; Birchmeier & Brohmann, 2000; Vasyutina & Birchmeier, 2006; Ackerman & Greer, 2007).

Unlike many skeletal muscles in the body, diaphragm is constantly active and most of muscle fibers in diaphragm are consisted of type I and type IIa which are relatively resistant to fatigue (Stubbings et al., 2008).

5.3.3. Muscle function of the diaphragm

The molecular machinery involving Ca^{2+} transport controls muscle contraction and relaxation. In mammalian muscle fibers, sarcoplasmic reticulum (SR) is the most important intracellular compartment for the storage of Ca^{2+} (Coirault et al. 1999; Carafoli, 2002; Clapham, 2007).

Release of the stored Ca^{2+} from the SR to the cytoplasm results in muscle contraction. On the contrary, when Ca^{2+} is taken up from the cytoplasm into the lumen of the SR, the low level of cytosolic Ca^{2+} induces muscle relaxation (Coirault et al. 1999; Carafoli, 2002; Clapham, 2007; Fig. 6). The import of Ca^{2+} into the SR is controlled by Sarco(endo)plasmic reticulum Ca^{2+} -ATPase (SERCA) proteins, which are encoded by various *Atp2a* genes (Olson et al., 2010; Inesi & Tadini-Buoninsegni, 2014).

In the adult diaphragm, two different isoforms of SR Ca^{2+} -ATPase, SERCA1 and SERCA2a have been detected (Sayen et al., 1992; Anger et al., 1995). SERCA1 is exclusively expressed in fast-twitch skeletal muscle fibers, whereas SERCA2a is expressed in slow-twitch muscle fibers as well as in cardiac and smooth muscles (Lytton et al., 1992; Coirault et al., 1999b). SERCA2a is also regulated by another integral membrane protein, phospholamban. The unphosphorylated phospholamban decreases the affinity between Ca^{2+} and SERCA (MacLennan et al., 1992; Coirault et al., 1999b; MacLennan, 2000).

SERCA1-deficient mice display cyanosis due to respiratory failure resulting in postnatal lethality. The lack of SERCA1 in fast-twitch skeletal muscle leads to a reduced Ca^{2+} pump activity to transport Ca^{2+} into the SR. Accordingly, the loss of the function of SERCA1 Ca^{2+} pump causes the impairment of relaxation of the skeletal muscle. This phenotype resembles a genetic myopathy in humans, Brody disease, which leads to defects in muscle relaxation, muscle stiffness, cramping and a shortened lifespan (Odermatt et al., 1996; MacLennan, 2000; Pan et al., 2003).

In the second publication (*Nature Comm.*, 2014), *Atp2a1* is described as a direct target gene of *Ebf3*, demonstrating that *Ebf3* is required for muscle relaxation in the diaphragm.

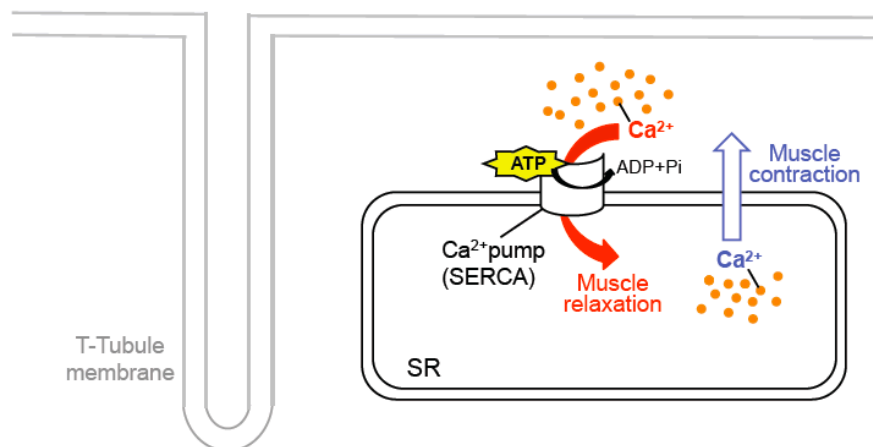


Figure 6. The mechanisms of muscle contraction and relaxation.

The energy-dependent transport of Ca^{2+} regulates muscle function. Release of Ca^{2+} from the sarcoplasmic reticulum (SR) to the cytoplasm causes muscle contraction. Muscle relaxation is achieved by the ATP-dependent transport of Ca^{2+} ions by SERCA proteins into the SR lumen (figure modified from Coirault et al., 1999b).

5.4. RNA interference

5.4.1. MicroRNA

MicroRNAs (miRNAs) have important roles in several biological processes including developmental timing control, hematopoiesis, apoptosis, cell proliferation and differentiation (Ambros, 2004; Barter, 2004). The first miRNA, *lin-4*, was discovered in *C. elegans* as a non-protein-coding small RNA that controls timing of *C. elegans* larval development (Lee et al., 1993). Meanwhile, hundreds of noncoding miRNA genes mediating gene-silencing have been identified (Lee et al., 2004; Murchison & Hannon, 2004; Kim 2005). To down-regulate specific gene expression, miRNAs can bind to complementary sites in target mRNAs frequently in the 3'-untranslated region (UTR) preventing protein synthesis (Lee et al., 1993).

miRNAs are tiny single-stranded RNAs ranging between 19-25 nucleotides in length (Ambros et al., 2003; Bartel, 2004). Compared to miRNAs, small interfering RNAs (siRNA) are a different type of small RNA consisting of a short duplex with 21-28 nucleotides (Kim et al., 2003, 2005). MiRNAs are processed from transcripts which contain a local hairpin structure, while siRNAs are made from long double-stranded RNA (dsRNA). The RNase III protein Dicer recognizes and cleaves the miRNA precursor and dsRNA into miRNA and siRNA (Ambros et al., 2003; Kim, 2003). Because these two classes of small RNAs, siRNAs and miRNAs, are generated by the same RNAi pathway in cells, it is difficult to distinguish them by means of their biochemical properties (Kim et al., 2003; Bartel, 2004; Ventura et al., 2004).

Both miRNAs and siRNAs are key players in the RNA silencing process, and although they share many aspects in their biogenesis, some characteristics are different. MiRNAs are classified as hetero-silencing RNAs that are derived from a different genomic locus than its targets. siRNAs are classified as auto-silencing RNAs that originate from the same genomic locus including mRNAs, transposons, viruses, or heterochromatic DNA (Bartel, 2004; Mack, 2007). Also, several different classes of endogenous siRNAs were discovered in various organisms (Kim et al., 2003, 2005).

5.4.2. RNA interference process

The RNAi pathway was originally found in *C. elegans* to silence specific gene expression (Fire et al., 1998). However, RNAi processing is not only a phenomenon in *C. elegans*, but constitutes an evolutionarily conserved mechanism for the down-regulation of target genes in many different organisms including vertebrates and plants (Kennerdell & Carthew, 1998; Wianny & Zernicka-Goetz, 2000; Kunath et al., 2003; Ventura et al., 2004). Thus, RNA interference (RNAi) also represents a powerful tool to silence gene expression in a sequence-specific manner.

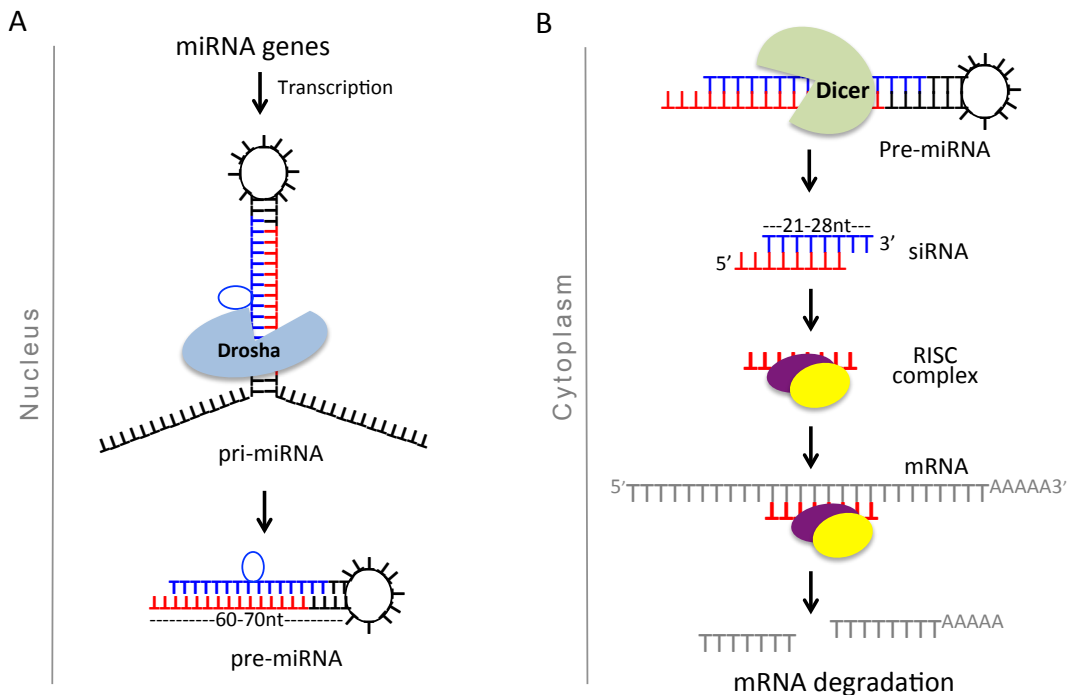


Figure 7. The RNA interference process.

(A) The biogenesis of miRNAs. In the cell nucleus, miRNA genes encode for the primary miRNA transcripts (pri-miRNAs) which are transcribed by RNA polymerase II. Drosha recognizes and cleaves the short hairpin structure of the pri-miRNA, generating pre-miRNAs (figure is modified from Kim, 2003). (B) RNA interference pathway. In the cytoplasm, Dicer cuts the double-stranded pre-miRNA to produce the siRNA. The siRNA is incorporated into the RISC complex which targets mRNA. The complementary mRNA to the siRNA is cleaved by active RISC (figure is modified from Kim, 2003).

In the nucleus, the endonuclease Drosha recognizes a stem loop in the long primary miRNA transcripts (pri-miRNAs) and cleaves the short hairpin structure, converting it into the miRNA precursor pre-miRNA (Lee et al., 2002; Kim, 2004; Fig. 7A). This cleaved pre-miRNA is exported from the nucleus to the cytoplasm by the Ran-dependent nuclear transport receptor exportin-5 (Yi et al., 2003; Lund et al., 2004).

In the cytoplasm, the pre-miRNA is processed into the mature miRNA by another endonuclease, Dicer (Hutvagner et al, 2001; Bernstein et al., 2001; Grishok et al., 2001). Dicer converts the pre-miRNA into the short double-stranded siRNA consisting of 21-22 nucleotides (Fire et al., 1998; Hamilton and Baulcombe, 1999; Bernstein et al., 2001). The RNA-induced silencing complex (RISC) is recruited to the single strand of siRNA as one ribonucleoprotein compound. The RISC endonuclease, AGO2 detects the sequence-complementary mRNA and cleaves it. Finally, this cleaved mRNA is degraded by other endogenous nucleases leading to a specific down-regulation of gene expression (Elbashir et al., 2001; Fig. 7B).

6. Publications

6.1. Contributions

Declaration of contributions to “An RNAi-based approach to down-regulate a gene family *in vivo*. Jeehee Kim, Aurora Badaloni, Torsten Willert, Ursula Zimmer-Strobl, Ralf Kühn, Wolfgang Wurst, Matthias Kieslinger. *PLoS ONE* 2013; 8(11): e80312”.

Fig. 1: Co-authors

Fig. 2: Co-authors

Fig. 3: Own contribution

Fig. 4: Own contribution

Fig. 5: Own contribution

Fig. 6: Co-authors

Fig. 7: Own contribution, together with Torsten Willert

In this project, I performed most of cellular and molecular biological experiments including FACS analysis, real-time PCR and western blotting. I prepared figures 3, 4, 5, 7 and supplementary figure S3. Together with Matthias Kieslinger, I wrote the Experimental Procedures section and proofread the manuscript.

Declaration of contributions to “Ebf factors and MyoD cooperate to regulate muscle relaxation via *Atp2a1*. Saihong Jin, Jeehee Kim, Torsten Willert, Tanja Klein-Rodewald, Mario Garcia-Dominguez, Matias Mosqueira, Rainer Fink, Irene Esposito, Lorenz C. Hofbauer, Patrick Charnay & Matthias Kieslinger. *Nature Communications* 2014; 5:3793”.

Fig. 1: Co-authors

Fig. 2: Co-authors

Fig. 3: Co-authors

Fig. 4: Co-authors

Fig. 5A, 5B, 5D & 5E: Own contribution together with various co-authors

Fig. 5C : Own contribution

Fig. 6 : Co-authors

Fig. 7 : Co-authors

I designed and performed interaction studies between DNA and Ebf3, including ChIP experiments and EMSA assays, contributed to the writing of the Methods section and proofread the manuscript.

An RNAi-Based Approach to Down-Regulate a Gene Family *In Vivo*

Jeehee Kim¹, Aurora Badaloni², Torsten Willert¹, Ursula Zimmer-Strobl³, Ralf Kühn⁴, Wolfgang Wurst⁴, Matthias Kieslinger^{1*}

1 Institute of Clinical Molecular Biology and Tumor Genetics, Helmholtz Zentrum München, German Research Center for Environmental Health, Munich, Germany, **2** Division of Neuroscience, San Raffaele Scientific Institute, Milan, Italy, **3** Department of Gene Vectors, Helmholtz Zentrum München, German Research Center for Environmental Health, Munich, Germany, **4** Institute of Developmental Genetics, Helmholtz Zentrum München, German Research Center for Environmental Health, Munich, Germany

Abstract

Genetic redundancy poses a major problem to the analysis of gene function. RNA interference allows the down-regulation of several genes simultaneously, offering the possibility to overcome genetic redundancy, something not easily achieved with traditional genetic approaches. Previously we have used a polycistronic miR155-based framework to knockdown expression of three genes of the early B cell factor family in cultured cells. Here we develop the system further by generating transgenic mice expressing the RNAi construct *in vivo* in an inducible manner. Expression of the transgene from the strong CAG promoter is compatible with a normal function of the basal miRNA/RNAi machinery, and the miR155 framework readily allows inducible expression from the *Rosa26* locus as shown by Gfp. However, expression of the transgene in hematopoietic cells does not lead to changes in B cell development and neuronal expression does not affect cerebellar architecture as predicted from genetic deletion studies. Protein as well as mRNA levels generated from *Ebf* genes in hetero- and homozygous animals are comparable to wild-type levels. A likely explanation for the discrepancy in the effectiveness of the RNAi construct between cultured cells and transgenic animals lies in the efficiency of the sequences used, possibly together with the complexity of the transgene. Since new approaches allow to overcome efficiency problems of RNAi sequences, the data lay the foundation for future work on the simultaneous knockdown of several genes *in vivo*.

Citation: Kim J, Badaloni A, Willert T, Zimmer-Strobl U, Kühn R, et al. (2013) An RNAi-Based Approach to Down-Regulate a Gene Family *In Vivo*. PLoS ONE 8(11): e80312. doi:10.1371/journal.pone.0080312

Editor: Marc Tjwa, University of Frankfurt - University Hospital Frankfurt, Germany

Received: July 5, 2013; **Accepted:** October 1, 2013; **Published:** November 12, 2013

Copyright: © 2013 Kim et al. This is an open-access article distributed under the terms of the Creative Commons Attribution License, which permits unrestricted use, distribution, and reproduction in any medium, provided the original author and source are credited.

Funding: This work was supported by grants from the German Research Foundation (DFG, TRR54, FOR1586). The funders had no role in study design, data collection and analysis, decision to publish, or preparation of the manuscript.

Competing interests: The authors have declared that no competing interests exist.

* E-mail: matthias.kieslinger@helmholtz-muenchen.de

Introduction

One of the surprising findings of gene targeting in mice are knock-out animals with no obvious phenotype. While a proportion of these cases is likely due to incomplete phenotypic testing or a manifestation only under certain non-standard conditions, it is estimated that 10 - 15% of knock-out mice do not have an obvious phenotype [1]. The vast majority of such cases is thought to derive from functional redundancy between duplicated and highly homologous genes [2]. In favour of this hypothesis, duplicate genes occur in all organisms, especially in multicellular eukaryotes with approximately 50% of mouse genes having a related member in the genome [3–5]. While these facts have interesting and sometimes hard to reconcile implications for evolutionary biology [6,7], gene duplications and redundancy often mask the true contribution of single

genes, making it difficult to discern the function of each copy by knocking out individual genes [8].

Interestingly, conserved gene duplicates in vertebrates are specifically enriched for signal transduction and developmental function [9]. Good examples of this are the MRF family of transcription factors, acting as master regulators of vertebrate skeletal muscle development, and the Hox gene cluster [10]. Another interesting case is the early B cell factor (Ebf) family of transcription factors. All four members show a high level of sequence conservation, reaching 80 - 90% at the nucleotide level within conserved domains, and all four members bind to the same DNA sequence [11,12]. Despite a strong expression in tissues like the olfactory epithelium and in many neuronal cells, deletion of *Ebf1* results in a distinct phenotype, i.e. the complete block of early B cell development [13]. This finding was unexpected, but *Ebf1* is the only family member expressed in hematopoietic cells, whereas the tissues mentioned above

express other Ebf genes in a largely overlapping manner [14–17]. In fact, in addition to B cells, Ebf1 is the only Ebf gene expressed in the embryonic striatum and in cranial nerve nuclei, and *Ebf1*-deficient mice display atrophy and abnormal cellular migration, axonal fasciculation and projection [18–20]. *Ebf2* and *Ebf3* are also expressed in a largely overlapping pattern, and deletion of the single genes leads to a mixture of distinct and overlapping phenotypes causing lethality at the age of approximately two months or immediately after birth respectively. *Ebf2* null mice display abnormalities in the cerebellum and peripheral nerve [21,22]. Mice double heterozygous for *Ebf2* and *Ebf3* recapitulate common defects, such as defective projection of olfactory neurons, but do not display some of the defects occurring only in single knock-outs, arguing that the function of *Ebf* genes is dose-dependent and at least partially redundant [23].

In an effort to overcome functional redundancy and examine the contribution of Ebf factors in general to the support of hematopoietic stem cells, we employed the SIBR (synthetic inhibitory BIC-derived RNA) vectors, a new approach to down-regulate several genes simultaneously based on RNA interference [24]. In this system shRNA sequences are embedded into the framework of miR155/BIC including the flanking sequences, which are cleaved by the RNaseIII enzyme Drosha. This allows the concatemerisation of several shRNAs, and the inclusion of a marker gene, in our case *Gfp*. Furthermore, regulated expression of the RNAi construct is possible since it uses RNA polymerase II-driven promoters. Overall, this results a flexible system to express several shRNAs together with a marker gene in a single polycistronic mRNA driven by PolIII [25]. We were able to successfully down-regulate Ebf1, Ebf2 and Ebf3 and to demonstrate redundancy between these genes in retrovirally infected cultures of osteoblastic cells [24]. The same vector has been used also by other groups to inhibit the Ebf proteins in a variety of different cells [26,27]. As this system proved useful in cell culture approaches in different contexts, we wanted to develop it further and overcome the limitations of *in vitro* approaches and retroviral infections. Here, we report the generation of transgenic mice with a targeted insertion of the SIBR-based *EbfRNAi* construct into the murine *Rosa26* locus, and describe the effects of its induced expression.

Results

Generation of EbfmiRNA transgenic mice

The successful down-regulation of Ebf1, Ebf2 and Ebf3 using one miRNA construct allowed us to analyse the biological effects of this highly conserved protein family in cell culture [24]. While this approach opens new possibilities in studying biological roles independent of redundancy, it remains limited to *in vitro* assays and the expression of the miRNA construct via transfection or viral infection. To overcome these limitations we wanted to develop this system further and use it *in vivo* by generating mice with a targeted insertion. We had previously generated two different miRNA constructs, RNAi-a and RNAi-b, targeting the mRNAs of *Ebf1*, *Ebf2* and *Ebf3* at different positions, primarily to control for off-target effects of the miRNA

generated [24,28]. The single shRNAs bind to regions of the Ebf mRNAs corresponding to the DNA binding or the adjacent IPT/TIG-domain (of unknown function) of the encoded proteins (Figure S1A) and are concatemerised as indicated (Figure S1B). Therefore, as two different constructs were available, we wanted to analyse the effectiveness of the RNAi constructs in detail before going *in vivo*. Therefore, HEK293T cells were transfected with expression plasmids for flag-tagged Ebf1, Ebf2 and Ebf3. In parallel, all six single constructs (two per *Ebf* gene), double and triple constructs were co-transfected. Co-expression of the single RNAi constructs resulted in the down-regulation of the respective Ebf protein, but left the other family members relatively unaffected, indicating specificity but also a high level of effectiveness. The double RNAi constructs against Ebf2 and Ebf3 led to their strong down-regulation, but left Ebf1 relatively unchanged, demonstrating that neither specificity nor effectiveness are compromised by the concatemerisation via the flanking region of miR155. Finally, expression of the triple RNAi constructs induced a loss of Ebf proteins to almost undetectable levels (Figure S2). Although the single RNAi constructs seemed to show slight differences in down-regulation efficiencies, these were minor and could be due to experimental variances. In fact, no differences were observed with the double and triple constructs, confirming data from the down-regulation of endogenous Ebf proteins [24]. Therefore, we decided to use both constructs for the generation of targeted mouse ES cells.

Since miRNAs are standard class II mRNAs driven by RNA polymerase II [29], yet depend on strong expression, we decided to target the insertion to the *Rosa26* locus. However, instead of relying on the endogenous transcriptional activity of the locus we decided to use the synthetic CAG (CMV early enhancer/ chicken β -actin) promoter, which has very strong transcriptional activity [30,31]. In combination with a transcriptional Stop site and a *PGK::Neo* resistance cassette, both flanked by *loxP* sites, immediately downstream of the CAG promoter (Figure 1A), this construct allows strong and tissue-specific expression of the insert [32]. The insert, which follows immediately after the *loxP* sites consists of the *Gfp* gene and the short hairpin sequences concatemerised by the flanking region of miR155 (Figure 1A). This sequence was cut from the pcDNA6.2-GW/EmGFP vector that was described before [24], and is also analysed here (Figure S2).

The targeting construct was used for electroporation of IDG3.2 murine ES cells, which were selected by G418. 600 resistant ES cell clones were picked and analysed for correct integration of the construct by Southern blot. In case of the external 5' probe, the appearance of a 6kb band in an *EcoRI* digestion and of a 12 kb band with a *Scal* digestion indicates the correct integration of the construct. Figure 1B shows two clones with integration of the RNAi-A (A-xx) and two clones with integration of the B construct (B-xx). Hybridising Southern Blot to the internal *Gfp* probe results in the predicted bands of 3 kb for the *EcoRI* digest and 12 kb for the *Scal* digest, confirming the correct and unique integration of the targeting vector (Figure 1C). In addition to the Southern Blot, all positive clones were also confirmed by sequencing. Overall, a 7.5% targeting efficiency was achieved over 600 clones tested,

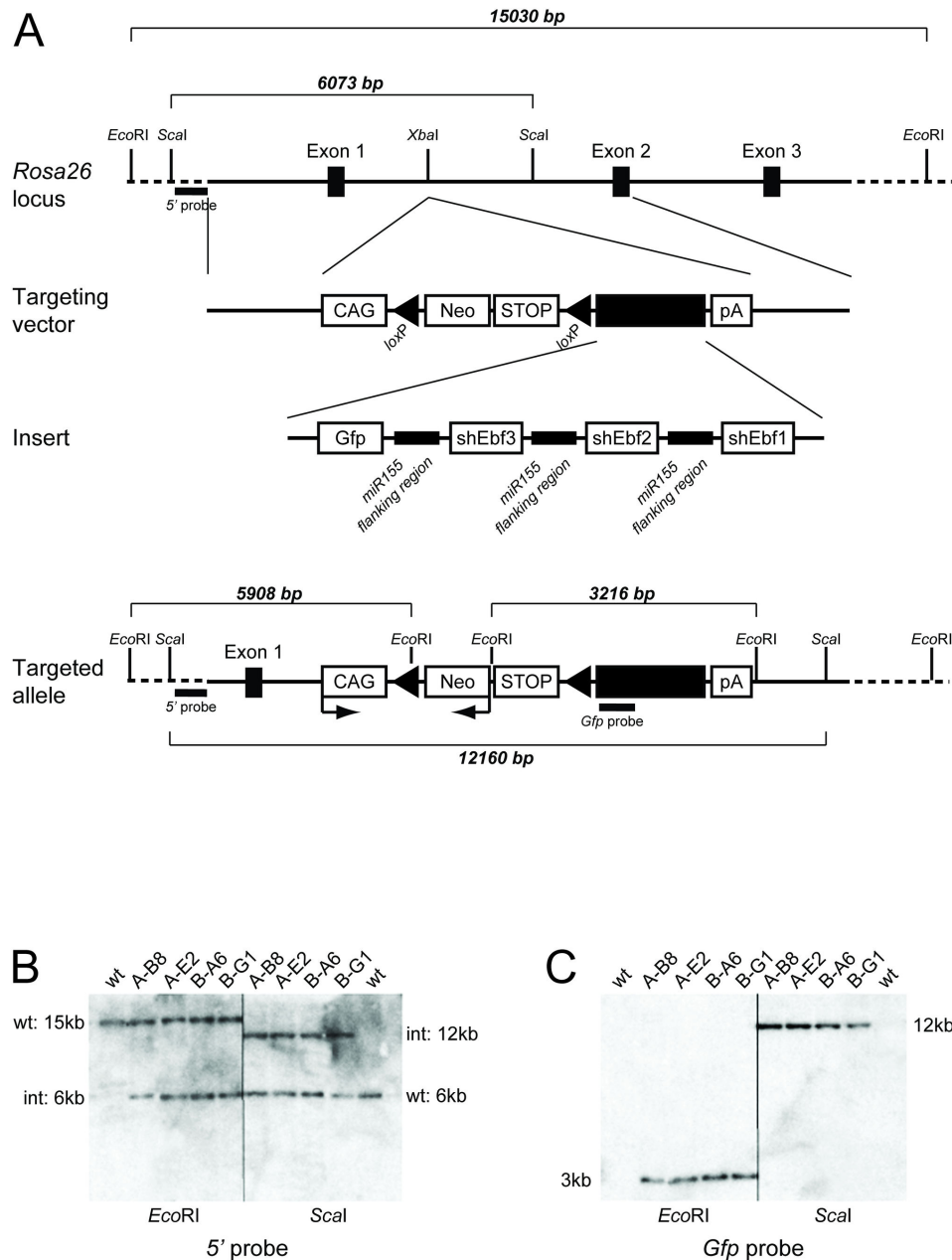


Figure 1. Generation of *EbfmiRNA* transgenic murine ES cells. (A) Schematic representation of the *Rosa26* wild-type locus. A solid line represents regions involved in the targeting construct, while a dashed line depicts genomic regions beyond the targeting construct. The targeting strategy consists of inserting the transgene into the *XbaI* site in intron 1, which is flanked by homology arms including exons 1, 2 and 3. The transgene consists of the synthetic CAG-promoter, a *PGK::Neo* cassette with a transcriptional Stop sequence flanked by *loxP* sites, the RNAi insert as a black box, and a polyA sequence. In the third line the insert is detailed as consisting of the *Gfp* gene, and DNA sequences encoding for short hairpin mRNA against *Ebf3*, *Ebf2* and *Ebf1*. These sequences are surrounded by the flanking region of miR155, which is recognised by the ribonuclease Droscha. The locus after recombination is depicted in line 4, also indicating the direction of transcription from the CAG promoter and the *PGK::Neo-Stop* cassette. Endogenous and newly introduced restriction sites are indicated and the resulting fragment lengths for wild-type and targeted allele with specific restriction enzymes are given. Southern blot probes corresponding to the 5' region and to the *Gfp* gene are indicated. (B) Southern blot of genomic DNA from one wild-type and four mutant ES cell clones digested with *EcoRI* and *Scal* as indicated, and hybridised to the 5' probe (as shown in A). Bands corresponding to the wild-type (wt) and the targeted (int) allele are indicated. (C) Southern blot of genomic DNA as in B, hybridised to the internal *Gfp* probe. Bands of the correct size appear in all four targeted ES cell clones as indicated.

doi: 10.1371/journal.pone.0080312.g001

confirming the high recombination efficiency published for this locus [33,34].

No leakiness and high inducibility of the transgene in murine ES cells

To test the transgene functionally before going *in vivo*, we transfected ES cell clones with the pGK-cre-bpA plasmid (kind gift of Dr. Kurt Fellenberg, Institute of Genetics, University of Cologne), which leads to the expression of the Cre-recombinase in transfected cells. In consequence, the transcriptional Stop sequence should be deleted and the transgene including the *Gfp* gene should come under control of the CAG promoter (Figure 2A). ES cells were harvested 48h post-transfection and analysed by flow cytometry for the expression of *Gfp*. Figure 2B indicates that cells transfected with the mock vector do not express *Gfp*, and a low percentage of cells shows apoptosis as detected by propidium iodide. Transfection of the Cre-encoding plasmid however, leads to an expression of *Gfp* in approximately 30% of cells, again with a low percentage of cells showing apoptosis (Figure 2B). This indicates that the construct is not leaky, i.e. there is no expression of the transgene in presence of the Stop sequence, and that the transgene is efficiently induced via Cre-mediated excision of the Stop cassette. Furthermore, expression of the transgene does not influence viability of the cells.

No leakiness, high inducibility and strong expression of the transgene *in vivo*

Since all tests in ES cells provided evidence for the correct insertion and the functioning of the transgene, we proceeded to generate transgenic mice by standard conditions. Two different ES cell clones for each RNAi construct were injected into blastocysts and chimeric mice were obtained with both transgenic constructs, RNAi-a and RNAi-b. However, germ-line transmission was only successful with chimeric mice transgenic for the RNAi-a construct. As RNAi-a and RNAi-b did not differ significantly in their ability to down-regulate *Ebf* proteins *in vitro* (Figure S2 and [24]), we continued to analyse these mice and will refer to them as *Rosa26^{RNAi}*.

To determine leakiness, inducibility and functionality *in vivo*, we wanted to induce expression of the transgene in hematopoietic cells. *Ebf1* is expressed in early B cells and is necessary for the transition from fraction A to fraction B during B cell development [13]. Furthermore, miRNAs and the protein machinery required for their processing are important for the development of other hematopoietic cells like T and B cells [35]. Thereby, the functionality of the transgene can be tested in early B cells and potentially unspecific or off-target effects by examining T cell development, making the hematopoietic system ideal to study both aspects. To this end, we crossed the *Rosa26^{RNAi}* mouse line to the *vav^{Cre}* line, which is active in hematopoietic stem cells and their derivatives [36]. In a first analysis, we wanted to determine the inducibility and the level of expression of the transgene, as these are two critical parameters for the effectiveness of RNAi. Single cell suspension from the bone marrow of adult mice from various genotypes was analysed by flow cytometry for the expression of *Gfp*. In all control mice, *wt::wt*, *wt::Rosa26^{RNAi/+}* and

vav^{Cre::wt}, no expression of *Gfp* and a percentage of approximately 50% B220-positive cells could be detected, indicating again no leakiness of the construct. A small reduction in the number of B220-positive cells was observed in the presence of the recombinase, but this phenotype did not reach statistical significance, therefore it might represent a slight tendency, but does not proof phenotypic changes due to the expression of the Cre recombinase. The vast majority of bone marrow from *vav^{Cre::Rosa26^{RNAi/+}}* is shifted into the *Gfp* positive channel, with virtually all B220-positive cells also expressing *Gfp*. The level of expression of *Gfp* varies between several different populations, but ranges between one to three shifts in logarithmic units above wild-type, with the majority of cells at around two log-shifts (Figure 3A). Bone marrow cells from *vav^{Cre::Rosa26^{RNAi/RNAi}}* show exactly the same pattern of *Gfp*-positive cells when plotted against B220, but the expression of *Gfp* is shifted to even higher levels, with very few cells remaining negative for *Gfp* (Figure 3A). Statistical analysis shows that the described differences in the expression of *Gfp* are highly significant, and also indicate that the number of B220-positive cells is reduced from 53.8% in wild-type animals to 40.4% in *vav^{Cre::Rosa26^{RNAi/+}}* and 38.6% in *vav^{Cre::Rosa26^{RNAi/RNAi}}* mice, indicating a potential but weak influence of the transgene on B cell development (Figure 3B).

No alterations in early B cell fractions mediated by expression of the transgene

As we detected a high expression of the transgene, particularly in B cells and a slight reduction of B220-positive cells, we continued to analyse the functionality of the RNAi transgene. Since *Ebf1* is the only *Ebf* family member expressed in hematopoietic cells and is required for the progression from fraction A to fraction B in early B cell development [13], we expected a block or at least a down-regulation of cells in the transition from fraction A to fraction B, depending on the efficiency of the construct. Single cell suspensions from mice of the indicated genotypes were stained for B220 and CD43, and double positive cells, which comprise fractions A - C were analysed. No differences in the percentage of these cells were detected (Figure S3). For further analysis, these cells were gated and analysed for expression of BP-1 and CD24, allowing the individual fractions to be distinguished. Again, no differences beyond standard variations in fractions A (BP-1⁻CD24⁻), B (BP-1⁻CD24⁺), or C (BP-1⁺CD24⁺) could be detected in the various genotypes tested. Neither in the B220⁺CD43⁺ Fractions A - C, nor in the individual fractions is it possible to detect any significant changes (Figure 4B).

Expression of the transgene does not interfere with *Ebf1* levels *in vivo*

As no differences in early B cell fractions could be detected in hematopoietic cells, yet the cells express the transgene, we wanted to determine the levels of *Ebf1* under these conditions. Therefore, we sorted fractions A, B and C according to the sorting gates indicated in Figure 5 A from mice carrying the same genotypes as before. Analysis of these early B cell

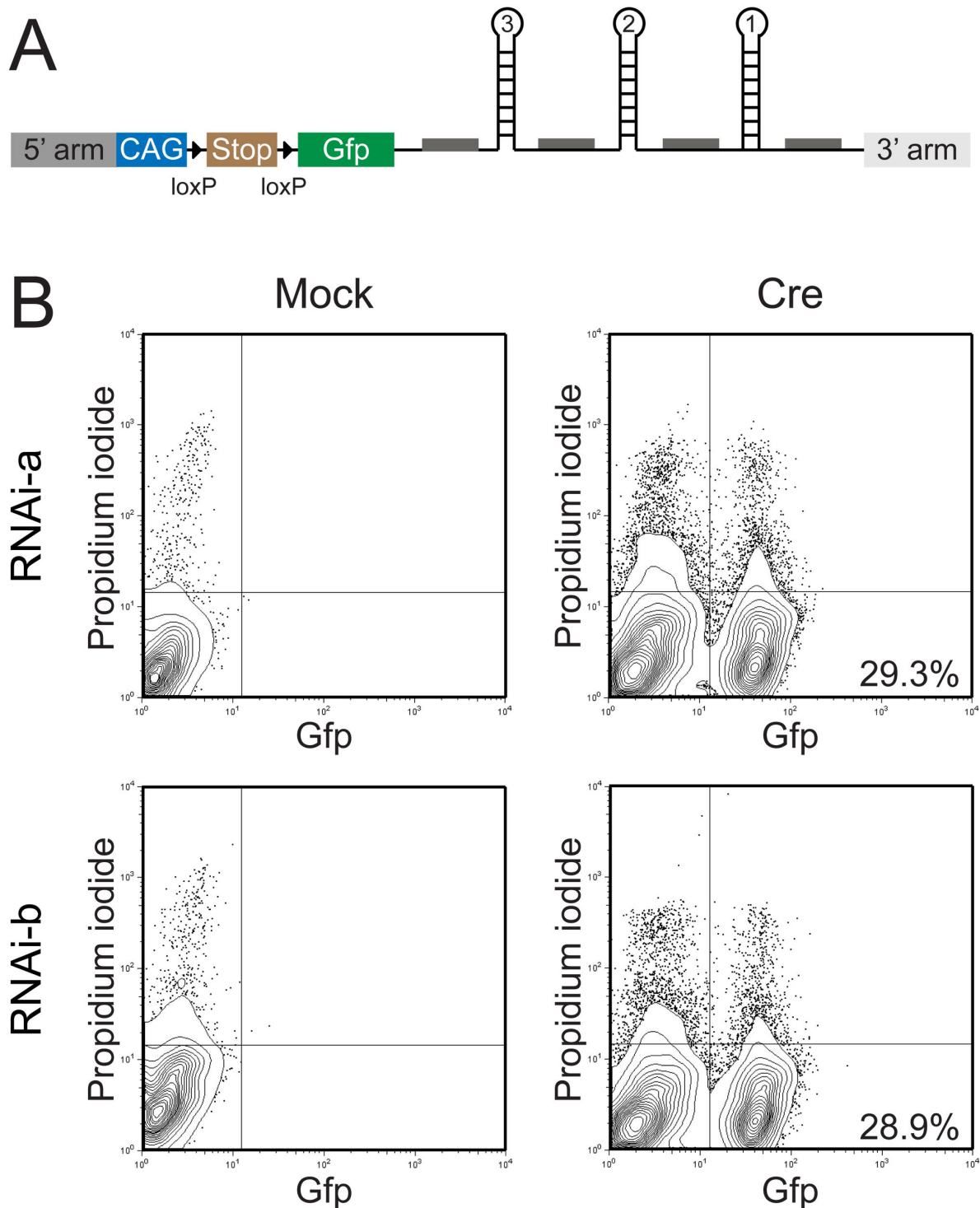


Figure 2. The transgene shows no leakiness and high inducibility in murine ES cells. (A) Schematic depiction of the transgene inserted into the *Rosa26* locus. Expression is driven by the strong CAG promoter, but aborted due to the presence of the transcriptional Stop sequence. Upon Cre mediated deletion, the stop cassette is removed and a polycistronic mRNA encoding for Gfp and short-hairpin sequences against *Ebf3*, *Ebf2* and *Ebf1* gets expressed. (B) ES cell clones tested by Southern blot as correctly targeted for either the RNAi-a or RNAi-b construct were transfected with the pGK-Cre-bpA plasmid encoding for the Cre recombinase or with the empty parental vector (mock). 48 h after transfection, cells were analysed by FACS for the expression of Gfp and for cell death by propidium iodide. Cells have been gated for FSC/SSC.

doi: 10.1371/journal.pone.0080312.g002

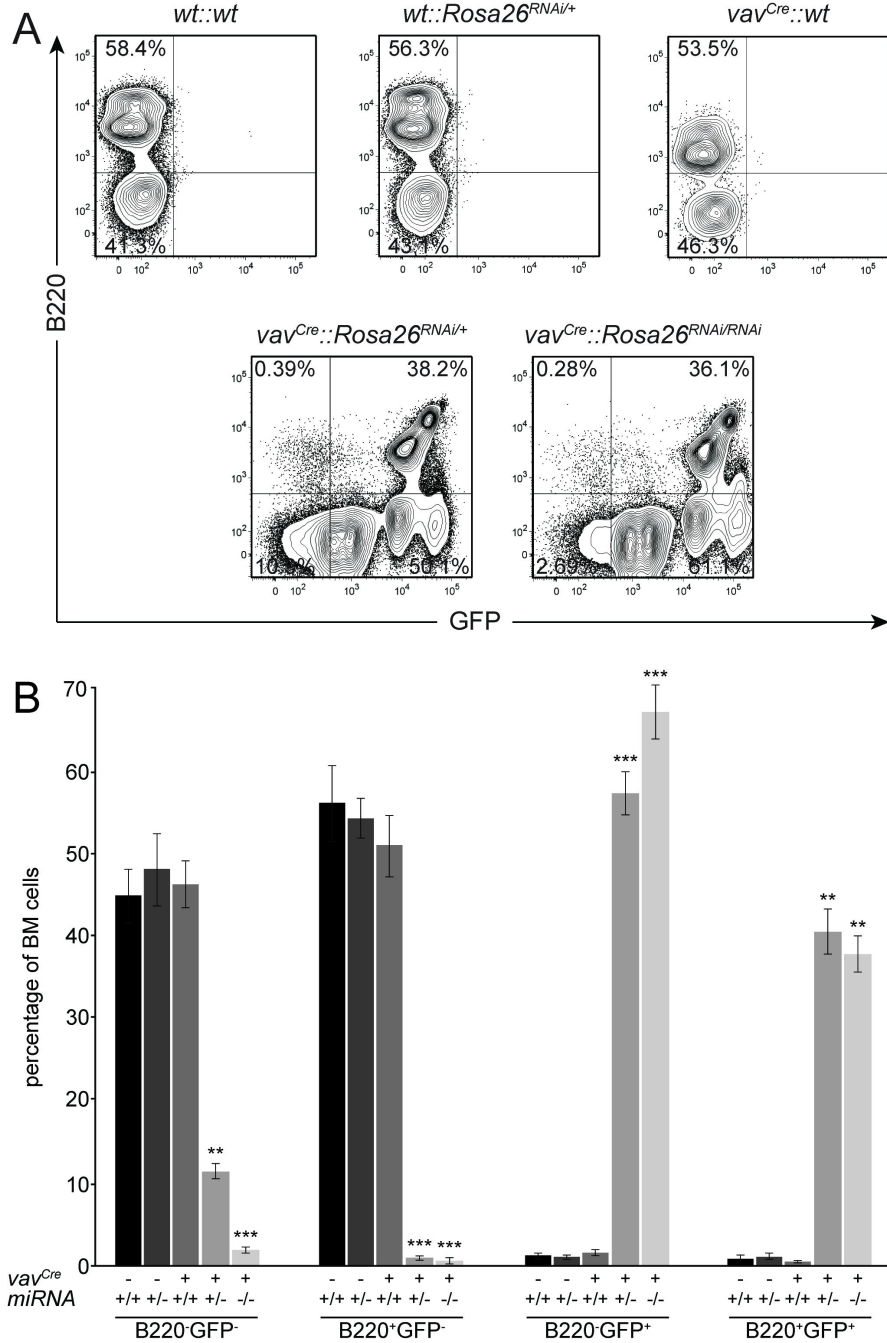


Figure 3. No leakiness, high inducibility and strong expression of the transgene *in vivo*. (A) Single cell suspensions from bone marrow of mice with the indicated genotypes were analysed for the expression of Gfp and the B cell marker B220. Gfp-positive cells are observed only in combination of the *vav^{Cre}* and the transgenic *Rosa26^{RNAi}* genotypes. All other genotypes show expression of B220, but a lack of Gfp. Note the slight shift in expression of Gfp from *Rosa26^{RNAi/+}* to *Rosa26^{RNAi/RNAi}*, due to the presence of two alleles of the transgene. Cell have been gated for FSC/SSC and as PI. (B) Statistical analysis of bone marrow cells stained and analysed as in A. Significant differences based on genotypes are observed only in combination of the *vav^{Cre}* and *Rosa26^{RNAi}* transgenes compared to all other genotypes; n=3-4; error bars=SD; ** p<0.01, *** p<0.001.

doi: 10.1371/journal.pone.0080312.g003

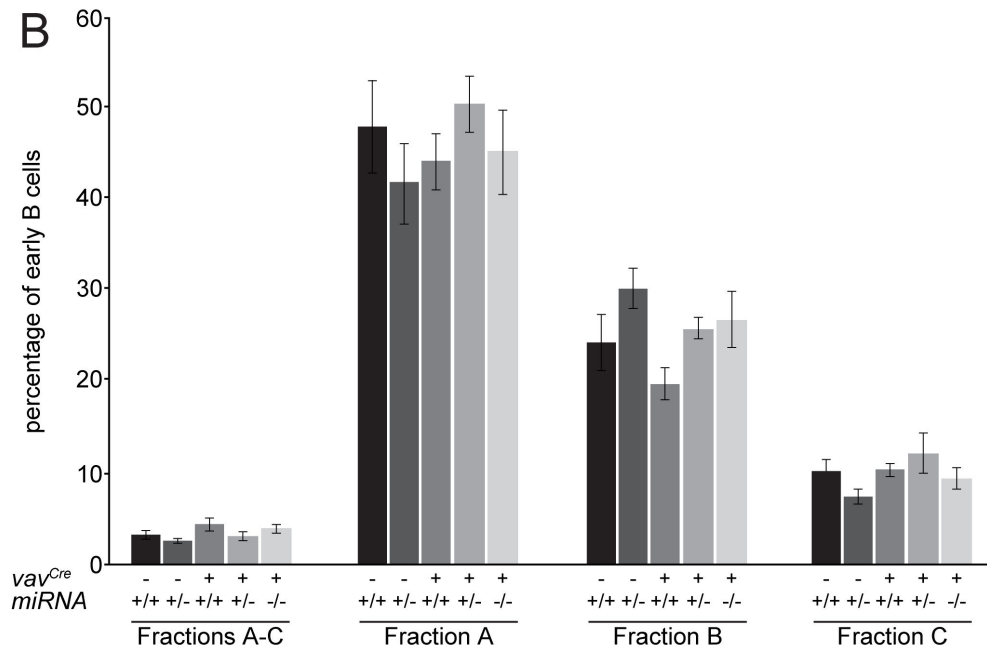
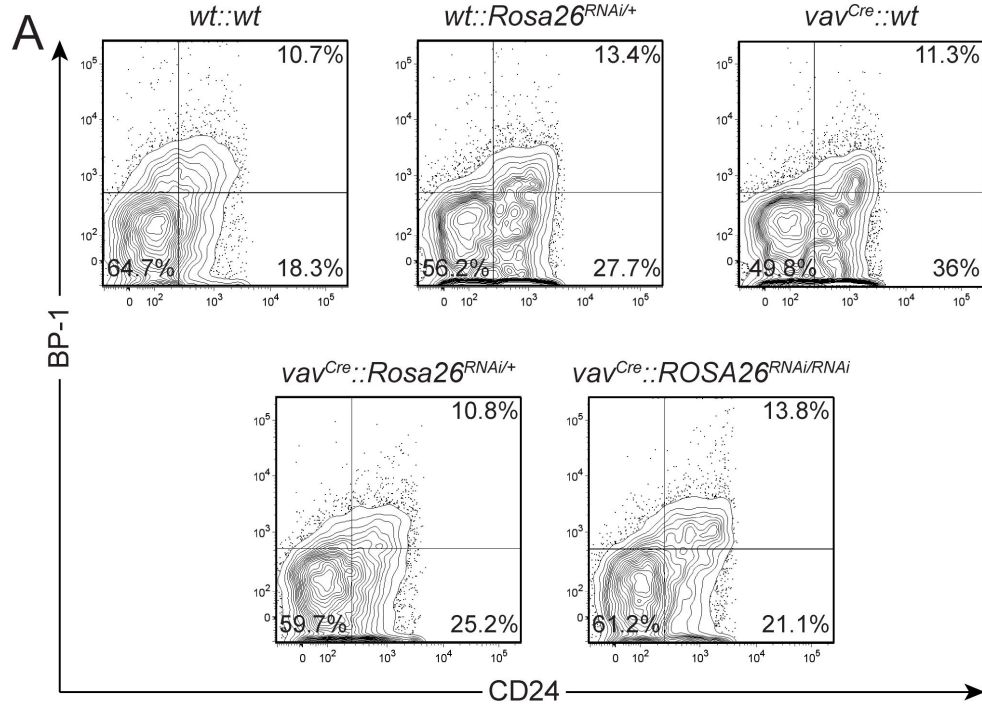


Figure 4. No alterations in early B cell fractions mediated by expression of the transgene. (A) Single cell suspensions from bone marrow of mice with the indicated genotypes were analysed for the percentage of early B cell fractions. Cells were stained with propidium iodide, B220, CD43, BP-1, HSA and CD24. Propidium iodide negative cells are gated as B220/CD43 double positive (see Figure S3), and analysed for expression of HSA/CD24 allowing to distinguish fractions A (B220⁺CD43⁺CD24⁻BP-1⁻), B (B220⁺CD43⁺CD24⁺BP-1⁻) and C (B220⁺CD43⁺CD24⁺BP-1⁺) of B cell development. Representative examples of the indicated genotypes are shown. Cells were further gated for FSC/SSC. (B) Statistical analysis of bone marrow cells stained and analysed as in A. No significant differences based on genotypes are observed; n=3-4; error bars=SD.

doi: 10.1371/journal.pone.0080312.g004

fractions for the expression of *Ebf1* revealed no significant differences in the amount of mRNA even in *vav^{Cre}::Rosa26^{RNAi/+}* versus *vav^{Cre}::Rosa26^{RNAi/RNAi}* mice (Fig. 5B). Since RNAi can also inhibit protein translation, we tested the protein levels of early B cells. As the number of cells after fractionation is too low to allow for testing of individual fractions, we sorted B220⁺CD43⁺ fractions A - C, and subjected those to Western blot analysis. Using a pan Ebf antibody recognising Ebf1, Ebf2 and Ebf3, we could detect comparable amounts of Ebf protein in cells from all genotypes. For control, bone marrow mononuclear cells were depleted of B220⁺ cells and included in the assay. No band was detected in these cells, confirming that no Ebf protein is expressed in hematopoietic cells besides Ebf1 in B cells (Figure 5C). Quantification of the protein amount by densitometry confirmed this observation by showing that no significant differences in Ebf protein levels exist based on the various genotypes (Figure 5D). Therefore we conclude that although the transgene mediates down-regulation of Ebf proteins in cell culture, and it is expressed at high levels in B cells from transgenic mice, its expression does not affect Ebf1 protein levels *in vivo*.

No alteration in cerebellar cyto-architecture in the *Ebf2^{GFPiCre}::Rosa26^{RNAi}* line

Previous studies have clearly indicated that targeted deletion of one member of the Ebf gene family (*Ebf2*) impairs cerebellar development. In particular, cerebellar Purkinje cells (PCs) are decreased in number affecting the size and lobulation of the null cerebellum. One PC subpopulation is selectively reduced, and PC migration into the cerebellar cortex is impaired or delayed [21,37]. *Ebf2* exerts an autocrine/paracrine control over PC survival by activating *Igf1* gene expression [27]. In light of these previous findings, we tested the combined effect of *Ebf1-3* down-regulation on cerebellar development. This analysis was conducted on the adult (P60) progeny of an *Ebf2^{Cre}* x *Rosa26^{RNAi/+}* cross. *Ebf2-Cre* is activated at the outset of PC development, and robust Cre levels are detected in the cerebellar primordium as early as E11.5 [26]. This transgene marks the PC lineage, as shown by genetic fate mapping (A.B., unpublished observations). Our results clearly indicate that *Ebf2^{Cre}::miRNA^{+/-}* mice feature no major cerebellar defects (Figure 6A-D). DAPI staining indicated that cerebellar lobulation is unaffected by RNAi activation in PC progenitors. Moreover, transgenic PCs express normal levels of Calbindin (CaBP), a Ca²⁺ binding protein whose levels decrease rapidly upon PC degeneration. Finally, RNAi-expressing PCs exhibit a normally branched dendritic tree. Thus, no obvious abnormalities were scored in RNAi-expressing cerebella.

Expression of Gfp and the miRNA-transgene are correlated but do not influence Ebf protein levels

The data indicate a clear discrepancy between the functionality of the construct *in vitro* and *in vivo*. One possible explanation is an insufficient expression level of the transgene. So far we have analysed Gfp-positive cells as one bulk population, but as shown in Figure 3A, the expression of Gfp shows a broad spectrum, from high to low expression in largely three distinct populations. This offers the possibility to analyse

these populations individually, to examine if expression-related effects are masked in the bulk analysis. To this end, we isolated low, middle and high Gfp-expressing cells in addition to Gfp-negative cells by flow cytometry from *vav^{Cre}::miRNA^{+/-}* and *vav^{Cre}::miRNA^{-/-}* mice. Interestingly, the percentage of cells in the respective gates does not differ between these two genotypes, but the expression of Gfp is clearly higher in *vav^{Cre}::miRNA^{-/-}*, reflecting the presence of two instead of one allele of the transgene (Figure 7A).

The expression of the transgene in these sorted populations was analysed in qPCR by primers spanning from the 3'-end of Gfp to the last inserted miRNA sequence. As shown in Figure 7B, Gfp-negative cells from all examined genotypes displayed no detectable expression of the transgene, while cells from gates 2 - 4 show increasing expression of the transgene (Figure 7B), revealing a correlation in the expression of the transgene with Gfp. Therefore, if expression plays a role, we might be able to see an influence on Ebf1 protein levels in the most highly expression populations. However, western blot analysis of cells sorted according to the gates showed that Ebf1 was present in the different fractions at comparable levels (Figure 7C), indicating that too low expression of the transgene alone does not explain the observed inefficiency *in vivo*.

Discussion

RNAi has evolved as a means to down-regulate the expression of single target genes *in vivo* [38]. Initially, short-hairpin RNAs were driven by RNA polymerase III-dependent promoters to affect the expression of a single target gene [39–44]. Tissue-specificity can be achieved via the disruption of the promoter by a neomycin-resistance cassette flanked by *loxP* sites [45–47]. However, neither does this system allow to incorporate a marker gene, nor to choose the activating potential of the promoter. When it was found that over-saturation of the cellular shRNA/miRNA pathway was sufficient to cause morphologic changes and even fatality in mice, it became clear that a regulated expression was important *in vivo* [48]. At the same time, shRNA sequences were discovered that are embedded in more complex RNAi transcripts, which are driven by RNA polymerase II, opening the possibility of tissue-specific expression and inclusion of a marker gene [29,49,50]. Among those, miRNA30 was first shown to mediate inhibition of cognate mRNAs with natural as well as designed miRNA sequences [51]. This system was developed further, and now allows the down-regulation of target RNAs in a tissue-specific and, by adding a doxycycline-inducible promoter, reversible manner [52–54].

In some situations however, as to overcome genetic redundancy or to inhibit more than one signalling pathway, it is desirable to inhibit several genes concomitantly. The miR155 precursor is embedded within the third exon of the non-coding BIC gene, and the miR155 precursor together with flanking regions is sufficient to confer the oncogenic activities of BIC/miR155 [55,56]. Based on this, a polycistronic expression vector for RNA polymerase II was developed, in which the flanking regions, which are subject to cleavage by the RNase Drosha, are used to concatemerise sequences encoding

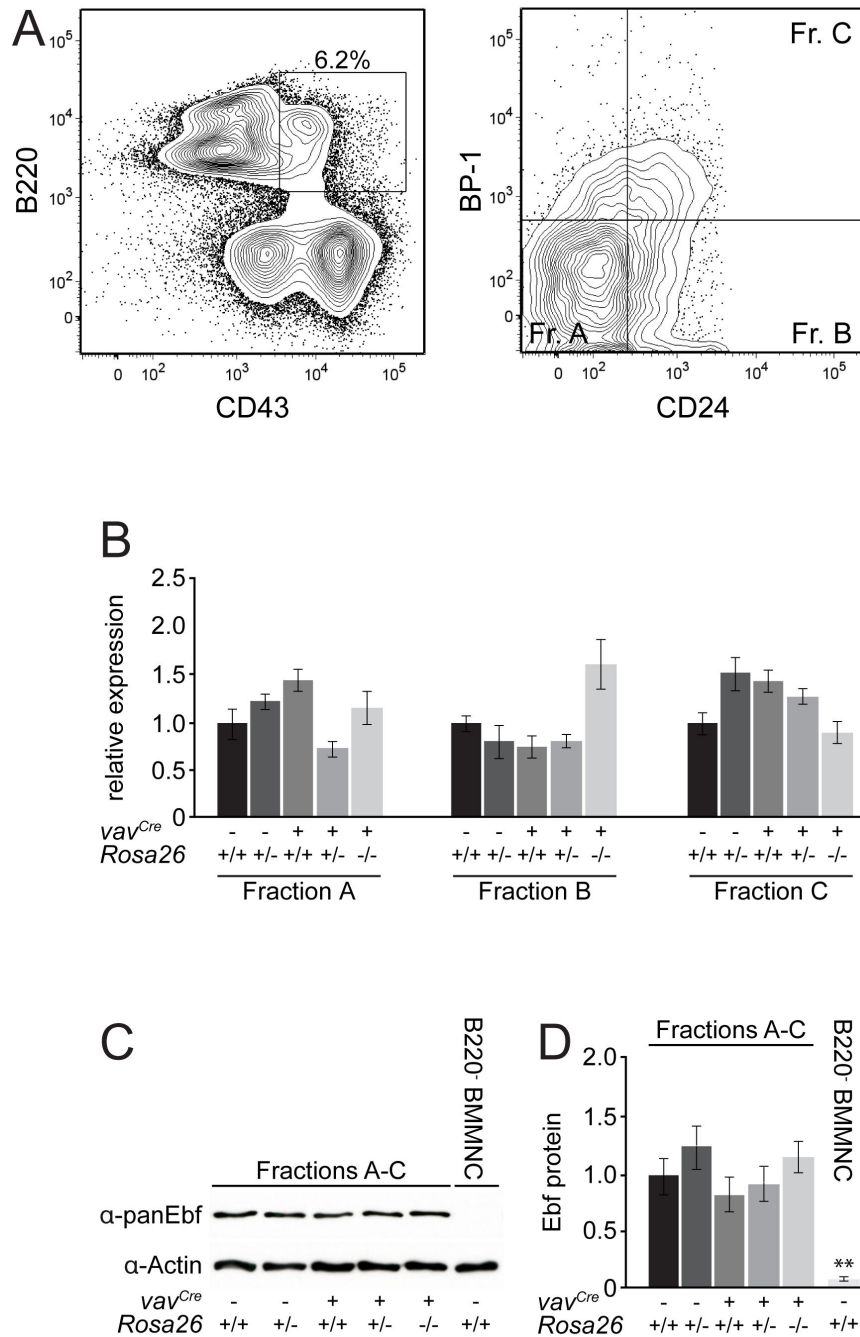


Figure 5. Expression of the transgene does not interfere with Ebf1 levels *in vivo*. (A) Single cell suspensions from bone marrow of mice with the same genotypes as before were prepared and stained for B220/CD43 and CD24/BP1. Cells were gated in flow cytometry for FSC/SSC and as B220⁺CD43⁺ as indicated in the left panel in a representative example. The right panel shows the gates used for sorting of cells from fraction A (B220⁺CD43⁺CD24⁻BP-1⁻), B (B220⁺CD43⁺CD24⁺BP-1⁻) and C (B220⁺CD43⁺CD24⁺BP-1⁺). These B cell fractions were sorted from all the genotypes used throughout this study. (B) Sorted cells from different B cell fractions of the indicated genotypes were subjected to qPCR analysis of Ebf1. All values were normalised to *HPRT* and the expression of Ebf1 in wild-type cells was set to 1 in each case; n=3-4; error bars=SD. (C) B220⁺CD43⁺ cells were sorted from total bone marrow of mice with the indicated genotypes and used for analysis of expression of Ebf1 by Western blot (Fractions A-C). Bone marrow from wild-type mice was depleted of B220⁺ cells (B220⁻ BMMNC) and used as negative control, β -actin is used as loading control. (D) Measurement of the amount of protein present in the B cell fractions and control as depicted in C using ImageJ; n=3-4; error bars=SD, ** p<0.01.

doi: 10.1371/journal.pone.0080312.g005

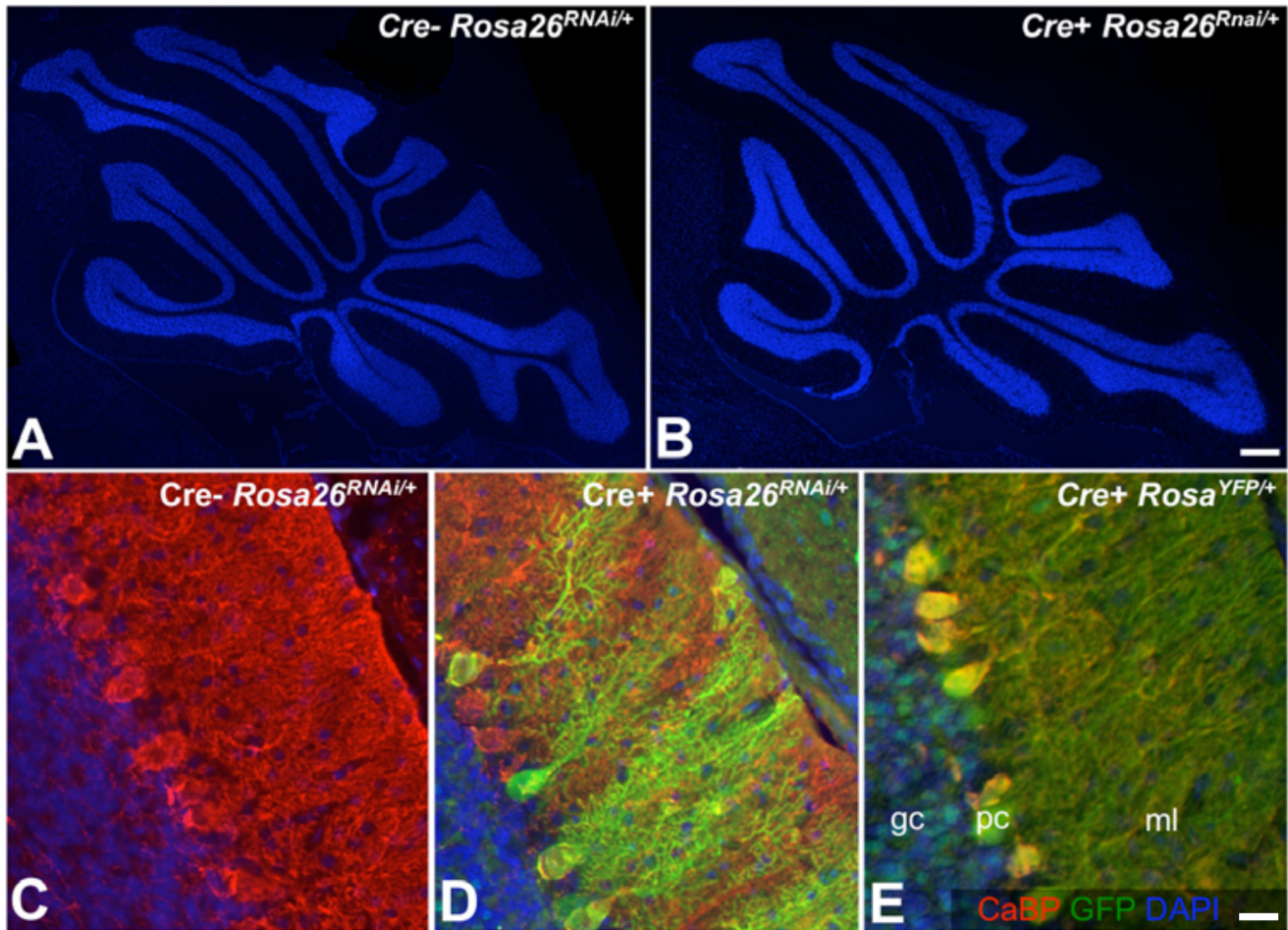


Figure 6. No relevant alterations in the adult cerebellum as a result of RNAi activation in the early cerebellar primordium. (A-B) Low magnification DAPI stainings of postnatal day 60 cerebella. Normal lobulation in the RNAi-expressing cerebellum (*Ebf2^{Cre}::Rosa26^{RNAi/+}*, panel B), compared to a Cre- control (A). (C-D) Sagittal sections of adult cerebella stained for the Purkinje cell (PC)-specific marker calbindin (CaBP, red) and for Gfp. RNAi-expressing PCs (Gfp⁺, panel D) develop normal somata and dendritic arbors positive for CaBP. Panel E (normal control) shows sagittally sectioned CaBP⁺ PCs from an *Ebf2^{Cre}::Rosa26^{YFP/YFP}* mouse. Size bars: B, 200 μ m; E, 25 μ m.

doi: 10.1371/journal.pone.0080312.g006

shRNAs [25]. At least two different synthetic shRNAs can be expressed from a single transcript and coupling to a marker gene like *Gfp* is possible without compromising the efficiency of the system. We used this framework to incorporate sequences directed against *Ebf1*, *Ebf2* and *Ebf3* and observed a strong down-regulation upon ectopic expression but also of the endogenous genes, allowing us to establish a redundant role of these proteins in the support of hematopoietic stem cells [24]. As these constructs also worked in various other cellular contexts [26,27], we wanted to extend the system and to overcome the limitations of cell culture and retroviral infections.

The most striking finding of our experiments is that an RNAi construct that mediates down-regulation of cognate RNA very efficiently in cell culture does not have a biological effect *in vivo*. Several possibilities with different likelihoods can explain this discrepancy. One of our major concerns was the level of

expression necessary to achieve a down-regulation *in vivo*. Originally, one of the reasons for choosing RNA polymerase III for the expression of shRNAs was the high level of expression that can be achieved. Therefore, we did not want to rely on the expression mediated by the endogenous *Rosa26* locus, which ranges from low to mid level, depending on cell type, but is not near typical RNA polymerase III or viral promoter driven expression [57,58]. Therefore, we chose the synthetic CAG promoter, which is among the strongest inducers of eukaryotic expression known [31]. We do observe a good inducibility of *Gfp* in ES cells and particularly in hematopoietic cells after *vav^{Cre}* mediated activation of the transgene. In this case, the expression results in a shift of three log units in flow cytometry, and can be further enhanced to a shift over four logarithmic units by crossing the transgene to homozygosity. This expression is very likely to be higher than the levels achieved

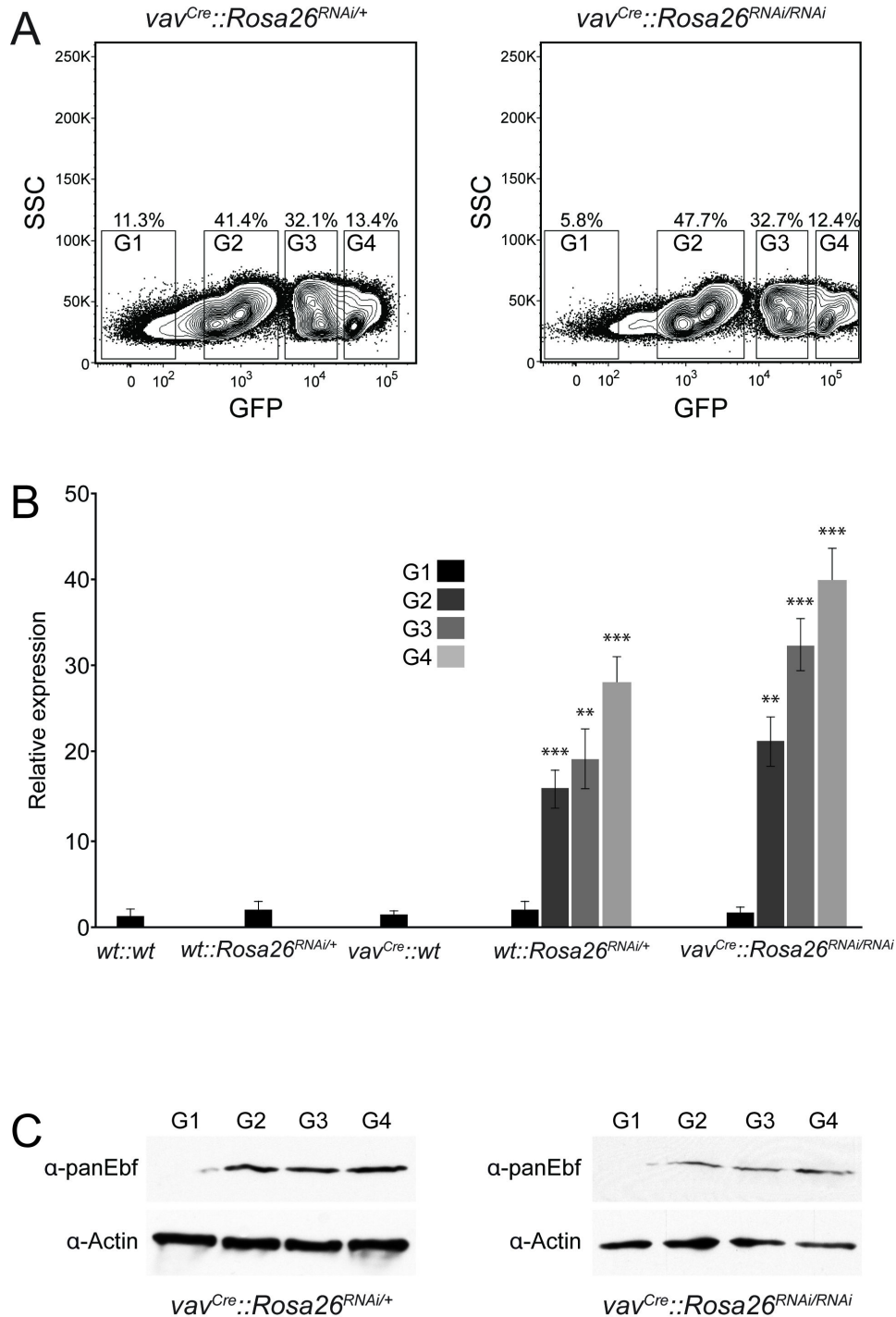


Figure 7. Expression levels of Gfp and transgene correlate, but do not influence Ebf protein. (A) Bone marrow cells from mice with the indicated genotypes were sorted as negative (G1), low (G2), middle (G3) and high (G4) for the expression of Gfp. (B) Cells sorted according to the gates in (A) were analysed for the expression of the miRNA by qPCR. Additionally, bone marrow was isolated from control mice as indicated and used in this analysis. n=3-4; error bars=SD, ** p<0.01, *** p<0.001. (C) Cells sorted according to the gates in (A) were analysed for the presence of Ebf1 protein by western blot. β -actin is used as loading control and the genotypes of the donor mice are indicated. For western blot, three biological replicates were pooled and analysed together.

doi: 10.1371/journal.pone.0080312.g007

using the tet-transactivator to down-regulate p53 [52]. Therefore, and as Ebf genes are not expressed at very high levels (own unpublished data), we consider it very unlikely that too low expression of the transgene is the reason for the lack of down-regulation of Ebf proteins. The expression of the transgene at different levels allowed us to study a potential influence on Ebf protein levels closer. The analysis of cells expressing GFP not at all, or at low, middle or high levels shows that the transgene encoding is detectable at corresponding levels, which is not surprising, given that both are encoded by one mRNA. This also shows that the transgene encoding for the miRNA sequences is really present in the transgene. However, no changes in Ebf protein level can be detected, not even in the highest expressing cells, ruling out that a potential effect is masked in the bulk analysis of Gfp-positive cells and showing that the observed expression levels alone do not explain the lack of down-regulation. Furthermore, a higher expression of the transgene in homozygous transgenic animals, but no down-regulation of Ebf proteins in these mice argues against a dose-dependent effect. In addition, we conclude that expression of the transgene from the CAG promoter does not saturate the miRNA/shRNA machinery, as miRNAs control many aspects of the development of hematopoietic cells, but we do not observe any phenotypic changes [35].

A second possibility might be problems with the processing of a complex polycistronic mRNA *in vivo*. To generate the knock-in mice, we used exactly the same DNA construct as in the retroviral vector used for the infection of cultured murine and human cells. Therefore, since cells of the same species were used, differences in the processing machinery between cultures cells and transgenic mice seem rather unlikely. Additionally many studies show that the basic RNAi machinery is ubiquitously expressed. The second possibility is that the basic machinery is the same *in vitro* and *in vivo*, but the artificial RNAi construct generated poses more problems in its correct processing than endogenous miRNAs. Chaining of more than three shRNA sequences strongly decreases the efficiency in mediating down-regulation for each shRNA and the expression of *Gfp* is attenuated by shRNA chaining, presumably due to increased processing (data not shown). Together, this might indicate that the construct is on the border of losing its effectiveness due to its complexity. Again, the expression of *Gfp in vitro* and *in vivo* and the down-regulation of Ebf proteins in cultured cells argues against this possibility, although we consider it more likely than the two afore mentioned possibilities.

A third general possibility is the design and efficiency of the RNAi sequences used to inhibit the Ebf proteins. The precise sequence requirements for efficient RNAi are not well understood [59], although it is known that thermodynamic asymmetry, low G/C content and a strong bias for A/U at the 5' end of the guide strand are important [60–62]. We have tested the RNAi sequences for down-regulation in cultured cells by transfection of the shRNA encoding plasmid and by retroviral infection of primary cells for efficient down-regulation of transfected and endogenous Ebf proteins [24]. In both cases however, the RNAi transcripts result from a multitude to several

origins of expression (plasmids / retroviral integration sites), but not from a single genomic locus as is the case in the transgenic mice. In fact it is this aspect where the biggest differences between the *in vitro* and *in vivo* approach occur. Based on a large scale approach, it has been estimated that only 3% of all possible RNAi sequences for a particular gene elicit efficient knockdown at the level of single copies [28]. Of all the possible explanations mentioned here, we consider problems with the design and the efficiency of the RNAi sequences as single genomic copies most likely to explain the discrepancy between *in vitro* and *in vivo*, i. e. the absence of a detectable down-regulation of Ebf proteins.

In summary, we have used a new miR155-based system to explore the potential to knockdown the expression of several genes simultaneously. This approach was successfully *in vitro*, however, its direct translation *in vivo* did not result in the expected down-regulation. We think that the most likely explanation for this discrepancy lies in the efficiency of the RNAi sequences as single genomic copies. This, together with the complexity of the whole RNAi transcript, consisting of three short hairpins and *Gfp*, likely results in an overall efficiency that is too low to detect and that potentially can be compensated for. We do not think that the overall expression or differences in the endogenous basic miRNA/RNAi machinery are likely explanations. The data presented here clearly show that expression of the transgene from the CAG promoter is compatible with a normal function of the basal miRNA/RNAi machinery in hematopoietic cells, and the miR155 framework works well in the context of inducible expression from the *Rosa26* locus as shown by *Gfp*. The data presented here provide the foundation for future work on the simultaneous knockdown of several genes *in vivo*, as the problems concerning the efficiency of the RNAi sequences can be overcome [59].

Experimental Procedures

Generation of transgenic mice

Two different sequences to inhibit *Ebf1*, *Ebf2* and *Ebf3* (RNAi-a and RNAi-b) were excised together with *EmGFP* from the pcDNA6.2-GW/EmGFP vector (Invitrogen, [24]), and inserted into the *XbaI* site of the pRTS targeting vector (kindly provided by D. Calado, Immune Disease Institute Inc., Boston, MA). Mouse ES cells derived from C57Bl/6 x 129S6/SvEvTac-F1 strains (IDG3.2) were electroporated with this construct and colonies were isolated in the presence of 170 µg/ml G418 (Gibco). DNA extraction and Southern Blots were performed as described [63]. The correct insertion of the targeting sequences was analysed using an external 550 bp 5' probe and an internal *Gfp* probe of 723 bp. The 5' probe was cut from the p*Rosa26*-5-pBS KS plasmid using *EcoRI* and *PacI*, the *Gfp* probe was isolated from the pcDNA6.2-GW/EmGFP vector using *DraI*. Hybridisation was carried out for 16 hours at 65°C in Church buffer (0.4 M Na₂HPO₄), membranes were washed 3 x 10 min at 58°C in wash buffer (0.2 x SSC, 0.5% SDS) and bands were detected using a phosphorimager (Fuji Bas 1000). Two correctly targeted clones representing RNA-a and RNA-b constructs were injected into C57Bl/6 blastocysts that were

implanted into pseudopregnant females. Chimeric mice were bred to obtain germ-line transmission. Two male chimera (80%) corresponding to the RNA-a clone were selected to get heterozygous mice. Mutant mice were backcrossed with C57Bl/6 wild-type mice for more than 6 generations. All experiments involving animals were designed in agreement with the stipulations of the San Raffaele Institutional Animal Care and Use Committee, the Helmholtz Zentrum München and the Regierung von Oberbayern. The protocol and all experiments involving animals was approved by the ethics committees of the afore mentioned institutions. All efforts were made to minimise animal suffering.

Genotyping

For genotyping of mice tails were digested for at least 1 h in lysis buffer [FirePol buffer B (Solis BioDyne), 1.25 mM MgCl₂, 50 µg/ml proteinase K] at 55 °C and inactivated for 15 min at 95 °C. PCR was carried out with genomic DNA; 20 pmol of each primer were used, for the miRNA line (5'-*Rosa* fwd 5'-GAGTTCTCTGCTGCCTCCTG-3', CAG rev 5'-TGAAC TAATGACCCCGTAATTG-3', 3'*Rosa* rev 5'-AGGAAAGGGAAAATGCCAAT-3' using FirePol (Solis BioDyne) under these conditions: 31 cycles of 94 °C for 45 sec, 60 °C for 45 sec, 72 °C for 1 min to amplify products of 600 bp for wild-type and 290 bp for the mutant allele; for *R26R^{YFP}* line (R523 5'-GGAGCGGGAGAAATGGATAT-3', R26F2: 5'-AAAGTCGCTCTGAGTTGTTAT-3', oIMR 316 5'-AAGACCGCGAAGAGTTTGTC-3') under these conditions: 35 cycles of 94 °C for 30 sec, 58 °C for 1 min, 72 °C for 1 min to amplify products of 600 bp for wild-type and 320 bp for the knock-in allele; for *Ebf2^{GFPiCre}* line (F 5'-ATGGTGCCAAGGATGACTC-3', R 5'-CCTCGAGCAGCCTCACCA-3') under these conditions: 30 cycles of 94 °C for 30 sec, 58 °C for 30 sec, 72 °C for 30 sec to amplify a 200 bp product corresponding to the transgene.

Cell-culture, Transfections, Plasmids

HEK293T cells were kept under standard conditions in DMEM medium (+ 10% FCS, 1% Pen/Str/Glu; Gibco), and transfected using polyethylenimine (Gibco) according to standard protocols. For ectopic expression *Ebf1*, *Ebf2* and *Ebf3* were cloned into the pcDNA3.1 vector (Invitrogen) in frame with an N-terminal Flag-tag (Sigma).

Flow cytometry, Antibodies

For flow cytometry single cell suspensions were prepared by trypsinising ES cells or by aspirating bone marrow according to standard procedures. Isolated cells were blocked for unspecific binding using CD16/32 and incubated with either biotinylated or directly fluorochrome-conjugated antibodies. Cells were measured or sorted using either an LSRFortessa or a FACSAriaIII (BD Biosciences) and data were analysed using FACSDiva (Becton Dickinson GmbH) and FlowJo 9.3 (Treestar Inc.) software. For depletion of dead cells propidium iodide was used. Antibodies directed against the following markers were obtained from BD Biosciences: B220 (RA3-6B2) and CD43 (RM4-5), BP-1 (6C3), CD24 (30-F1), CD16/32 (=FcyRII/III; 2.4G2).

Isolation of RNA and Quantitative RT-PCR

mRNA was isolated using peqGOLD TriFast™ (Peqlab) according to manufacturer's instructions, cDNA was synthesised using SuperScript II reverse transcriptase (Invitrogen) and the oligo-dT primer (Roche). qPCR reactions were performed in duplicate with SYBR Green I Master in a LightCycler® 480II (Roche) with standard conditions: 95 °C for 10 min followed by 45 cycles of 95 °C for 10 s, 65 °C for 10 s and 72 °C for 10 s. Primer sequences: *Hprt* fwd 5'-tgc tgg tga aaa gga cct ctc g-3', rev 5'-tct ggg gac gca gca act ga-3'; β -Actin fwd 5'-tgt ggt ggt gaa gct gta gc-3', rev 5'-gac gac atg gag aag atc tgg-3'; *Ebf1* fwd 5'-ggg gac agt gca gat ggt aa-3', rev 5'-caa ctc act cca gac cag ca-3'; *Gfp* fwd 5'-acc tac ggc gtg cag tgc ttc agc-3', rev 5'-gtc ctc gat gtt gtg gcg gat ctt g-3'; *miRNA*-fwd: 5'-ggc atg gac gag ctg tac aa-3', *miRNA*-rev3: ctc tag atc aac cac ttt gt-3'. Three independent measurements were performed for each qPCR analysis, error bars represent the standard deviation of the mean. The comparative CT method was used to calculate the expression levels of RNA transcripts, and the quantified individual RNA expression levels were normalised for the respective β -actin expression levels, unless stated otherwise. Since we measured the relative RNA expression levels, the indicated expression levels were set as 1 or 100.

Histological procedures

Postnatal mice were anaesthetised with Avertin (Sigma, St Louis, MO, USA) and perfused with 0.9% NaCl followed by 4% paraformaldehyde (PFA). Tissues were fixed with 4% PFA, cryoprotected in 30% sucrose overnight, embedded in OCT (Bioptica), sectioned on a cryotome (18 µm). Cryosections were immunostained with the following antibodies: rabbit or mouse anti-calbindin (1:1000, Swant, Bellinzona, Switzerland); rabbit anti-GFP (1:700; Invitrogen); chicken anti-GFP (1:500; Abcam, Cambridge, UK).

Statistics

P-values were determined with the Student's two-tailed t-test for independent samples, assuming equal variances on all experimental datasets.

Immunoblotting, Antibodies

Protein isolation and immunoblotting was carried out according to standard procedures, antibodies used were α -panEbf [24], α - β -Actin (AC-74, Sigma), α -Flag (M2, Sigma), The secondary α -mouse-IgG-HRP antibodies were obtained from Sigma, the secondary α -rat-IgG + IgM-HRP antibody was purchased from Jackson Immuno Research. Bands in western blot experiments were quantified using the open source software ImageJ (<http://rsb.info.nih.gov/ij/>; W. S. Rasband, NIH, National Institutes of Health, Bethesda, MD).

Supporting Information

Figure S1. Schematic overview of the DNA sequences used for RNAi. (A) The structure of the transcripts of *Ebf1*, *Ebf2* and *Ebf3* is depicted including 5'- and 3'-UTR. Protein

domains encoded by the transcripts are indicated above (HLH = helix-loop-helix domain) and the beginning and end of the coding sequence are given underneath in base pairs relative to the start site. The sequences used to inhibit the individual members and their positions are plotted against the transcripts. Two sequences are indicated for each gene, as two different RNAi constructs have been generated, and their identifying numbers are given underneath. (B) Schematic representation of the organisation of the RNAi used for the transgene. Grey boxes represent the flanking region from miR155, and the numbers within the loops indicate the Ebf gene against which the sequences at this position are directed. The composition of the two constructs used for RNAi is given below.

(TIF)

Figure S2. Down-regulation of Ebf1, Ebf2 and Ebf3 by a single RNAi construct. To analyse the efficiency and specificity of bioinformatically predicted sequences to down-regulate the expression of Ebf1, Ebf2 and Ebf3, HEK293T cells were transfected with expression plasmids encoding the individual Ebf proteins together with an N-terminal Flag tag. Expression vectors containing the shRNA sequences either alone or in combination were co-transfected, and 48 h after transfection cells were harvested and analysed by Western blot. α -Flag antibody was used to detect Ebf expression levels, and α -actin as loading control. Mock is referring to a co-transfection of the empty parental vector (pcDNA6.2-GW/EmGFP), no RNAi leaves out the shRNA containing vectors.

References

- Barbaric I, Miller G, Dear TN (2007) Appearances can be deceiving: phenotypes of knockout mice. *Brief Funct Genomic Proteomic* 6: 91-103. doi:10.1093/bfgp/elm008. PubMed: 17584761.
- Cooke J, Nowak MA, Boerlijst M, Maynard-Smith J (1997) Evolutionary origins and maintenance of redundant gene expression during metazoan development. *Trends Genet* 13: 360-364. doi:10.1016/S0168-9525(97)01233-X. PubMed: 9287491.
- Mouse Genome Sequencing Consortium, Waterston RH, Lindblad-Toh K, Birney E, Rogers J, et al. (2002) Initial sequencing and comparative analysis of the mouse genome. *Nature* 420: 520-562. doi:10.1038/nature01262. PubMed: 12466850.
- Lynch M, Conery JS (2003) The origins of genome complexity. *Science* 302: 1401-1404. doi:10.1126/science.1089370. PubMed: 14631042.
- Zhang J (2003) Evolution by gene duplication: an update. *Trends Ecol Evol* 18: 292-298. doi:10.1016/S0169-5347(03)00033-8.
- Thomas JH (1993) Thinking about genetic redundancy. *Trends Genet* 9: 395-399. doi:10.1016/0168-9525(93)90140-D. PubMed: 8310537.
- Nowak MA, Boerlijst MC, Cooke J, Smith JM (1997) Evolution of genetic redundancy. *Nature* 388: 167-171. doi:10.1038/40618. PubMed: 9217155.
- Tautz D (1992) Redundancies, development and the flow of information. *Bioessays* 14: 263-266. doi:10.1002/bies.950140410. PubMed: 1596275.
- Putnam NH, Butts T, Ferrier DE, Furlong RF, Hellsten U et al. (2008) The amphioxus genome and the evolution of the chordate karyotype. *Nature* 453: 1064-1071. doi:10.1038/nature06967. PubMed: 18563158.
- Kafri R, Springer M, Pipel Y (2009) Genetic redundancy: new tricks for old genes. *Cell* 136: 389-392. doi:10.1016/j.cell.2009.01.027. PubMed: 19203571.
- Liberg D, Sigvardsson M, Akerblad P (2002) EBF/Olf/Collier family of transcription factors: regulators of differentiation in cells originating from all three embryonal germ layers. *Cell Biol* 22: 8389-8397.
- Dubois L, Vincent A (2001) The COE--Collier/Olf1/EBF--transcription factors: structural conservation and diversity of developmental functions. *Mech Dev* 108: 3-12. doi:10.1016/S0925-4773(01)00486-5. PubMed: 11578857.
- Lin H, Grosschedl R (1995) Failure of B-cell differentiation in mice lacking the transcription factor EBF. *Nature* 376: 263-267. doi:10.1038/376263a0. PubMed: 7542362.
- Mella S, Soula C, Morello D, Crozatier M, Vincent A (2004) Expression patterns of the coe/ebf transcription factor genes during chicken and mouse limb development. *Gene Expr Patterns* 4: 537-542. doi:10.1016/j.modgep.2004.02.005. PubMed: 15261831.
- Wang SS, Tsai RY, Reed RR (1997) The characterization of the Olf-1/EBF-like HLH transcription factor family: implications in olfactory gene regulation and neuronal development. *J Neurosci* 17: 4149-4158. PubMed: 9151732.
- Green YS, Vetter ML (2011) EBF factors drive expression of multiple classes of target genes governing neuronal development. *Neural Dev* 6: 19. doi:10.1186/1749-8104-6-19. PubMed: 21529371.
- Jin K, Jiang H, Mo Z, Xiang M (2010) Early B-cell factors are required for specifying multiple retinal cell types and subtypes from postmitotic precursors. *J Neurosci* 30: 11902-11916. doi:10.1523/JNEUROSCI.2187-10.2010. PubMed: 20826655.
- Garel S, Marin F, Grosschedl R, Charnay P (1999) Ebf1 controls early cell differentiation in the embryonic striatum. *Development* 126: 5285-5294. PubMed: 10556054.
- Garel S, Garcia-Dominguez M, Charnay P (2000) Control of the migratory pathway of facial branchiomotor neurones. *Development* 127: 5297-5307. PubMed: 11076752.
- Garel S, Yun K, Grosschedl R, Rubenstein JL (2002) The early topography of thalamocortical projections is shifted in Ebf1 and Dlx1/2 mutant mice. *Development* 129: 5621-5634. doi:10.1242/dev.00166. PubMed: 12421703.
- Croci L, Chung SH, Masserdotti G, Gianola S, Bizzoca A et al. (2006) A key role for the HLH transcription factor EBF2COE2, O/E-3 in Purkinje neuron migration and cerebellar cortical topography. *Development* 133: 2719-2729. doi:10.1242/dev.02437. PubMed: 16774995.
- Corradi A, Croci L, Broccoli V, Zecchini S, Previtali S et al. (2003) Hypogonadotropic hypogonadism and peripheral neuropathy in Ebf2-null mice. *Development* 130: 401-410. doi:10.1242/dev.00215. PubMed: 12466206.

(TIF)

Figure S3. Analysis of B cell fractions A - C in Rosa26^{RNAi} transgenic mice. Single cell suspensions from bone marrow of mice with the indicated genotypes were analysed for the percentage of early B cell fractions. Cells were stained with propidium iodide, B220, CD43, and gated for FSC/SSC and as PI negative, and B220 CD43 double positive. The gating window and the percentage of cells are shown. Cells were further stained for BP-1 and HSA/CD24, and analysed for fractions A - C in detail (Figure 4). Representative examples of the indicated genotypes are shown. The statistical analysis of fraction A - C in Figure 4B is referring to this setting.

(TIF)

Acknowledgements

We thank Marc Schmidt-Supprian for the targeting vector, Dinis Calado from Klaus Rajewski's laboratory for providing the pRTS-vector, and Dimitris Kioussis (MRC, London, UK) for providing the *vav^{Cre}* mice.

Author Contributions

Conceived and designed the experiments: MK UZS. Performed the experiments: JK AB TW. Analyzed the data: JK AB MK. Contributed reagents/materials/analysis tools: RK WW. Wrote the manuscript: MK.

23. Wang SS, Lewcock JW, Feinstein P, Mombaerts P, Reed RR (2004) Genetic disruptions of O/E2 and O/E3 genes reveal involvement in olfactory receptor neuron projection. *Development* 131: 1377-1388. doi: 10.1242/dev.01009. PubMed: 14993187.
24. Kieslinger M, Hiechinger S, Dobrev G, Consalez GG, Grosschedl R (2010) Early B cell factor 2 regulates hematopoietic stem cell homeostasis in a cell-nonautonomous manner. *Cell Stem Cell* 7: 496-507. doi:10.1016/j.stem.2010.07.015. PubMed: 20887955.
25. Chung KH, Hart CC, Al-Bassam S, Avery A, Taylor J et al. (2006) Polycistronic RNA polymerase II expression vectors for RNA interference based on BIC/miR-155. *Nucleic Acids Res* 34: e53. doi: 10.1093/nar/gkl143. PubMed: 16614444.
26. Chiara F, Badaloni A, Croci L, Yeh ML, Cariboni A et al. (2012) Early B-cell factors 2 and 3 (EBF2/3) regulate early migration of Cajal-Retzius cells from the cortical hem. *Dev Biol* 365: 277-289. doi:10.1016/j.ydbio.2012.02.034. PubMed: 22421355.
27. Croci L, Barili V, Chia D, Massimino L, van Vugt R et al. (2011) Local insulin-like growth factor I expression is essential for Purkinje neuron survival at birth. *Cell Death Differ* 18: 48-59. doi:10.1038/cdd.2010.78. PubMed: 20596079.
28. Dow LE, Premrsirut PK, Zuber J, Fellmann C, McJunkin K et al. (2012) A pipeline for the generation of shRNA transgenic mice. *Nat Protoc* 7: 374-393. doi:10.1038/nnano.2012.65. PubMed: 22301776.
29. Lee Y, Kim M, Han J, Yeom KH, Lee S et al. (2004) MicroRNA genes are transcribed by RNA polymerase II. *EMBO J* 23: 4051-4060. doi: 10.1038/sj.emboj.7600385. PubMed: 15372072.
30. Alexopoulou AN, Couchman JR, Whiteford JR (2008) The CMV early enhancer/chicken beta actin (CAG) promoter can be used to drive transgene expression during the differentiation of murine embryonic stem cells into vascular progenitors. *BMC Cell Biol* 9: 2. doi: 10.1186/1471-2121-9-2. PubMed: 18190688.
31. Niwa H, Yamamura K, Miyazaki J (1991) Efficient selection for high-expression transfectants with a novel eukaryotic vector. *Gene* 108: 193-199. doi:10.1016/0378-1119(91)90434-D. PubMed: 1660837.
32. Xiao C, Calado DP, Galler G, Thai TH, Patterson HC et al. (2007) MiR-150 controls B cell differentiation by targeting the transcription factor c-Myb. *Cell* 131: 146-159. doi:10.1016/j.cell.2007.07.021. PubMed: 17923094.
33. Soriano P (1999) Generalized lacZ expression with the ROSA26 Cre reporter strain. *Nat Genet* 21: 70-71. doi:10.1038/5007. PubMed: 9916792.
34. Zambrowicz BP, Imamoto A, Fiering S, Herzenberg LA, Kerr WG et al. (1997) Disruption of overlapping transcripts in the ROSA beta geo 26 gene trap strain leads to widespread expression of beta-galactosidase in mouse embryos and hematopoietic cells. *Proc Natl Acad Sci U S A* 94: 3789-3794. doi:10.1073/pnas.94.8.3789. PubMed: 9108056.
35. Xiao C, Rajewsky K (2009) MicroRNA control in the immune system: basic principles. *Cell* 136: 26-36. doi:10.1016/j.cell.2008.12.027. PubMed: 19135886.
36. de Boer J, Williams A, Skavdis G, Harker N, Coles M et al. (2003) Transgenic mice with hematopoietic and lymphoid specific expression of Cre. *Eur J Immunol* 33: 314-325. doi:10.1002/immu.200310005. PubMed: 12548562.
37. Chung SH, Marzban H, Croci L, Consalez GG, Hawkes R (2008) Purkinje cell subtype specification in the cerebellar cortex: early B-cell factor 2 acts to repress the zebrin II-positive Purkinje cell phenotype. *Neuroscience* 153: 721-732. doi:10.1016/j.neuroscience.2008.01.090. PubMed: 18403128.
38. Kleinhammer A, Wurst W, Kühn R (2011) Constitutive and conditional RNAi transgenesis in mice. *Methods* 53: 430-436. doi:10.1016/j.ymeth.2010.12.015. PubMed: 21184828.
39. Kunath T, Gish G, Lickert H, Jones N, Pawson T et al. (2003) Transgenic RNA interference in ES cell-derived embryos recapitulates a genetic null phenotype. *Nat Biotechnol* 21: 559-561. doi:10.1038/nbt813. PubMed: 12679785.
40. Hemann MT, Fridman JS, Zilfou JT, Hernandez E, Paddison PJ et al. (2003) An epi-allelic series of p53 hypomorphs created by stable RNAi produces distinct tumor phenotypes in vivo. *Nat Genet* 33: 396-400. doi:10.1038/ng1091. PubMed: 12567186.
41. Hasuwa H, Kaseda K, Einarsdottir T, Okabe M (2002) Small interfering RNA and gene silencing in transgenic mice and rats. *FEBS Lett* 532: 227-230. doi:10.1016/S0014-5793(02)03680-3. PubMed: 12459495.
42. Rubinson DA, Dillon CP, Kwiatkowski AV, Sievers C, Yang L et al. (2003) A lentivirus-based system to functionally silence genes in primary mammalian cells, stem cells and transgenic mice by RNA interference. *Nat Genet* 33: 401-406. doi:10.1038/ng1117. PubMed: 12590264.
43. Carmell MA, Zhang L, Conklin DS, Hannon GJ, Rosenquist TA (2003) Germline transmission of RNAi in mice. *Nat Struct Biol* 10: 91-92. doi: 10.1038/nsb896. PubMed: 12536207.
44. Tiscornia G, Singer O, Ikawa M, Verma IM (2003) A general method for gene knockdown in mice by using lentiviral vectors expressing small interfering RNA. *Proc Natl Acad Sci U S A* 100: 1844-1848. doi: 10.1073/pnas.0437912100. PubMed: 12552109.
45. Coumoul X, Shukla V, Li C, Wang RH, Deng CX (2005) Conditional knockdown of Fgfr2 in mice using Cre-LoxP induced RNA interference. *Nucleic Acids Res* 33: e102. doi:10.1093/nar/gni100. PubMed: 15987787.
46. Ventura A, Meissner A, Dillon CP, McManus M, Sharp PA et al. (2004) Cre-lox-regulated conditional RNA interference from transgenes. *Proc Natl Acad Sci U S A* 101: 10380-10385. doi:10.1073/pnas.0403954101. PubMed: 15240889.
47. Chang HS, Lin CH, Chen YC, Yu WC (2004) Using siRNA technique to generate transgenic animals with spatiotemporal and conditional gene knockdown. *Am J Pathol* 165: 1535-1541. doi:10.1016/S0002-9440(10)63411-6. PubMed: 15509524.
48. Grimm D, Streetz KL, Jopling CL, Storm TA, Pandey K et al. (2006) Fatality in mice due to oversaturation of cellular microRNA/short hairpin RNA pathways. *Nature* 441: 537-541. doi:10.1038/nature04791. PubMed: 16724069.
49. Cai X, Hagedorn CH, Cullen BR (2004) Human microRNAs are processed from capped, polyadenylated transcripts that can also function as mRNAs. *RNA* 10: 1957-1966. doi:10.1261/ma.7135204. PubMed: 15525708.
50. Lee Y, Jeon K, Lee JT, Kim S, Kim VN (2002) MicroRNA maturation: stepwise processing and subcellular localization. *EMBO J* 21: 4663-4670. doi:10.1093/emboj/cdf476. PubMed: 12198168.
51. Zeng Y, Wagner EJ, Cullen BR (2002) Both natural and designed microRNAs can inhibit the expression of cognate mRNAs when expressed in human cells. *Mol Cell* 9: 1327-1333. doi:10.1016/S1097-2765(02)00541-5. PubMed: 12086629.
52. Dickens RA, McJunkin K, Hernandez E, Premrsirut PK, Krizhanovskiy V et al. (2007) Tissue-specific and reversible RNA interference in transgenic mice. *Nat Genet* 39: 914-921. doi:10.1038/ng2045. PubMed: 17572676.
53. McJunkin K, Mazurek A, Premrsirut PK, Zuber J, Dow LE et al. (2011) Reversible suppression of an essential gene in adult mice using transgenic RNA interference. *Proc Natl Acad Sci U S A* 108: 7113-7118. doi:10.1073/pnas.1104097108. PubMed: 21482754.
54. Premrsirut PK, Dow LE, Kim SY, Camiolo M, Malone CD et al. (2011) A rapid and scalable system for studying gene function in mice using conditional RNA interference. *Cell* 145: 145-158. doi:10.1016/j.cell.2011.03.012. PubMed: 21458673.
55. Tam W, Ben-Yehuda D, Hayward WS (1997) bic, a novel gene activated by proviral insertions in avian leukosis virus-induced lymphomas, is likely to function through its noncoding RNA. *Mol Cell Biol* 17: 1490-1502. PubMed: 9032277.
56. Tam W, Dahlberg JE (2006) miR-155/BIC as an oncogenic microRNA. *Genes Chromosomes Cancer* 45: 211-212. doi:10.1002/gcc.20282. PubMed: 16252262.
57. Medina MF, Joshi S (1999) RNA-polymerase III-driven expression cassettes in human gene therapy. *Curr Opin Mol Ther* 1: 580-594. PubMed: 11249665.
58. Casola S (2010) Mouse Models for miRNA Expression: The ROSA26 Locus. *Methods Mol Biol* 667: 145-163. doi: 10.1007/978-1-60761-811-9_10. PubMed: 20827532.
59. Fellmann C, Zuber J, McJunkin K, Chang K, Malone CD et al. (2011) Functional identification of optimized RNAi triggers using a massively parallel sensor assay. *Mol Cell* 41: 733-746. doi:10.1016/j.molcel.2011.02.008. PubMed: 21353615.
60. Reynolds A, Leake D, Boese Q, Scaringe S, Marshall WS et al. (2004) Rational siRNA design for RNA interference. *Nat Biotechnol* 22: 326-330. doi:10.1038/nbt936. PubMed: 14758366.
61. Tomari Y, Zamore PD (2005) Perspective: machines for RNAi. *Genes Dev* 19: 517-529. doi:10.1101/gad.1284105. PubMed: 15741316.
62. Schwarz DS, Hutvagner G, Du T, Xu Z, Aronin N et al. (2003) Asymmetry in the assembly of the RNAi enzyme complex. *Cell* 115: 199-208. doi:10.1016/S0092-8674(03)00759-1. PubMed: 14567917.
63. Sambrook J, Fritsch EF, Maniatis T (1989) *Molecular cloning : a laboratory manual*. Cold Spring Harbor, NY: Cold Spring Harbor Laboratory. Getr. Zählung. p. 2

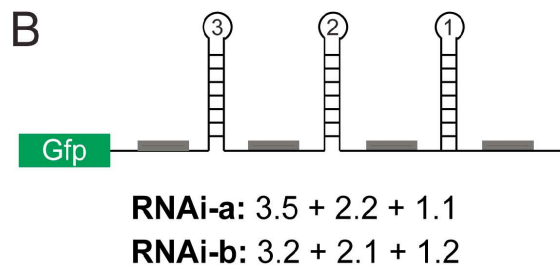
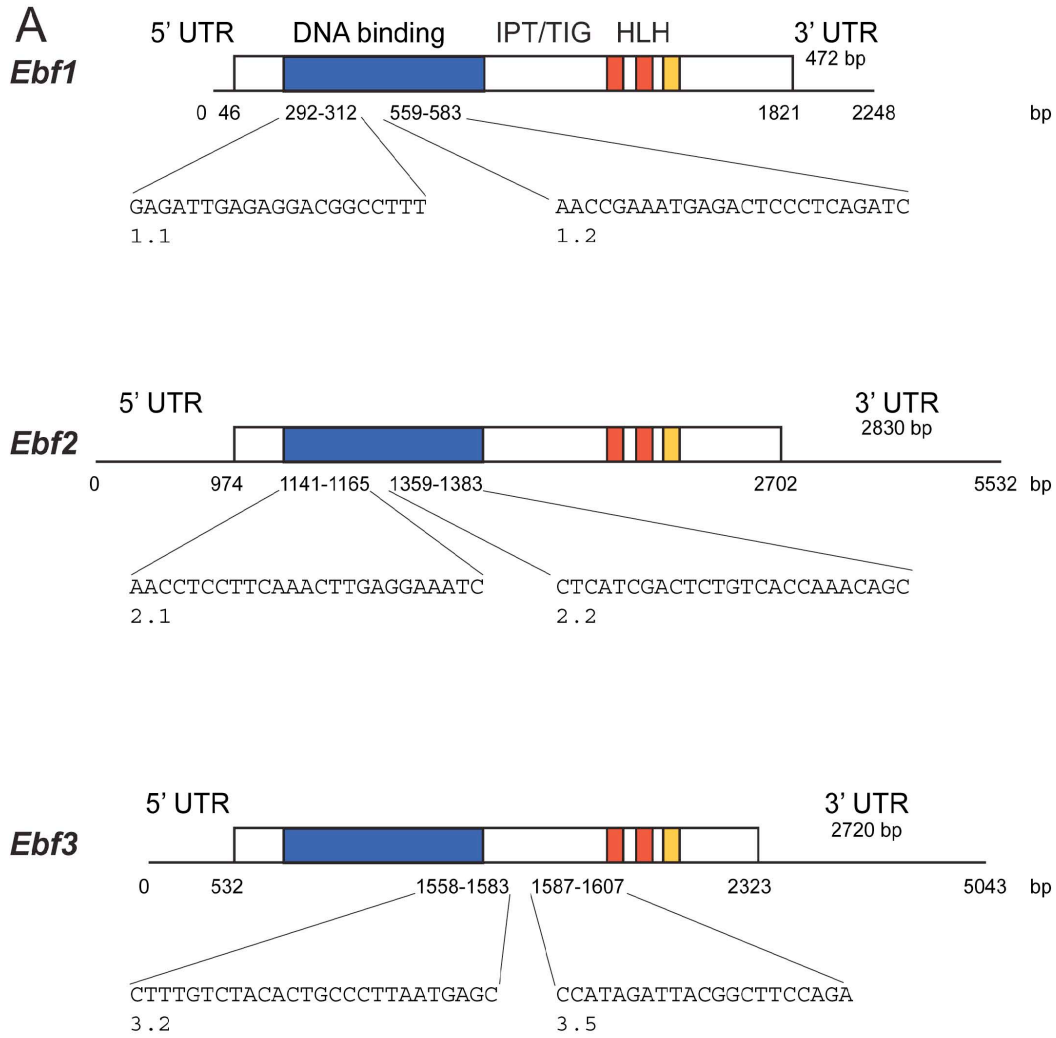
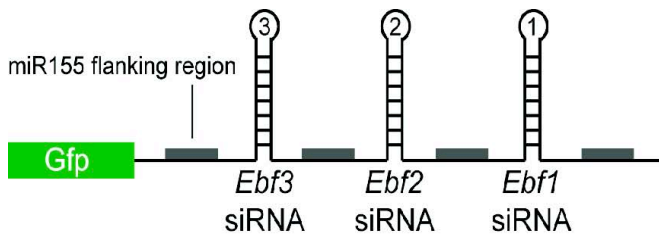


Figure S1.



RNAi-a: 3.5 + 2.2 + 1.1

RNAi-b: 3.2 + 2.1 + 1.2

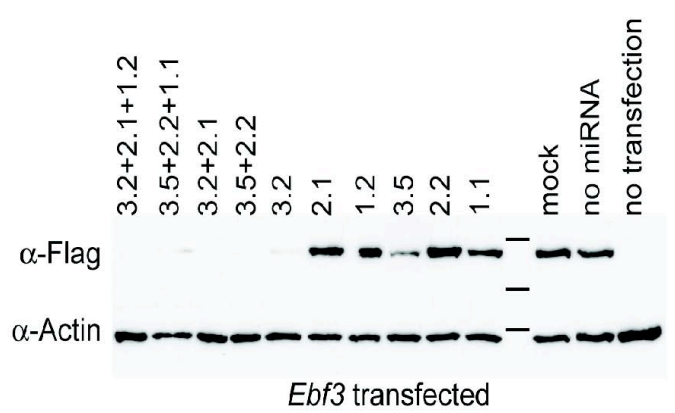
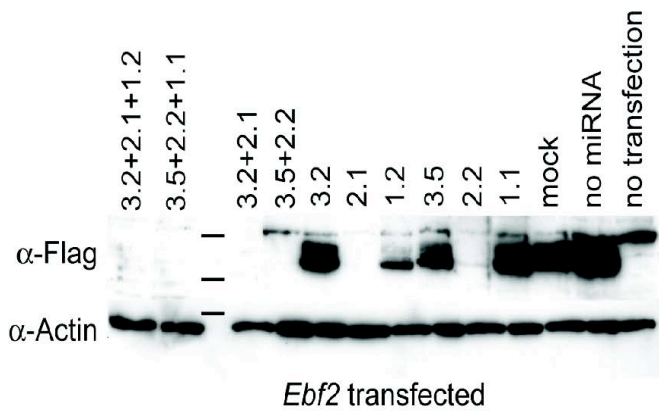
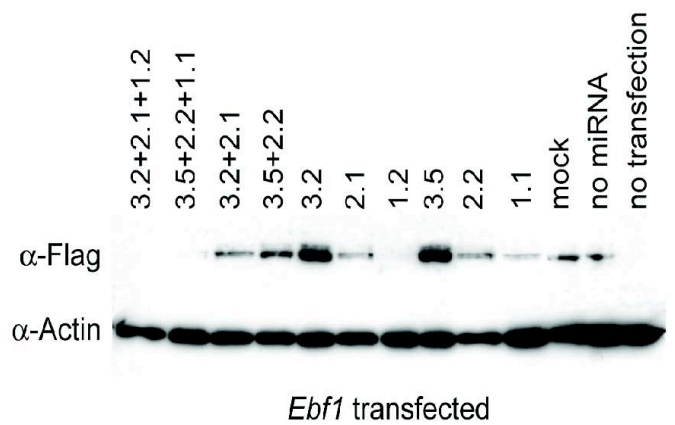


Figure S2.

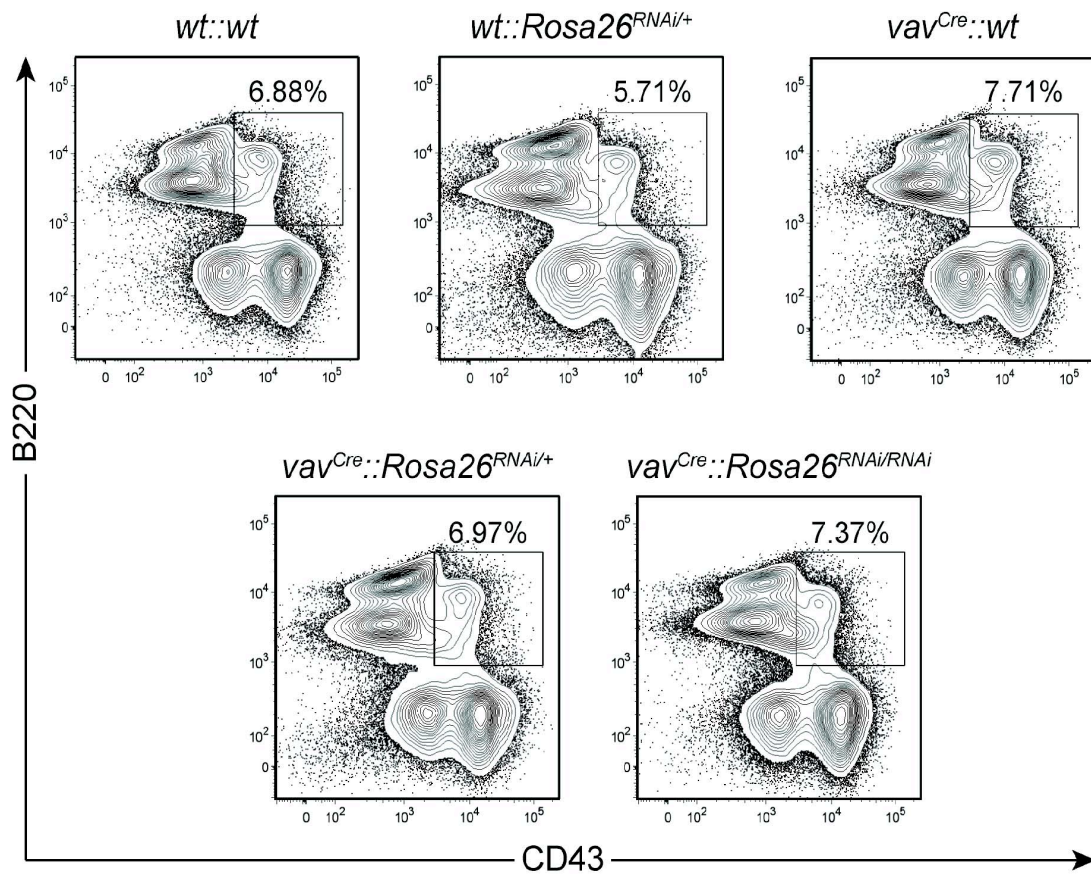


Figure S3.

Supporting Information

Figure S1.

Schematic overview of the DNA sequences used for RNAi. (A) The structure of the transcripts of Ebf1, Ebf2 and Ebf3 is depicted including 5'- and 3'-UTR. Protein domains encoded by the transcripts are indicated above (HLH = helix-loop-helix domain) and the beginning and end of the coding sequence are given underneath in base pairs relative to the start site. The sequences used to inhibit the individual members and their positions are plotted against the transcripts. Two sequences are indicated for each gene, as two different RNAi constructs have been generated, and their identifying numbers are given underneath. (B) Schematic representation of the organisation of the RNAi used for the transgene. Grey boxes represent the flanking region from miR155, and the numbers within the loops indicate the Ebf gene against which the sequences at this position are directed. The composition of the two constructs used for RNAi is given below.
doi:10.1371/journal.pone.0080312.s001

Figure S2.

Down-regulation of Ebf1, Ebf2 and Ebf3 by a single RNAi construct. To analyse the efficiency and specificity of bioinformatically predicted sequences to down-regulate the expression of Ebf1, Ebf2 and Ebf3, HEK293T cells were transfected with expression plasmids encoding the individual Ebf proteins together with an N-terminal Flag tag. Expression vectors containing the shRNA sequences either alone or in combination were co-transfected, and 48 h after transfection cells were harvested and analysed by Western blot. α -Flag antibody was used to detect Ebf expression levels, and α -actin as loading control. Mock is referring to a co-transfection of the empty parental vector (pcDNA6.2-GW/EmGFP), no RNAi leaves out the shRNA containing vectors.
doi:10.1371/journal.pone.0080312.s002

Figure S3.

Analysis of B cell fractions A - C in *Rosa26^{RNAi}* transgenic mice. Single cell suspensions from bone marrow of mice with the indicated genotypes were analysed for the percentage of early B cell fractions. Cells were stained with propidium iodide, B220, CD43, and gated for FSC/SSC and as PI negative, and B220 CD43 double positive. The gating window and the percentage of cells are shown. Cells were further stained for BP-1 and HSA/CD24, and analysed for fractions A - C in detail (Figure 4). Representative examples of the indicated genotypes are shown. The statistical analysis of fraction A - C in Figure 4B is referring to this setting. doi:10.1371/journal.pone.0080312.s003

ARTICLE

Received 12 Feb 2014 | Accepted 2 Apr 2014 | Published 2 May 2014

DOI: 10.1038/ncomms4793

Ebf factors and MyoD cooperate to regulate muscle relaxation via *Atp2a1*

Saihong Jin¹, Jeehee Kim¹, Torsten Willert¹, Tanja Klein-Rodewald², Mario Garcia-Dominguez^{3,4}, Matias Mosqueira⁵, Rainer Fink⁵, Irene Esposito^{2,6}, Lorenz C. Hofbauer⁷, Patrick Charnay³ & Matthias Kieslinger¹

Myogenic regulatory factors such as MyoD and Myf5 lie at the core of vertebrate muscle differentiation. However, E-boxes, the cognate binding sites for these transcription factors, are not restricted to the promoters/enhancers of muscle cell-specific genes. Thus, the specificity in myogenic transcription is poorly defined. Here we describe the transcription factor Ebf3 as a new determinant of muscle cell-specific transcription. In the absence of *Ebf3* the lung does not unfold at birth, resulting in respiratory failure and perinatal death. This is due to a hypercontractile diaphragm with impaired Ca^{2+} efflux-related muscle functions. Expression of the Ca^{2+} pump *Serca1* (*Atp2a1*) is downregulated in the absence of Ebf3, and its transgenic expression rescues this phenotype. Ebf3 binds directly to the promoter of *Atp2a1* and synergises with MyoD in the induction of *Atp2a1*. In skeletal muscle, the homologous family member *Ebf1* is strongly expressed and together with MyoD induces *Atp2a1*. Thus, Ebf3 is a new regulator of terminal muscle differentiation in the diaphragm, and Ebf factors cooperate with MyoD in the induction of muscle-specific genes.

¹Institute of Clinical Molecular Biology and Tumor Genetics, Helmholtz Zentrum München, National Research Center for Environmental Health, Marchioninistrasse 25, 81377 Munich, Germany. ²Institute of Pathology, Helmholtz Zentrum München, National Research Center for Environmental Health, Ingolstädter Landstr. 1, 85764 Neuherberg, 81377 Munich, Germany. ³Developmental Biology Section, Ecole Normale Supérieure, Rue d'Ulm 46, 75230 Paris, France. ⁴Stem Cells Department, CABIMER (CISC), Av Américo Vespucio, 41092 Sevilla, Spain. ⁵Medical Biophysics Unit, Institute of Physiology and Pathophysiology, University of Heidelberg, Im Neuenheimer Feld 326, 69120 Heidelberg, Germany. ⁶Institute of Pathology, Technische Universität München, Ismaningerstrasse 22, 81675 Munich, Germany. ⁷Division of Endocrinology, Diabetes and Metabolic Bone Diseases, Department of Medicine III, TU Dresden Medical Center, Fetscherstrasse 74, 01307 Dresden, Germany. Correspondence and requests for materials should be addressed to M.K. (email: matthias.kieslinger@helmholtz-muenchen.de).

Muscle cells in the body of vertebrates specify and differentiate from mesenchymal progenitor cells in the somites¹. This process is initiated by the combined action of the transcription factors Pax3 and Pax7 (ref. 2). Together with the myogenic regulatory factors (MRF) Myf5 and MyoD they form a regulatory network that is central to all early muscle cell differentiation^{3,4}. Once immature myoblasts have formed, they fuse to generate multinucleated mature muscle cells or myotubes, which constitute the minimal functional unit of all muscles in the body. The transcription factors Myogenin and Mrf4 regulate the later steps of differentiation by influencing the expression of muscle-specific genes encoding contractile proteins in fast and slow twitch fibres⁵. Contraction of skeletal muscles is achieved via the influx of Ca²⁺ into the cytosol and its interaction with Troponin C, triggering the ATP-dependent sliding of α -actin and myosin filaments along each other. For relaxation, Ca²⁺ is actively removed from the cytosol into the sarcoplasmic reticulum by Serca proteins, which are ATP-dependent Ca²⁺-specific ion pumps^{5,6}.

All MRF proteins bind to E-box sequences that are present in the enhancers or promoters of genes coding for most muscle contractile proteins⁴ and also a great many that are not related to muscle-specific genes⁷. Genome-wide Chromatin immunoprecipitation (ChIP)-seq analysis revealed that MyoD binds to a large number of E-boxes including non muscle-specific ones⁸. Therefore, additional transcription factors are required to regulate MRF specificity for particular target genes. Mef2 is such an example, as it binds to sites often present in contractile protein enhancers and interacts cooperatively with MRFs^{9,10}.

Among the skeletal muscles, the diaphragm is one of the most essential ones, separating the pleural and abdominal body cavities. It consists of two different muscles, the crural muscle, which has a central and dorsal location surrounding the oesophagus and aorta, and the costal muscle, which connects the diaphragm's central tendon to the surrounding ribs. During embryonic development, muscle progenitor cells migrate from cervical somites to the pleuroperitoneal folds, transient structures surrounding the oesophagus¹¹. These are assumed to fuse with the septum transversum, which is thought to give rise to the central tendon. Many important aspects of diaphragm development are still unclear, despite its requirement for the unfolding of the lung at birth and subsequent respiration¹².

The family of *early B cell factor* (*Ebf*) genes encodes a highly homologous group of transcription factors consisting of four members in mammals. The proteins possess a N-terminal DNA-binding domain, which also harbours transactivation potential, followed by an IPT/TIG (immunoglobulin, plexins, transcription factors-like/transcription factor immunoglobulin) domain, presumably mediating protein-protein interaction, and an atypical helix-loop-helix domain required for the formation of homo- and heterodimers. A transactivation domain (TAD) at the C terminus mediates activation of Ebf target genes^{13,14}. As all four proteins share over 90% sequence homology within these domains, except for the TAD, all Ebf proteins bind to the same DNA sequence and can act redundantly^{15–17}.

Ebf3 is a member of this protein family that is poorly characterized compared with other Ebf factors. Originally identified in neuronal cells^{18,19}, *Ebf3* is important for cell migration in the developing cortex¹⁷ and in the projection of olfactory neurons to the olfactory bulb¹⁶. In *Xenopus* the homologue *Xebf3* acts as a regulator of neuronal differentiation downstream of *XNeuroD*²⁰. Furthermore, *Ebf3* has been implicated as a negative regulator of cell proliferation²¹. Ectopic expression suppresses proliferation and induces apoptosis of tumour cell lines²² and *Ebf3* was found to be silenced in most high-grade brain tumour cases in a genome-wide screen

for tumour suppressors²³. Silencing of *Ebf3* via promoter methylation was also observed in gastric cancer, and ectopic expression induced cell cycle arrest and apoptosis²⁴.

Here, we present evidence that mammalian muscle cells express *Ebf3*. Its function is critical in the relaxation of muscle fibres of the diaphragm and essential to allow respiration immediately after birth preventing postnatal lethality. Ebf3 synergises with MyoD in directly regulating the expression of a Ca²⁺ pump necessary for muscle relaxation. Thereby, Ebf3 is a new transcription factor involved in the regulation of muscle cell-specific transcription.

Results

Expression of Ebf3. To analyse the biological role of *Ebf3*, we disrupted its gene locus in murine ES cells. Therefore, a targeting vector was constructed in which an *NLS-lacZ* gene and a *PGK::neo* cassette, flanked by *loxP* sites, were cloned in frame after the translational start codon of *Ebf3*, replacing the first four exons of *Ebf3* (Supplementary Fig. 1A). These exons (representing the first 138 amino acids) encode for essential parts of the DNA-binding and transactivation domain of Ebf3 (ref. 19). Two out of 800 clones of mouse embryonic stem cells analysed had correctly incorporated the targeting construction (clones #1 and #2; Supplementary Fig. 1B). Analysis of genomic DNA from E18.5 embryos from heterozygous matings by PCR revealed the presence of all three possible genotypes (Supplementary Fig. 1C; primers indicated in Supplementary Fig. 1A). To confirm the disruption of *Ebf3* independently of the genomic status, semiquantitative RT-PCR was performed, revealing the loss of the *Ebf3* transcript in bones of embryonic day (E)18.5 embryos (Supplementary Fig. 1D).

As a first step in the biological analysis of Ebf3, we determined its expression during embryonic development. Initial but low expression of *Ebf3* can be detected in the second branchial arch around E8.5 (Supplementary Fig. 3A). Although somites are present at this stage, *Ebf3* is expressed in these structures only later, at around E9.0 (Supplementary Fig. 3B). In the following stages, the expression of *Ebf3* becomes more complex with prominent sites in the midbrain, the branchial arches, the dorsal root ganglia and the olfactory epithelium (Supplementary Fig. 2). To analyse the expression of *Ebf3* independently, qPCR was performed on whole wild-type embryos between E7.5 and E18.5 (Supplementary Fig. 3C). In this approach, *Ebf3* is first detectable at E9.5, strongly increases at E10.5, and is present throughout embryonic development thereafter with a pronounced decrease at E15.5 and E16.5. These results confirm data from EST databases, which list *Ebf3* expression from E9.5 on, and are also in line with the β -gal staining shown here, with the only exception that the very first expression was probably below the detection limit in the settings used for qPCR. Furthermore, the data show that the loss of *Ebf3* does not alter overall morphology during embryonic development (Fig. 1a–c and Supplementary Fig. 2). A more detailed analysis of tissues and cells in E16.5 embryos reveals prominent expression of *Ebf3* in neuronal structures such as the midbrain, the cerebellar primordium and the mantle layer of the spinal cord (Fig. 1b). Strong expression is also observed in the olfactory epithelium, adipose tissue and at sites of skeletogenesis such as ribs and vertebrae. Moreover, expression is seen in developing skeletal muscle tissues like the diaphragm and in the limbs. Again, no developmental defects were observed in the absence of *Ebf3* (Fig. 1c). Staining of E16.5 wild-type embryos indicates the specificity of the observed signals except for the inner lumen of the duodenum (Fig. 1a). To quantify the expression of *Ebf3* in various tissues, we isolated different organs of E18.5 embryonic and 3-week-old wild-type mice and analysed

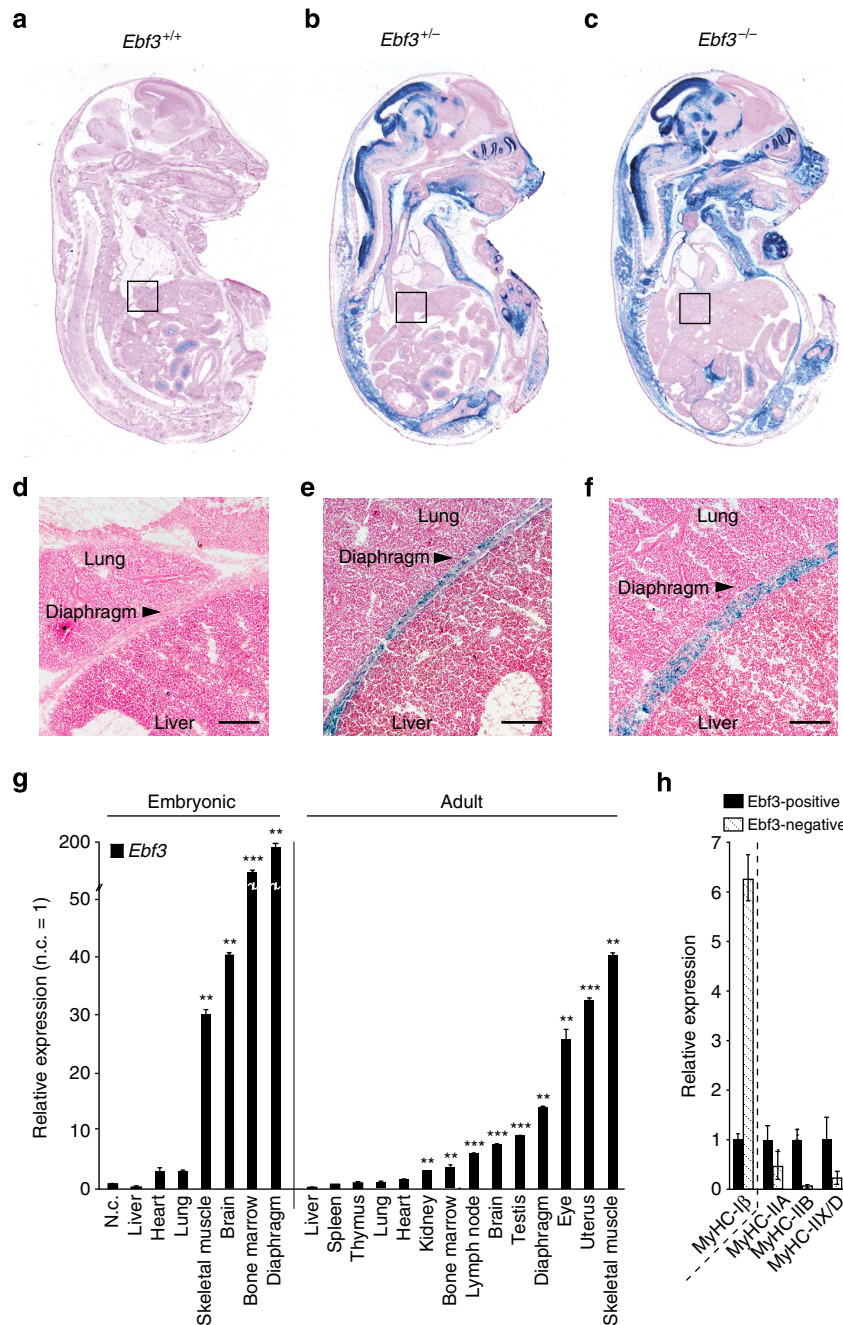


Figure 1 | Expression of *Ebf3* at sites of osteogenesis and muscle formation. (a–c) Staining for β -galactosidase in cryosections of E16.5 *Ebf3*^{+/+} (a), *Ebf3*^{+/-} (b) and *Ebf3*^{-/-} (c) embryos. *Ebf3*- β -gal-positive cells can be detected in neuronal, olfactory and adipocytic tissues and at sites of osteogenesis and muscle formation. Staining in the lumen of the duodenum is background. (d–f) Magnification of *Ebf3*- β -gal staining in the area surrounding parts of the diaphragm in *Ebf3*^{+/+} (d), *Ebf3*^{+/-} (e) and *Ebf3*^{-/-} (f) embryos as indicated by black boxes in a–c. The diaphragm in this magnification is surrounded by the lung and liver tissue as indicated. Bar, 100 μ m. (g) Quantitative PCR analysis of the expression of *Ebf3* in various tissues of wild-type E18.5 embryos (left) or adult animals (right). The pro-B cell line Ba/F3 was used as a negative control and set to 1. *n* = 3; error bars = s.d. Significance is calculated in comparison with Ba/F3. ***P* < 0.01, ****P* < 0.001. (h) Single-cell suspensions from the diaphragm of E18.5 *Ebf3*^{+/-} embryos were sorted into *Ebf3*- β -gal-positive and -negative cells and subjected to expression analysis of the indicated marker genes for slow (MyHC- β) and fast (MyHC-IIa, MyHC-IIb, MyHC-IIx/D) twitch muscle types by qPCR. *n* = 3; error bars = s.d., **P* < 0.05 ***P* < 0.01.

them by qPCR. Accordingly *Ebf3* shows the highest expression in the diaphragm, followed by bone marrow, brain and skeletal muscle in the embryo (Fig. 1g). Adult mice express *Ebf3* at the highest levels in skeletal muscle followed by the uterus, eye and diaphragm. Intermediate expression levels can be detected in the eye, testis, brain and lymph node, and low expression is seen in the bone marrow and kidney. No expression of *Ebf3* was

detected in the lung, thymus, spleen, liver and heart (Fig. 1g). As diaphragm showed the highest expression among all organs and tissues examined, we analysed its expression in further details using *in situ* detection of β -galactosidase activity. *Ebf3* expression delineates the diaphragm at E18.5, is expressed in the majority, but not all cells (Fig. 1e), and is specific in comparison with wild type (Fig. 1d). Deletion of one or both alleles of *Ebf3* does

not change overall morphology, but seems to induce a slightly thickened appearance of the diaphragm (Fig. 1f). The diaphragm consists of ~10% type I (slow twitch) and 90% type II (fast twitch) fibres, which can be distinguished by the expression of different isoforms of the myosin heavy chain^{25,26}. *Ebf3* is strongly enriched in cells expressing the type II-associated isoforms MyHC-IIa, MyHC-IIb and MyHC-IIx/D, whereas the type I-associated MyHC-I β prevails in *Ebf3*-negative cells, indicating that *Ebf3* is preferentially expressed by type II or fast twitch fibres (Fig. 1h).

Deletion of *Ebf3* leads to respiratory failure. Embryonic development proceeds normally in the absence of *Ebf3*, and, to define the biological role of *Ebf3* postnatally, we evaluated genotypes from offspring of heterozygous matings at various time points after birth. From postnatal day 0.5 (D0.5) on, we could not detect any *Ebf3*-deficient mice (Fig. 2a), and therefore analysed earlier time points observing a normal Mendelian ratio of wild type, heterozygous and knock-out embryos at E18.5 (Fig. 2a). This finding suggests lethality around birth, and indeed a close observation of animals at birth revealed that pups were born alive, and *Ebf3*^{-/-} mice were indistinguishable from wild-type and heterozygous littermates in their overall appearance. However, immediately after birth, *Ebf3*-deficient mice displayed gasping respiration and progressive cyanosis (Fig. 2b), and died within 0.5 to 2 h after birth. Examination of wild-type newborn mice showed that the lungs are unfolded and have a normal appearance of alveolar ductal lumens, alveoli and small pulmonary vessels (Fig. 2c–e, upper row). In contrast, lungs from *Ebf3*^{-/-} mice have a congested appearance, do not unfold, and in consequence air-containing passages are not formed as in wild-type lungs (Fig. 2c–e, lower row). This result suggests that the postnatal lethality and the cyanotic appearance are very likely due to respiratory failure caused by an inability to unfold the lung at birth. However, it seems to be a secondary effect, as *Ebf3* is not expressed in the lung (Fig. 1a–g), the morphology of the compact lung is normal (Fig. 2c–e, lower row) and unfolding is not a lung-intrinsic property.

The diaphragm and the rib cage are necessary to support lung function and breathing, and muscle cells of the diaphragm strongly express *Ebf3* (Fig. 1g). As osteoblastic cells express *Ebf3* during *in vitro* differentiation²⁷, we examined the expression of *Ebf3* in bone and bone marrow *in vivo* to elucidate its role in skeletogenesis and bone formation. The bone marrow is a complex mixture of various cell types, and haematopoietic cells do not express *Ebf3* as shown by *Ebf3*- β -gal staining (Supplementary Fig. 5A) or by semiquantitative RT-PCR of E18.5 fetal liver cells (Supplementary Fig. 5B). As primary *Ebf3*-positive mesenchymal cells of the bone marrow express high levels of *Scleraxis*, *aP2* and *Prx1*, but no markers of chondrocytes or mature osteoblasts (Supplementary Fig. 4A), we conclude that *Ebf3* is expressed by immature mesenchymal cells, including mesenchymal stem cells, skeletal progenitors and adipocytes. A slight increase in CFU-F numbers, that is, in the frequency of immature mesenchymal cells of the bone marrow, was observed (Supplementary Fig. 4B), but loss of *Ebf3* has no effect on the formation of bone and cartilage as exemplified by Alcian blue/Alizarin red staining of E18.5 embryos (Fig. 2f) or at various other developmental stages (Supplementary Fig. 4C). In addition, analysis of calcified mineral bone by von Kossa staining revealed no differences in the absence of *Ebf3* (Supplementary Fig. 4D). Furthermore, no defects in fetal haematopoiesis were observed (Supplementary Fig. 5C). In contrast, thickening of muscle fibres was observed in the diaphragm of *Ebf3*^{-/-} newborn mice, suggesting that deletion of *Ebf3* might cause defects in muscle function (Fig. 2g,h).

Defects in diaphragm contraction in absence of *Ebf3*. As the diaphragm has a central role in facilitating the unfolding of the lung and supporting breathing after birth²⁸, we followed this observation closer. Electron microscopy revealed hypercontracted regions within the diaphragm in the absence of *Ebf3* and a shortening of Z-stacks (Fig. 3A,B). Within these regions, sarcomere length was reduced 38% from 2.11 μ m in wild-type diaphragm to about 1.34 μ m in *Ebf3*^{-/-} newborn mice (Fig. 3C). The phenotype described so far indicates problems with the relaxation of muscle cells in the absence of *Ebf3*. To study potential defects in muscle function in more detail, we isolated the diaphragm from *Ebf3* wild-type and mutant newborn animals and analysed their reaction to defined electrical stimulation. In a first set of experiments the diaphragm was electrically stimulated with a single pulse of 50 V for 1 ms. Measurement of the resulting twitch shows that the force produced by the *Ebf3*-deficient diaphragm was reduced by a factor of 18 compared with wild-type levels (Fig. 3D). The total duration of the contraction in response to a single stimulation was prolonged 11.6-fold (Fig. 3E). As muscle function normally involves sustained activation, we also measured the same parameters during tetanus stimulation of the isolated diaphragm (50 V, 1 ms, 120 Hz for 500 ms; Supplementary Fig. 6A,B). The force produced in response to tetanus stimulation was reduced by a factor of 3.6 (Supplementary Fig. 6A), confirming data from the single stimulation experiment. Furthermore, the full duration of the contraction after tetanus stimulation was prolonged 23-fold (Supplementary Fig. 6B). Taken together, the results indicate a strongly reduced force produced by the diaphragm in response to stimulation, which explains the missing expansion of the lung in *Ebf3*-deficient mice and the resulting failure of respiration and cyanotic death. Furthermore, the fact that the muscle can be stimulated, but the duration of the contraction is strongly prolonged, suggests an impairment in muscle relaxation after stimulation.

***Ebf3* is required for expression of *Atp2a1*.** To gain an understanding of the molecular mechanism behind this deficiency, we analysed the expression of genes implicated in muscle contraction and relaxation in the diaphragm of E18.5 wild-type and *Ebf3*-deficient mice. The vast majority of these candidate genes did not show differences in expression in absence of *Ebf3* (Fig. 3F). A slight but significant decrease was observed with *Mlc1f*, *Tnni2* and skeletal muscle-specific α -actin, which are all required for contraction as well as relaxation. Interestingly, the expression of *Atp2a1*, which encodes a sarcoplasmic reticulum Ca²⁺-ATPase required for muscle relaxation, was decreased by a factor of ~10, and *Ebf3*-deficient mice display an almost exact phenocopy of the deletion of the *Atp2a1* gene²⁹. As not all cells of the diaphragm express *Ebf3* (Fig. 1e,f), we sorted *Ebf3*- β -gal-expressing cells from the diaphragm by flow cytometry from *Ebf3*^{+/-} and *Ebf3*^{-/-} mice. In heterozygous cells *Ebf3* was detected almost exclusively in the β -gal-positive population, showing a high level of purification by this method (Fig. 3G). *Atp2a1* is a marker for fast twitch muscle cells and was strongly enriched among the *Ebf3*- β -gal-positive cells in *Ebf3*^{+/-} animals, confirming our previous finding that *Ebf3*-expressing cells constitute most, if not all, fast twitch type muscle cells of the diaphragm (Fig. 1h). In *Ebf3*-deficient cells this expression, and thereby the vast majority of overall *Atp2a1* expression, was reduced to undetectable levels, whereas a minor level among *Ebf3*- β -gal-negative cells remained unchanged, indicating a cell-autonomous defect. As expected, *Ebf3* expression was reduced to background levels in *Ebf3*-deficient cells (Fig. 3G).

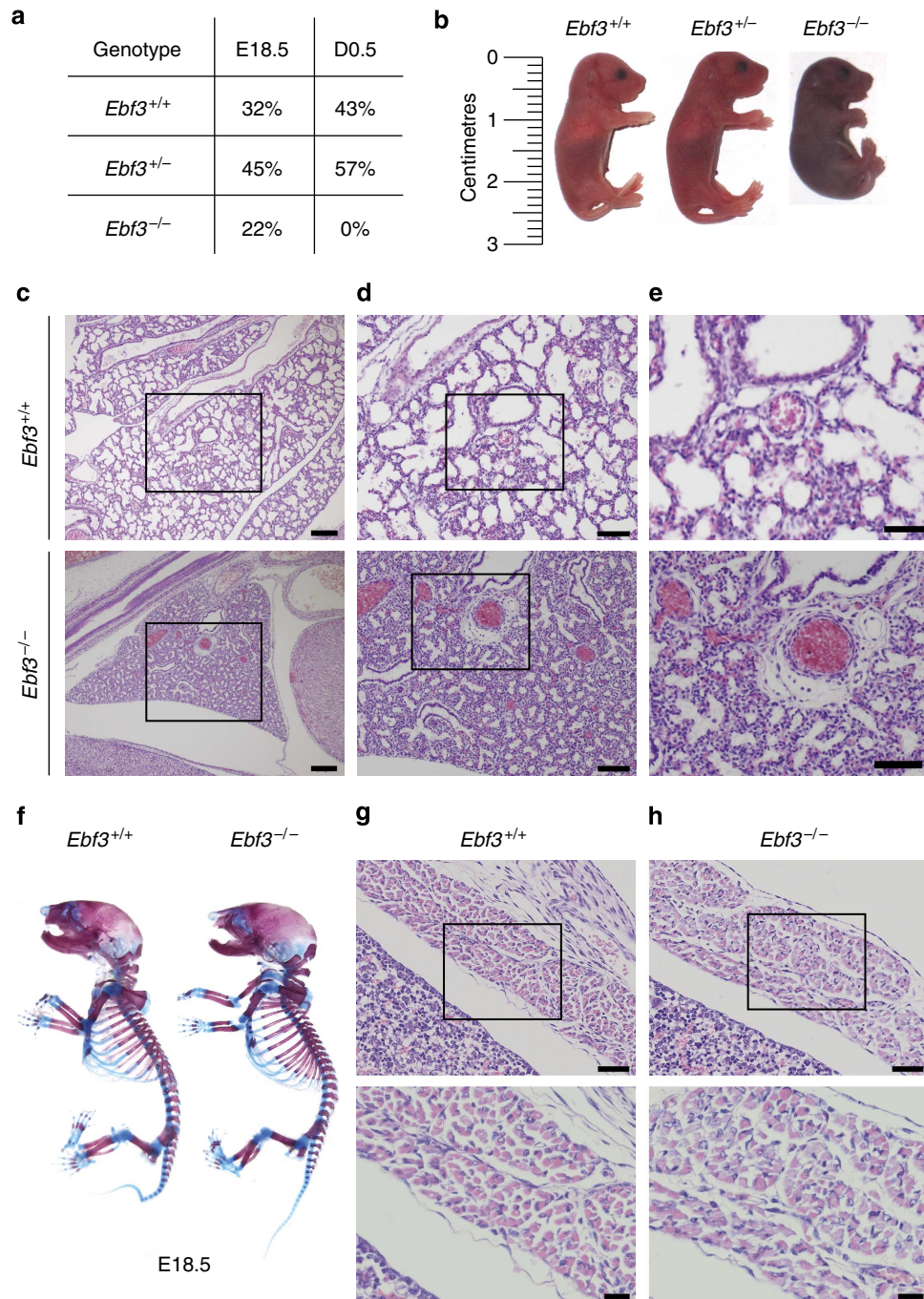


Figure 2 | Deletion of *Ebf3* leads to respiratory failure, postnatal death and alterations in muscle morphology. (a) Frequencies of *Ebf3* wild-type and mutant genotypes before and after birth. No *Ebf3*-deficient mice can be detected 12 h after birth; E18.5: $n = 415$, D0.5: $n = 58$. (b) Comparison of wild-type (left), *Ebf3*-heterozygous (middle) and *Ebf3*-deficient (right) newborn mice shortly after birth. Length is indicated in centimetres. (c–e) Histological analysis of longitudinal sections of the lung of wild-type (upper row) and *Ebf3*-deficient (lower row) newborn mice stained with haematoxylin/eosin. **d** and **e** are increasing magnifications as indicated by the insets. Bar, **c**: 200 μm ; **d**: 100 μm ; **e**: 50 μm . (f) Alcian blue/alizarin red staining of cartilage and bone of wild-type or *Ebf3*^{-/-} skeletons at E18.5. (g,h) Cross-sections of diaphragm muscle fibres of newborn wild-type (g) or *Ebf3*-deficient (h) mice stained with haematoxylin/eosin. Lower panels are higher magnifications as indicated by the inset in the upper panels. Bars, upper panels: 50 μm ; lower panels: 20 μm .

To evaluate whether compensatory mechanisms are active, or whether other members of the *Atp2a* gene family are also affected by the deletion of *Ebf3*, we analysed the diaphragms of E18.5 mice as described²⁹. Loss of *Ebf3* reduced not only *Atp2a1a* and *Atp2a1b*, the two isoforms of *Atp2a1*, but also *Atp2a2* by a factor of 7.5 and its two isoforms *Atp2a2a* and *Atp2a2b* by a factor of 73 and 14, respectively

(Supplementary Fig. 6E). Conversely, *Atp2a3*, the third gene of this family, showed a slight but significant upregulation in absence of *Ebf3* (Supplementary Fig. 6E). Taken together, loss of *Ebf3* leads to a decrease in the expression of the *Atp2a1* and *Atp2a2* genes and their isoforms, whereas *Atp2a3* shows a minor upregulation. The product of the *Atp2a1* gene is the Serca1 protein, which has a size of 110 kDa. In *Ebf3*-deficient

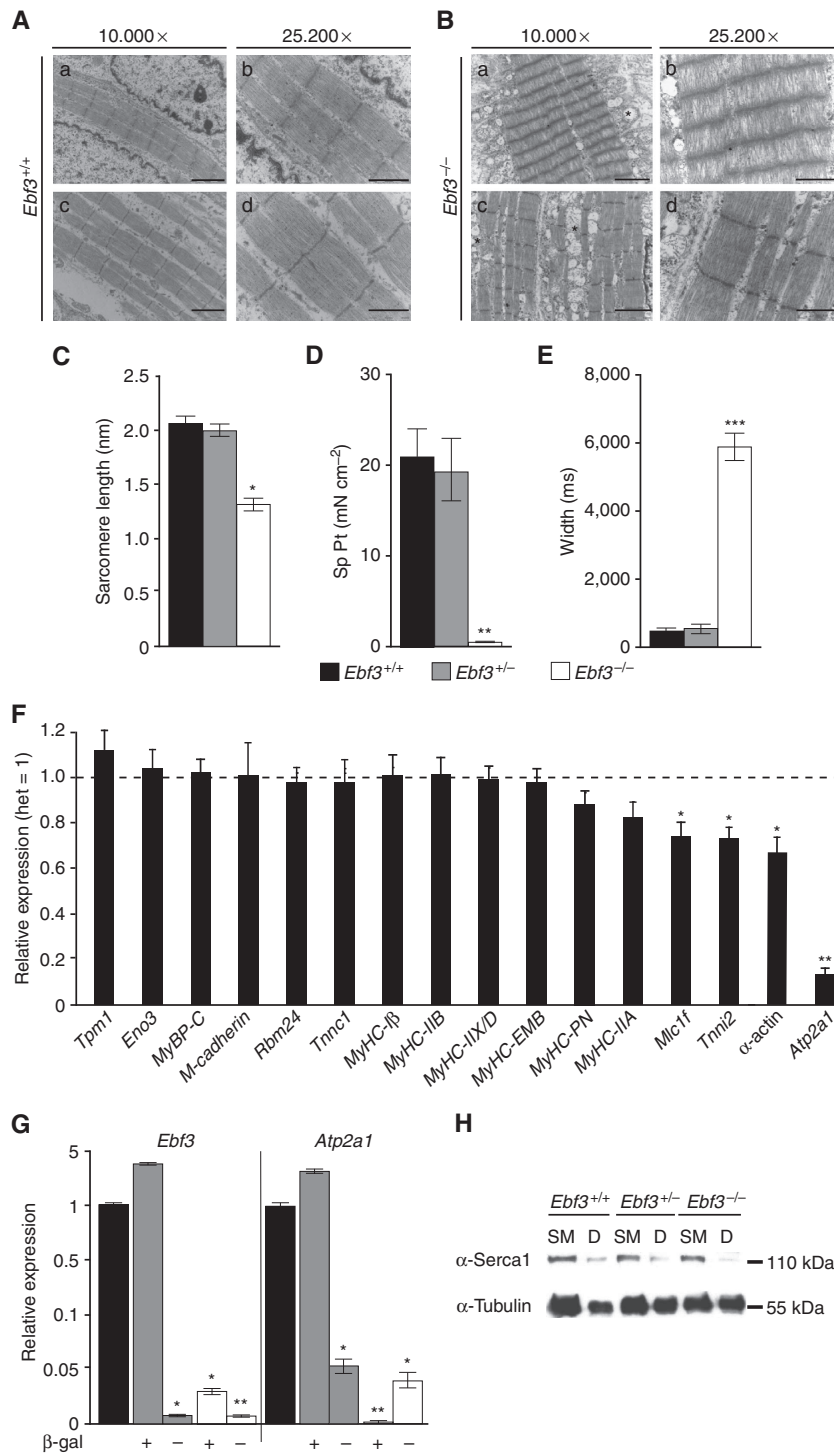


Figure 3 | Deletion of *Ebf3* impairs muscle relaxation and expression of *Atp2a1*. (A,B) Analysis of the ultrastructure of muscle fibres of the diaphragm by electron microscopy of wild-type (a) and *Ebf3*-deficient (b) newborn mice. Representative electron microscopy pictures of sarcomeres showing myofilaments at 10.000 × (bar, 2.5 nm) and 25.200 × magnification (bar, 1 nm); b shows hypercontracted myofibres. (C) Determination of sarcomere length in the diaphragm of *Ebf3*^{+/+}, *Ebf3*^{+/-} and *Ebf3*^{-/-} newborn mice. *n* = 3; error bars = s.d.; **P* < 0.05. (D,E) Single twitch stimulation (50 V, 1 ms) of diaphragm muscle from newborn mice of the indicated genotypes. (D) Measurement of single twitch normalized to the cross-sectional area, representing muscle force in response to the stimulation. (E) Total duration of muscle contraction after single twitch stimulation. *n* = 5 *Ebf3*^{+/+}, *n* = 7 *Ebf3*^{+/-}, *n* = 4 *Ebf3*^{-/-}; error bars = s.d.; **P* < 0.05, ***P* < 0.01, ****P* < 0.001. (F) *Ebf3*-β-gal-expressing cells were isolated from the diaphragm of E18.5 *Ebf3*^{+/-} embryos by flow cytometry and analysed for the expression of the indicated genes by qPCR. Expression in *Ebf3*^{+/-} cells was set to 1 and relative expression in *Ebf3*^{-/-} cells is shown. *n* = 3, **P* < 0.05, ***P* < 0.01. (G) Cells of the diaphragm of E18.5 animals were sorted as positive or negative for the expression of *Ebf3*-β-gal and analysed by quantitative PCR for the expression of *Ebf3* and *Atp2a1*. Unsorted cells of wild-type diaphragm were used as control and set to 1; *n* = 3, **P* < 0.05, ***P* < 0.01. (H) Representative western blot analysis of Serca1 expression in skeletal muscle (SM) and diaphragm (D) of E18.5 embryos of the indicated genotypes; *n* = 3. In all PCR experiments, values are normalized to wild-type levels, error bars represent s.d., and *P*-values were calculated in comparison to the wild-type control.

diaphragm, the protein was barely detectable and thus strongly reduced in comparison with wild-type levels (Fig. 3H). Quantification of the protein levels indicated a reduction of Serca1 in *Ebf3*-deficient diaphragm by a factor of 3.2. In contrast, Serca1 from skeletal muscle did not show a significant reduction in *Ebf3*^{-/-} diaphragm compared with *Ebf3*^{+/+}.

***Atp2a1* rescues *Ebf3*-dependent respiratory failure.** Since *Ebf3*^{-/-} mice phenocopy *Atp2a1*-deficient mice and the expression of *Atp2a1* is strongly downregulated in the absence of *Ebf3*, we wanted to determine the importance of *Atp2a1* as a downstream target of *Ebf3*. Transgenic animals expressing *Atp2a1* under the control of the skeletal muscle-specific skeletal α -actin promoter have been reported³⁰. These mice show transgenic expression in skeletal muscles including the diaphragm, but do not have any overt phenotype on their own, allowing us to genetically assess the biological relevance of *Atp2a1* as an *Ebf3* target gene *in vivo*. Genotyping of litters from *Ebf3*^{+/-}/*Atp2a1*^{tg} double-heterozygous crossings revealed a 50% distribution of the *Atp2a1* transgene as expected (Fig. 4a) from the breeding scheme (Supplementary Fig. 7). Among the *Atp2a1* wild-type animals, the frequency of *Ebf3*^{+/+}, *Ebf3*^{+/-} and *Ebf3*^{-/-} corresponds to the frequency observed previously before and after birth (Fig. 4a, left panel). In the presence of the *Atp2a1* transgene, the ratio of *Ebf3*^{-/-} mice at E18.5 surprisingly is not 12.5% as would be expected as a normal Mendelian ratio but 3%, indicating either a genetic interference between *Ebf3* and the *Atp2a1* transgene or a synthetic phenotype (Fig. 4a, right panel). We killed mice at stages E12.5 to E16.5, but did not observe a higher percentage of the compound *Ebf3*^{-/-}/*Atp2a1*^{tg} genotype, arguing against a synthetic phenotype. A defect earlier than E12.5 seems highly unlikely as the skeletal α -actin promoter is not active at these stages. The genomic insertion locus of the *Atp2a1* transgene is unknown, but we think the most likely explanation for the low frequency is genetic linkage, that is, the transgene is on the same chromosome as *Ebf3*. Strikingly, we observe the same frequency of *Ebf3*^{-/-}/*Atp2a1*^{tg} animals at D0.5, clearly distinguishing them from *Ebf3*^{-/-} mice. *Ebf3*^{-/-}/*Atp2a1*^{tg} mice do not show any signs of cyanosis or gasping respiration, but display normal morphology and movement at D0.5 (Fig. 4b). To determine the level of functional rescue exactly, we analysed sarcomere length in muscle fibres of the diaphragm from *Ebf3*^{+/+}/*Atp2a1*^{tg} and *Ebf3*^{-/-}/*Atp2a1*^{tg} mice and found no significant difference (Fig. 4c). Furthermore, we subjected whole diaphragms to defined electrical stimulation as described for the single deletion of *Ebf3*. Single twitch stimulation (50 V, 1 ms) induced a force from *Ebf3*-deficient diaphragms that was comparable to *Ebf3*-expressing muscle (Fig. 4d). In addition, the duration of contraction was also comparable in the diaphragm from *Ebf3*^{+/+}/*Atp2a1*^{tg} and *Ebf3*^{+/+}/*Atp2a1*^{tg} mice (Fig. 4e). The force produced under tetanus stimulation (50 V, 1 ms, 120 Hz for 500 ms) was also rescued by the transgenic expression of *Atp2a1* (Supplementary Fig. 6C) just as the duration of contraction (Supplementary Fig. 6D). Therefore, we conclude that *Atp2a1* is the critical target gene downstream of *Ebf3* causing the defects in muscle relaxation and the associated cyanotic appearance and postnatal lethality. However, the transgenic expression of *Atp2a1* did not allow for prolonged survival of *Ebf3*-deficient mice. In a time period from 24 h after birth up to 4 days, all double-mutant mice died, but again did not display a cyanotic appearance (Fig. 4f). As *Ebf3*^{-/-}/*Atp2a1*^{tg} mice seemed slightly weaker and less active over time than their littermates, we determined their weight and found that the gain in newborn mice, particularly from postnatal day 3 on, is not achieved by *Ebf3*^{-/-}/*Atp2a1*^{tg} mice (Fig. 4g).

Taken together, the data show that skeletal muscle-specific expression of *Atp2a1* rescues the defect in muscle relaxation of the diaphragm, but is unable to compensate for all defects associated with loss of *Ebf3*.

***Atp2a1* is a direct target gene of *Ebf3*.** The biological importance of *Atp2a1* downstream of *Ebf3* and its downregulation in absence of this transcription factor prompted us to investigate a potential direct molecular link. *Atp2a1* maps to mouse chromosome 7 (ref. 31), and analysis of DNA sequence upstream of the transcriptional initiation site³² reveals four potential binding sites for Ebf proteins in its promoter/enhancer (Fig. 5a). Two of these possess exactly the same DNA sequence as the Ebf-binding site in the *mb-1* promoter where Ebf1 was first identified³³; therefore, we named them as M1 and M2, and two sites as E1 and E2, which have the inner palindrome of the ideal consensus site for Ebf proteins³⁴. Ebf3 bound with high affinity to the M1 and E2 sites but only weakly to the E1 site as shown by electrophoretic mobility shift assay (EMSA; Fig. 5b). Ebf3 also bound to the M2 site, but slightly different conditions used for the binding buffer prevent a direct comparison. The binding is specific, as single-nucleotide mutation abolished it (the mutant versions are indicated in Fig. 5a), and the addition of unlabelled (cold) oligonucleotides in 10-fold excess also leads to a loss of binding activity. Furthermore, the binding activity could be super-shifted by an α -flag antibody, demonstrating complex formation between Ebf3 and the indicated oligonucleotides (Fig. 5b). ChIP assay using protein extracts from C2C12 cells expressing flag-tagged Ebf3 showed binding to sites M1, E2 and M2, but not to E1, largely corresponding to the data from the EMSA assay (Fig. 5c) and confirming the binding of Ebf3 to these promoter sites *in vivo*. To determine whether Ebf3 can transactivate from the *Atp2a1* promoter via the identified Ebf3-binding sites, a DNA fragment containing over 1 kb of its promoter was cloned into a luciferase reporter construct, and point mutations as indicated in Fig. 5a were introduced into the Ebf-binding sites either alone or in combination. Figure 5d shows that Ebf3 can transactivate from the *Atp2a1* promoter fragment 4.2-fold. Mutation of site M2 almost completely abolished transactivation, whereas mutation of site E1 did not have any influence. Mutation of site M1 or E2 gave intermediary results. Therefore, we conclude that site M2, which is closest to the transcriptional start site, is most important for transactivation of *Atp2a1* by Ebf3, and that sites M1 and E2 contribute to reach full activity. Site E1 seems dispensable as Ebf3 binds with low affinity in EMSA, no binding is detected in ChIP assay and transactivation is not influenced by its mutation. In fact, site E1 or neighbouring sequences might negatively influence transactivation, as its deletion together with M1 or E2 results in diminished loss of transactivation (Fig. 5d). Finally, to determine whether Ebf3 is not only required but also sufficient for the expression of *Atp2a1*, C2C12 cells were transfected with *Ebf3* and cultivated in the presence or absence of horse serum to induce myoblast differentiation. Within 2 days, horse serum alone did not induce the expression of *Atp2a1* (Fig. 5e). Ebf3 alone also had no effect, but in combination with horse serum leads to a strong upregulation of *Atp2a1*. After 5 days, Ebf3 had again no effect on the expression of *Atp2a1*, and horse serum had a small inductive effect, but together, horse serum and Ebf3 strongly induced the expression of *Atp2a1*. These data suggest that Ebf3 alone is not sufficient to induce the expression of endogenous *Atp2a1*, but likely acts in concert with other factors expressed during myoblast differentiation.

Ebf3 and MyoD synergistically induce expression of *Atp2a1*. Other members of the Ebf protein family cooperate with basic helix-loop-helix transcription factors in the induction of target

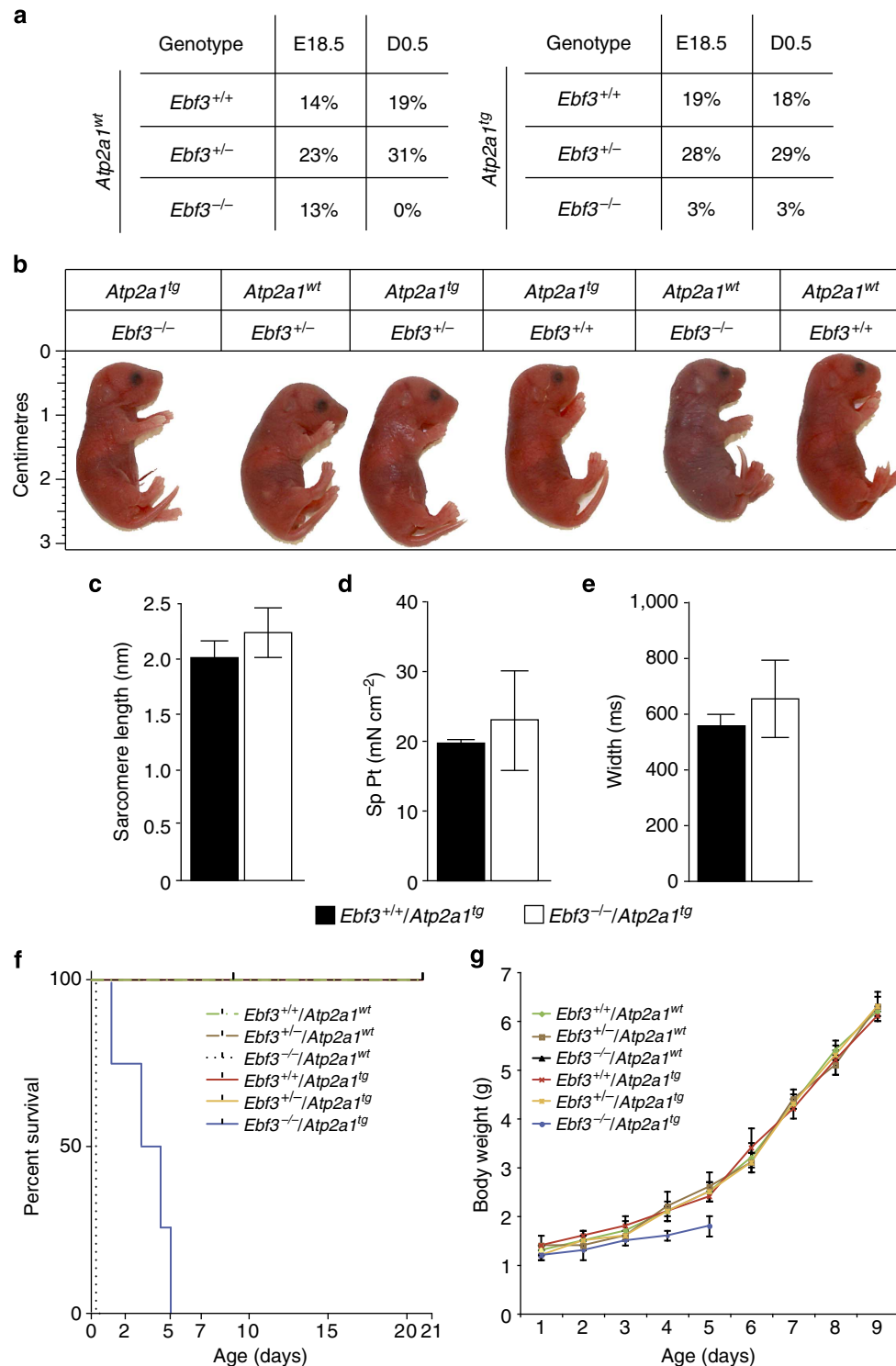


Figure 4 | Transgenic expression of *Atp2a1* rescues *Ebf3*-dependent respiratory failure. (a) *Ebf3*-mutant animals were crossed to *Atp2a1*-transgenic mice and frequencies of *Ebf3* wild-type and mutant genotypes on an *Atp2a1* wild-type or transgenic background are shown before and after birth; E18.5: $n = 115$, D0.5: $n = 231$. (b) Comparison of compound *Ebf3*-mutant and *Atp2a1*-transgenic animals as indicated shortly after birth. Note the cyanotic appearance only in *Ebf3*^{-/-}/*Atp2a1*^{wt} mice; *Ebf3*^{-/-}/*Atp2a1*^{tg} mice can be detected 12 h after birth. Length is indicated in centimetres. (c) Determination of sarcomere length in the diaphragm of *Ebf3*^{+/+}/*Atp2a1*^{tg} and *Ebf3*^{-/-}/*Atp2a1*^{tg} newborn mice. $n = 3$; error bars = s.d. (d,e) Single twitch stimulation (50 V, 1 ms) of diaphragm muscle from newborn mice of the indicated genotypes. (d) Measurement of single twitch normalized to the cross-sectional area, representing muscle force in response to the stimulation. (e) Total duration of muscle contraction after single twitch stimulation. $n = 3$; error bars = s.d. (f) Transgenic expression of *Atp2a1* in *Ebf3*-mutant animals does not allow prolonged survival. Survival of animals of the indicated genotypes is followed over time and plotted against days; $n = 3$ to 5 each. (g) Impaired weight gain in *Ebf3*-deficient, *Serca1* transgenic mice. Animals of the indicated genotypes were weighed every 24 h, and weight is plotted against age of the mice; $n = 4$ to 5 each; error bars = s.d.

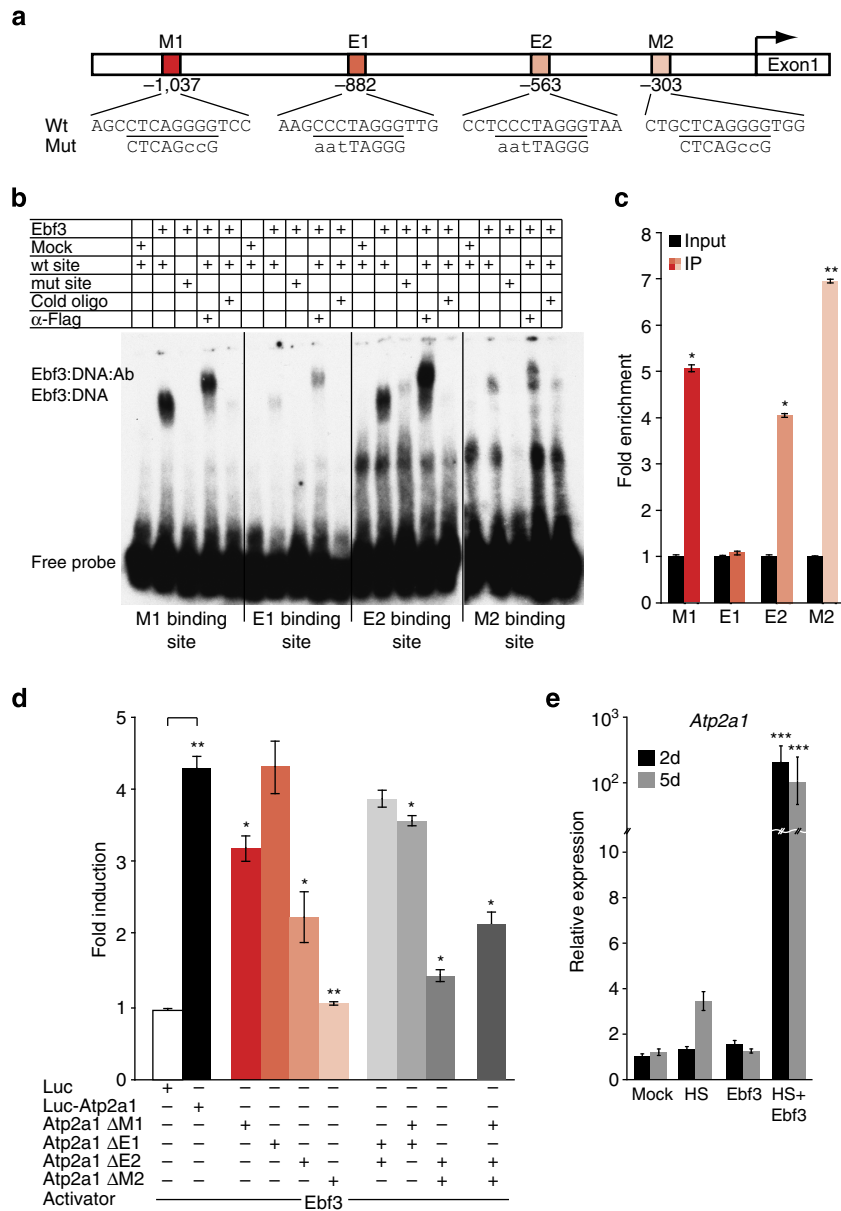


Figure 5 | *Atp2a1* is a direct target gene of Ebf3. (a) Schematic overview of the promoter structure of the *Atp2a1* gene. Red boxes indicate potential binding sites for Ebf proteins, numbers give the position relative to the transcriptional start site of *Atp2a1*. The sequence of each potential binding site is indicated and mutations used in the experiments in this figure are shown in small letters. (b) EMSA of HEK293T protein extract containing flag-tagged Ebf3 with oligonucleotides corresponding to potential binding sites. For specificity control non-radioactive (cold) or mutated oligonucleotides were used, identity was confirmed by supershift using α -Flag antibody (Ab); $n = 3$. (c) Chromatin immunoprecipitation (ChIP) of flag-tagged Ebf3 protein from C2C12 cells; qPCR analysis of ChIP using primers specific for all four individual binding sites. Fold enrichment indicates the ratio of DNA amplification comparing ChIP with beads-only control; $n = 3$; error bars = s.d.; * $P < 0.05$, ** $P < 0.01$. (d) Analysis of the transactivation potential of Ebf3 from the *Atp2a1* locus. HEK293T cells were transfected with plasmids comprising all four potential binding sites in wild-type or mutated form as indicated in a. Activity of luciferase was determined, and values were normalized to β -galactosidase. Transfections of the pBL-Luc plasmid not containing promoter elements together with pCMV-Ebf3 were set to 1; $n = 3$; error bars = s.d.; P -values were calculated in comparison with activation of pBL-Luc-*Atp2a1* if not otherwise indicated. * $P < 0.05$, ** $P < 0.01$. (e) Quantitative PCR analysis of *Atp2a1* expression in C2C12 cells 2 and 5 days after transfection of mock- or Ebf3-plasmid and initiation of *in vitro* differentiation by horse serum (HS). $n = 3$; error bars = s.d.; P -values are relative to mock; **** $P < 0.001$.

genes, like Ebf1 with E2A in B-cell development^{35,36}. Moreover, E-boxes, the consensus binding sites for bHLH transcription factors, are found highly enriched in the vicinity of Ebf-binding sites^{37,38}. A detailed examination of the *Atp2a1* promoter yielded five E-boxes within the *Atp2a1* promoter fragment (X1–X5, Fig. 6a). MyoD and Myf5 are two bHLH transcription factors binding to E-boxes that are important for myogenic differentiation. ChIP-seq analysis for both factors during proliferation and differentiation of primary myoblasts has been

reported and reveals that MyoD binds to two sites in the *Atp2a1* promoter during myoblast differentiation, whereas Myf5 does not bind under both conditions³⁹. We examined binding of MyoD to E-boxes present in the *Atp2a1* promoter by ChIP and could confirm strong binding to site X1 and weaker but significant binding also to site X5. Also, sites X3 and X4 gave an increased signal, but the values did not reach statistical significance (Fig. 6b). In contrast to Ebf3, ChIP-grade antibodies specific for MyoD are available, allowing us to examine its binding in

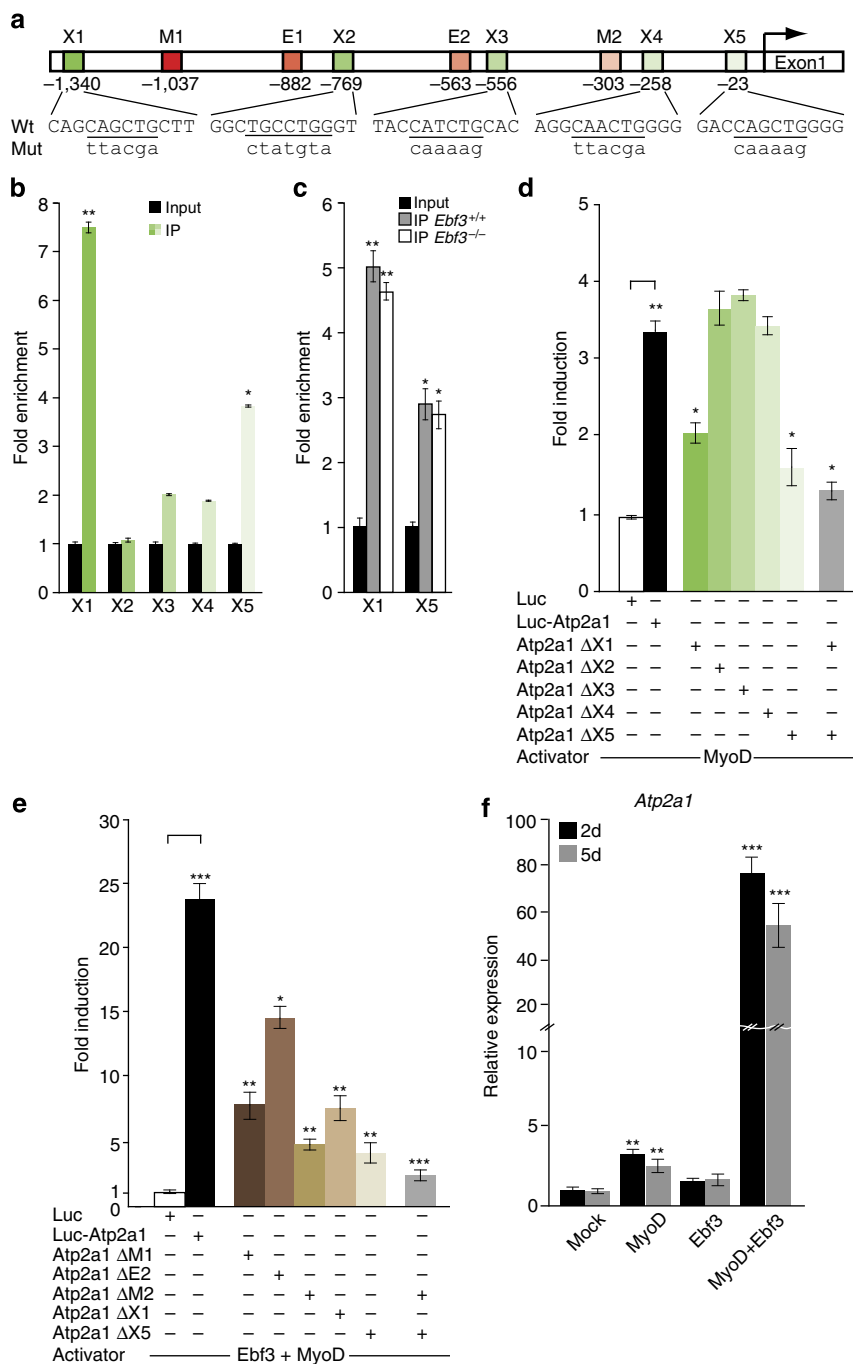


Figure 6 | Ebf3 synergises with MyoD in the induction of the *Atp2a1* gene. (a) Schematic overview of the promoter structure of the *Atp2a1* gene. Ebf consensus sites are indicated in red, E-boxes X1 to X5 in green, and their position relative to the transcriptional start site is shown. The sequence of each potential binding site is indicated, and mutations used in the experiments in this figure are shown in small letters. (b) Chromatin immunoprecipitation (ChIP) of flag-tagged MyoD protein from C2C12 cells; qPCR analysis of ChIP using primers specific for all five individual binding sites. Fold enrichment indicates the ratio of DNA amplification comparing ChIP with beads-only control; $n=3$; error bars = s.d.; $*P<0.05$, $**P<0.01$. (c) ChIP assay of MyoD protein from diaphragm of E18.5 *Ebf3*^{+/+} and *Ebf3*^{-/-} embryos as indicated; qPCR analysis of ChIP using primers specific for the two binding sites determined in b. Fold enrichment indicates the ratio of DNA amplification comparing ChIP with beads-only control; $n=3$; error bars = s.d.; $*P<0.05$, $**P<0.01$. (d) HEK293 cells were transfected with an expression plasmid for MyoD and a reporter construct containing all indicated consensus sites as wild-type or mutated sequence as shown in a, followed by the luciferase gene. Transfections of the pBL-Luc plasmid not containing promoter elements together with pCMV-*Ebf3* were set to 1 for each reporter plasmid; $n=3$; error bars = s.d.; P -values were calculated in comparison with activation of pBL-Luc-*Atp2a1* if not otherwise indicated. $*P<0.05$, $**P<0.01$. (e) HEK293 cells were transfected as in d, but expression plasmids for *Ebf3* and MyoD were used in parallel, and reporter plasmids with mutations in binding sites were used as indicated. Transfections of the pBL-Luc plasmid not containing promoter elements together with pCMV-*Ebf3* were set to 1 for each reporter plasmid; $n=3$; error bars = s.d.; P -values were calculated in comparison with pBL-Luc-*Atp2a1* if not otherwise indicated. $*P<0.05$, $**P<0.01$, $***P<0.001$. (f) Quantitative PCR analysis of *Atp2a1* expression in C2C12 cells 2 and 5 days after transfection of *Ebf3* and/or MyoD encoding expression plasmids. Mock (transfection of parental plasmid) is set to 1 for 2 and 5 days. $n=3$; error bars = s.d.; P -values are relative to mock; $**P<0.01$, $***P<0.001$.

primary diaphragm cells in the presence and absence of Ebf3. Figure 6c confirms binding of MyoD to sites X1 and X5 under wild-type conditions and also shows that MyoD can bind to these sites in the absence of Ebf3. To analyse the functional importance of these E-boxes, we tested them individually with wild-type or mutated sequences together with MyoD. Figure 6d shows that MyoD can transactivate 3.4-fold from the *Atp2a1* promoter, which is comparable to the induction with Ebf3 alone. Mutation of the individual E-boxes as indicated in Fig. 6a leads to a reduction in transactivation potential in case of sites X1 and X5 to 2- and 1.8-fold, respectively, whereas sites X2 to X4 have no influence. Combining mutations in sites X1 and X5 leads to a reduction of transactivation to 1.4-fold (Fig. 6d). To test potential synergistic effects between Ebf3 and MyoD, we combined these two factors with reporter constructs used before. Together, these two transcription factors lead to a 24.4-fold induction of the *Atp2a1* promoter, displaying strong synergy in their transactivation capacity. Mutation of Ebf-binding sites M1 or M2 in this context results in a reduction of transactivation to 7.6-fold and 4.8-fold, respectively, and in a reduction to 14.5-fold in case of site E2 (Fig. 6e). E-boxes X1 and X5 are important for co-transactivation, as their mutation reduces induction to 6.8-fold and 4.6-fold. Finally, the combination of the two strongest mutations for each class of transcription factors, M2 and X5, reduced the combined transactivation potential of Ebf3 and MyoD to 2.4-fold (Fig. 6e). As Ebf3 alone is not sufficient to induce the expression of endogenous *Atp2a1* in C2C12 cells within 2 to 5 days, but can do so in combination with horse serum (Fig. 5f), we tested whether Ebf3 and MyoD together have this ability. MyoD alone can induce the expression of *Atp2a1* 3.2-fold and 2.8-fold after 2 and 5 days, whereas expression of Ebf3 alone does not significantly induce *Atp2a1*. Together, however, Ebf3 and MyoD have the potential to strongly induce the expression of *Atp2a1* by 74.6-fold and 53.4-fold after 2 and 5 days post-transfection (Fig. 6f). The synergistic activity between Ebf3 and MyoD prompted us to investigate a potential direct interaction between these transcription factors. To this end, we transfected C2C12 cells with tagged versions of both factors, and tried co-immunoprecipitation under various conditions, but failed to detect a direct interaction.

Redundancy between Ebf factors in the induction of *Atp2a1*.

The finding that deficiency for *Ebf3* leads to a downregulation of *Serca1* in the diaphragm, but not in skeletal muscle, (Fig. 3h) is surprising and indicates that either the regulation of *Atp2a1* expression is different between these muscle types or that compensation between Ebf proteins is going on. As mentioned in the introduction, Ebf3 is part of a highly homologous family of proteins consisting of four members, of which functional redundancy has already been demonstrated¹⁶. To analyse whether the mechanism described here might be more general and not restricted to the diaphragm, we isolated RNA from diaphragm and skeletal muscle of wild-type mice and determined the expression of all four *Ebf* genes by qPCR. *Ebf3* shows the strongest expression in the diaphragm, followed by an approximately threefold lower expression of *Ebf1*, whereas *Ebf2* and *Ebf4* are only weakly expressed (Fig. 7a). In contrast, *Ebf1* is the most strongly expressed family member in the skeletal muscle, *Ebf3* is 3.4-fold lower, and *Ebf2* and *Ebf4* again are only weakly expressed (Fig. 7b). To determine whether there is functional redundancy between the individual Ebf factors in the induction of the *Atp2a1* gene, we first tested their ability to transactivate from the *Atp2a1* promoter. In reporter assays *Ebf1*, *Ebf2* and *Ebf4* have a transactivation potential that is comparable to the activity of *Ebf3* (Figs 5d and 7c), indicating potential

redundancy between these factors. To test this ability with the endogenous gene, we ectopically expressed Ebf factors either alone or in combination with MyoD in C2C12 cells and determined the expression of endogenous *Atp2a1* after 2 days. *Ebf1*, *Ebf2* and *Ebf4* alone can induce the expression of *Atp2a1* approximately two- to threefold, again largely recapitulating the ability of *Ebf3* alone. In combination with MyoD, however, all Ebf factors show a strong synergistic effect, resulting in a 60- to 80-fold induction of *Atp2a1* (Fig. 7d). To test these results also genetically, we examined the expression of *Atp2a1* in skeletal muscle from *Ebf1* wild-type and mutant mice. Loss of one allele of *Ebf1* leads to a downregulation of *Atp2a1* by 21%, whereas its complete deletion reduces *Atp2a1* by 51% (Fig. 7e), confirming a more general role for Ebf proteins in its regulation and also indicating dose-dependency of Ebf factors in the induction of the *Atp2a1* gene.

Taken together, the data show that Ebf3 is necessary for the relaxation of the diaphragm by binding to three consensus sites in the promoter/enhancer of the *Atp2a1* gene, where it synergises with MyoD to induce the expression of *Serca1*, which is necessary for Ca^{2+} -uptake into the sarcoplasmic reticulum (Fig. 7f). This mechanism, however, is not restricted to Ebf3 and the diaphragm but general in muscle cells as all Ebf factors can synergise with MyoD and transactivate from the *Atp2a1* promoter. An overlapping, but also distinct expression pattern, between mostly *Ebf1* and *Ebf3* in the diaphragm versus the skeletal muscle is responsible for biological effects.

Discussion

The transcription factor Ebf3 was originally identified because of its expression in the olfactory epithelium and neuronal cells^{18,19}, and *Ebf3*-deficient mice have defects in olfactory receptor neuron projection¹⁶. However, *Ebf3* is also expressed outside of the neural system and *Ebf3*^{-/-} mice die immediately after birth, but only very little is known about its role in other tissues. Here, we identify respiratory failure caused by the inability of the lung to unfold at birth as the reason for the postnatal death. Multiple organs might account for such a phenotype, including the lung, the rib cage and the muscles involved in respiration, that is, mainly the diaphragm and the heart. *Ebf3* is not expressed in the lung and the heart, and development of the lung, heart and bone proceeds normally in the absence of *Ebf3*. However, Ebf3 is expressed strongly in the diaphragm, suggesting an involvement of muscle cells in the *Ebf3*-dependent respiratory failure. Consistent with this notion, the function of *Ebf3*-deficient muscle cells of the diaphragm is impaired, resulting in less force produced in response to single or persistent stimulation and prolonged duration of muscle contraction after stimulation. This phenotype of impaired muscle relaxation is highly reminiscent of the deletion of *Atp2a1*, which encodes for a Ca^{2+} -ATPase that catalyses the ATP-dependent transport of Ca^{2+} from the cytosol to the lumen of the sarcoplasmic reticulum⁴⁰. Interestingly, *Serca1* is strongly downregulated in the diaphragm but not in skeletal muscle of *Ebf3*-deficient mice. *Ebf1*, a highly homologous member of this family of transcription factors, is most strongly expressed in skeletal muscle. *Ebf1* can act via the same binding sites in the *Atp2a1* promoter, synergises with MyoD, and loss of *Ebf1* leads to a downregulation of *Atp2a1* expression in skeletal muscle, indicating redundancy between individual Ebf factors. It is an interesting question why the diaphragm differs in its expression of Ebf factors from other skeletal muscles, however, as the promoters of Ebf genes have not been characterized with the exception of *Ebf1*, this remains subject for further study. An important question is also why there is a downregulation of *Atp2a1* in the absence of *Ebf3* since *Ebf1* is expressed in the

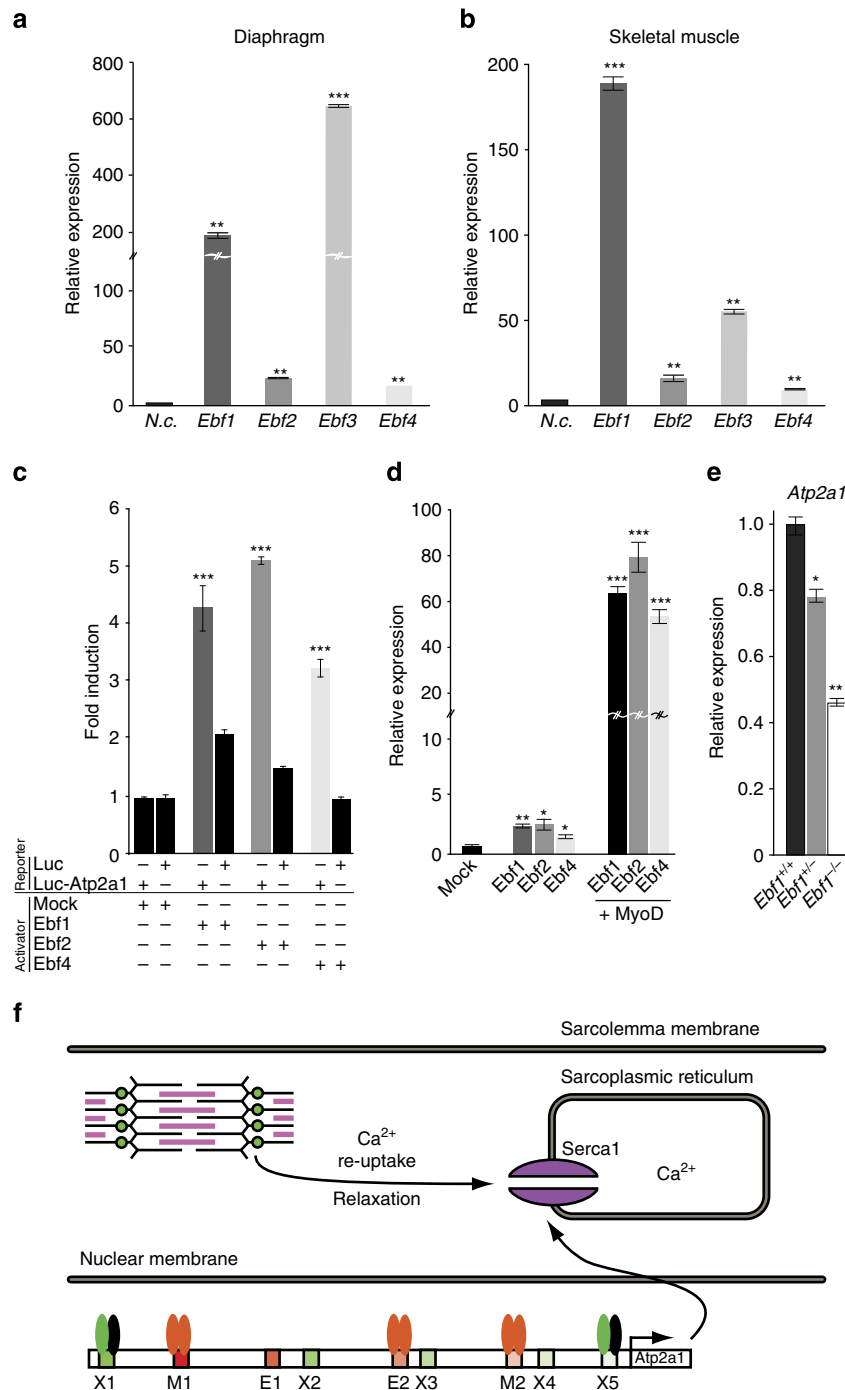


Figure 7 | Overlapping expression and redundancy between Ebf genes. (a) Expression of Ebf factors as indicated in the diaphragm from E18.5 embryos determined by quantitative PCR. Ba/F3 cells were used as negative control (n.c.). $n=3$, error bars = s.d., $**P<0.01$, $***P<0.001$. (b) Same as a, but skeletal muscle from adult mice was used for analysis. $n=3$, error bars = s.d., $**P<0.01$, $***P<0.001$. (c) Analysis of the transactivation potential of Ebf factors from the *Atp2a1* promoter. HEK293T cells were transfected with reporter plasmids comprising all four Ebf consensus sites in wild-type form as in Fig. 7d. Ebf1, Ebf2 and Ebf4 in pCMV were co-transfected as activators as indicated. Transfections of the empty pCMV plasmid were set to 1, and all other values are given accordingly. $n=3$, error bars = s.d., $***P<0.001$, P -values are in comparison with mock control of the respective reporter. (d) Analysis of the expression of *Atp2a1* in C2C12 cells by qPCR in response to ectopic expression of Ebf1, Ebf2, Ebf4 and MyoD as indicated 2 days after transfection. $n=3$, error bars = s.d., $*P<0.05$, $**P<0.01$, $***P<0.001$. (e) Expression of *Atp2a1* determined by qPCR from skeletal muscle of *Ebf1*^{+/+}, *Ebf1*^{+/-} and *Ebf1*^{-/-} mice (E18.5); $n=3$, error bars = s.d., $*P<0.05$, $**P<0.01$. (f) Model for the role of Ebf factors in muscle physiology. Ebf (orange ovals) and MyoD (green ovals) directly bind to consensus sequences present in the promoter of the *Atp2a1* gene and synergistically transactivate the expression of *Atp2a1*. Serca1 mediates Ca²⁺ re-uptake and muscle relaxation, which are defective in absence of Ebf3.

diaphragm as well and is also able to induce its expression. Ebf factors have dose-dependent effects in other cellular contexts like B-cell and neuronal development^{16,35} and, in fact, deletion of

only one allele of *Ebf1* also leads to a slight reduction of *Atp2a1* in skeletal muscle. Therefore, dose dependency seems to be responsible for this effect.

The large phenotypic overlap between loss of *Ebf3* and *Atp2a1* is striking and together with its downregulation already indicates the potential importance of *Atp2a1* as a target gene of Ebf3. The genetic rescue of *Ebf3*-dependent muscle relaxation and respiratory failure by ectopic expression of *Atp2a1* *in vivo* identifies it as the biologically most relevant downstream target of *Ebf3* in the diaphragm. However, *Serca1* does not completely rescue deficiency for *Ebf3* as mice die within 4 days after birth. This is likely the result of a complex situation in the compound *Ebf3/Atp2a1* mutant animals. The skeletal α -actin promoter does not recapitulate the expression pattern of the endogenous *Atp2a1* promoter, and in addition the expression of *Atp2a2* is strongly downregulated. We failed to identify Ebf-binding sites in the promoter/enhancer of the *Atp2a2* gene, and ectopic expression of *Ebf3* and *MyoD* alone or in combination did not alter *Atp2a2* expression levels in C2C12 cells. In addition, since *Atp2a2* is expressed in slow twitch fibres, its downregulation seems to be indirect. As this situation is not only complex, but due to the expression of the transgene to some degree also artificial, we decided not to follow the synthetic phenotype any further. Therefore, the analysis of the biological role of Ebf3 after birth awaits the generation of conditional knock-out mice.

Interestingly, many muscle-specific genes harbour E-boxes in their promoter, which act as binding sites for MRF proteins^{4,7}. However, E-boxes are not tissue-specific as they occur not only in muscle-specific genes, but also have a much broader distribution, and MRF factors bind to many E-boxes in nonmuscle-specific promoters⁸. Consequently, an important question in muscle development is how specificity is achieved. A combinatorial action between MRF and other transcription factors has been suggested, and a few examples have been identified^{10,41}. In B-cell development, Ebf1 acts synergistically with the transcription factor E47, a product of the *E2A* gene, which also binds to E-boxes³⁵. Although no direct interaction could be demonstrated so far, they cooperate in the induction of B-cell-specific genes³⁶. There are several striking parallels to the data presented here, like the involvement of Ebf factors and E-box binding proteins, direct binding to neighbouring sites in the promoter, no detectable physical interaction but cooperation in the induction of the downstream gene. Furthermore, *MyoD* can replace products of the *E2A* gene in the synergistic induction of the B-cell-specific *lambda5* gene, demonstrating redundancy between bHLH transcription factors in the cooperation with Ebf proteins⁴². Therefore, synergistic effects between E-box-binding factors and Ebf proteins seem to be a broader phenomenon and not restricted to B cells. Consequently, although Ebf3 just as other Ebf factors is clearly not muscle specific, it could be part of a transcriptional module that together mediates muscle-specific gene expression.

In parallel to the high conservation of *Ebf* genes at the sequence level during evolution^{13,14,43}, there seems to be also a considerable level of conservation of their biological role. *Collier*, the only *Ebf* gene in *Drosophila*, is expressed by cells that support immature haemocytes and is necessary to maintain this pool of progenitor cells⁴⁴. This is highly reminiscent of *Ebf2* and its role in the support of immature haematopoietic stem and progenitor cells⁴⁵. Besides the support of haemocytes, *collier* is also required for the formation of the dorsal/acute 3 (DA3) embryonic muscle, which does not develop in its absence^{46,47}. Together with *nautilus*, the only homologue of MRF bHLH factors in *Drosophila*, *collier* controls shape and morphology of the DA3 muscle⁴⁸. Here we report that *Ebf3* is required for the relaxation of the diaphragm and that it synergises with *MyoD* in inducing a critical cell-type specific gene. To our knowledge this is the first implication of *Ebf* genes in muscle cell function in mammals, but the phenotype described here differs considerably from the loss of *collier* in *Drosophila*. Hence, either the

requirement for Ebf factors has changed during evolution or the expression of other Ebf family members and redundancy might mask a broader role for this gene family in muscle development. Indeed, it was recently shown that Ebf proteins participate in transcriptional regulation of muscle development in *Xenopus*⁴⁹, favouring the second possibility.

In parallel to a strong evolutionary conservation at the sequence level, there might be also a conservation at the level of interaction partners like bHLH transcription factors. Although *collier* and *Ebf3* are required for development and function of a specific muscle, such a conservation seems true at the broad biological level, but not in detailed aspects. The diaphragm is a derivative of myoblasts from myotomes C3, C4 and C5, which migrate into the septum transversum, a condensation of mesenchymal cells pre-figuring large parts of the diaphragm, where they expand and differentiate. This process is not homologous to the generation of the DA3 muscle, but it is tempting to speculate that a conservation in the specification of muscle identity might exist at the molecular level despite different organ development at the cellular level. Therefore, rather than postulating a relationship between the DA3 muscle in *Drosophila* and the diaphragm in the mouse, it seems more likely that Ebf factors probably in combination with the E-box-binding MRF factors form a module in muscle cell differentiation that has been adopted during evolution.

Brody's disease is a rare myopathy, characterized by exercise-induced impairment of skeletal muscle relaxation, stiffness and cramps, resulting from impaired Ca^{2+} -uptake and Ca^{2+} -ATPase activity⁵⁰. Mutations of *Atp2a1* were found in 50% of Brody's patients and are genetically associated with Brody disease⁵¹. The reason for the remaining cases of Brody myopathy is unclear, as the genomic sequence of *Atp2a1* is unchanged. Among these, cases have been reported in which the expression of *Serca1* is strongly reduced⁵². As *Serca1* is strongly downregulated and barely detectable in the diaphragm of *Ebf3*-deficient mice, we suggest that *Ebf3* might be involved in at least a subgroup of the remaining cases of Brody disease. This might be either via mutation of *Ebf3* itself, but this is the more unlikely possibility as the broad expression of *Ebf3* will probably result in more defects after birth. Alternatively, binding sites for Ebf proteins might be mutated, preventing Ebf3 from transactivating from the human *Atp2a1* promoter.

Methods

Generation of mice. Two DNA fragments corresponding to the *Ebf3* genomic region were isolated from a mouse 129/Ola genomic cosmid library. The first fragment (5'-region) expanded 4.85 kb from a *Pml1* site upstream of the *Ebf3* coding region to the translation start codon. The second region was a *PstI* fragment of 4.6 kb from intron 4 to intron 6. The targeting construct was obtained by cloning these fragments in the pBluescript KS vector, followed by insertion of an *NLS-lacZ* gene and a *PGK::Neo* cassette flanked by *loxP* sites between both fragments. *NLS-LacZ* was cloned in frame with the *Ebf3* translation start codon. Mouse ES cells were electroporated with this construct, and colonies were isolated in the presence of 400 $\mu\text{g ml}^{-1}$ G418. For DNA extraction, cells were digested with 100 $\mu\text{g ml}^{-1}$ Proteinase K in the presence of 50 mM Tris-HCl pH 7.5, 100 mM NaCl and 10% SDS. DNA was ethanol precipitated and analysed by Southern Blot⁵³. Two clones (#1 and #2) out of the 800 clones analysed had correctly incorporated the targeting construct, as established by Southern blot. Both clones were injected into C57BL/6 blastocysts that were implanted into pseudopregnant females. Chimeric mice were bred to obtain germline transmission. Two male chimera (80%) corresponding to clone #1 were selected to get heterozygous mice. The *PGK::Neo* cassette was removed by crossing with PGK-Cre transgenic mice⁵⁴. Mutant mice were backcrossed with C57BL/6 wild-type mice for more than 10 generations. All experiments involving animals were designed in agreement with the stipulations of the animal care committee of the Helmholtz Zentrum München and the 'Regierung von Oberbayern'.

Genotyping. For genotyping of mice tails were digested for at least 1 h in lysis buffer (FirePol buffer B (Solis BioDyne), 1.25 mM MgCl_2 , 50 $\mu\text{g ml}^{-1}$ proteinase K) at 55 °C and inactivated for 15 min at 95 °C. PCR was carried out with genomic

DNA and 20 pmol of each primer (*Ebf3* fwd 5'-GGGCACACCACAGTCTGTC-3', *Ebf3* wt rev 5'-GGAGGATATACAGGGTCACAC-3', *Ebf-lacZ* rev 5'-GCGCCG GTCACCATTACC-3') using FirePol (Solis BioDyne) under these conditions: 35 cycles of 94 °C for 30 s, 61 °C for 1 min, 72 °C for 30 s. *Atp2a1*-transgenic mice were obtained from Jeffery Molkentin (University of Cincinnati, USA) and genotyped as described³⁰.

Isolation of primary cells. Bone marrow cells were isolated as described⁵⁵. For isolating bone marrow cells, bones (two tibia and two femurs per mouse) from embryos at day E18.5, bones were pre-digested in DMEM supplemented with 0.1% collagenase (Sigma) and 0.2% dispase (Roche) twice for 20 min. After washing with PBS, bones were cut and digested three times as above, and supernatant was collected. For cell isolation from whole organs, adult or embryonic mice were killed, organs removed and detached by a 100- μ m cell strainer. Diaphragm cells were digested in DMEM supplemented with 0.2% collagenase for 30 min, fractionated and resuspended.

Electrophysiology and force measurements. Experiments were conducted on diaphragm muscle strips from newborn mice. The pups were killed by cervical dislocation and after the laparotomy, the rib cage containing the whole diaphragm was excised and kept in cold MEM-Glutamax (Gibco) supplemented with fetal bovine serum for dissection. A strip from the right ventral costal hemi-diaphragm was excised keeping both insertions from ribs and central tendon intact. The muscle strips were horizontally mounted in Ringer-Krebs-Henseleit solution (140 mM NaCl, 5 mM KCl, 1.2 mM KH₂PO₄, 1.2 mM MgCl₂, 2 mM CaCl₂, 20 mM Hepes, 6 mM glucose; pH 7.4; osmolarity between 290–315 mOsm). At constant perfusion, the solution was kept at 25 °C and bubbled with gas mixture of 95% O₂ and 5% CO₂. The costal end was held in a stationary end and the central tendon attached to the force transducer (SI-H Force Transducer, 0–50 mN, SI-KG4, WPI). The optimal length (*L*_o) was defined as the muscle length at which twitch tension development was maximal, corresponding to the apex of the length-active tension curve. Stimulation was applied using a Grass stimulator SD9 (Grass Instruments, Quincy, MA) via closely flanking platinum wire electrodes. Supramaximal stimulation during single twitch was reached at 50 V, with 1 ms squared pulse duration. Duration of tetanus stimulation was set for 500 ms. The diaphragm force-frequency relationship was assessed at supramaximal stimulation by sequential excitation of muscles at 50 V with pulse duration of 1 ms at 1, 5, 10, 15, 30, 60, 90, 120, 150 and 180 Hz, during 500 ms, every 3 min. The cross-sectional area (CSA) of the muscle strip was calculated by dividing the mass of the muscle (without rib bone and central tendon; mg) by the product of the optimal length (*L*_o, mm) and muscle density (1.056 g cm⁻³). The tension was calculated as force (mN) per CSA (cm²). The traces were acquired at 4 KB s⁻¹ and analysed using PowerLab and LabChart 7.0 (AD Instruments, Australia).

Cell Culture. 70Z/3, 18-81 TK+ and Ba/F3 cells were cultured in RPMI 1640, supplemented with 10% fetal calf serum (FCS; PAA), 1% penicillin and streptomycin, 1% L-glutamine. For 70Z/3 and 18-81 TK+, 1% sodium pyruvate and 0.003% β -mercaptoethanol was used additionally. For the maintenance of Ba/F3 cells, the culture medium was supplemented in addition with 10% conditioned medium from WEHI3 cells as a source of IL-3. WEHI-3B and Whitlock-Witte cultures were propagated in RPMI 1640 supplemented with 10% FCS and 0.0003% β -mercaptoethanol. Stromal cell lines (2018, AFT024, C2C12, GP + E86, HEK293T) were grown in Dulbecco's modified Eagle medium with Glutamax (DMEM), and osteoblastic cells (C3H10T $\frac{1}{2}$, MC3T3) were cultured in minimum essential medium (MEM α) with in addition supplemented 10% FCS, penicillin and streptomycin and L-Glutamine. All reagents described were purchased from Gibco unless stated otherwise. *In vitro* differentiation assay was performed as described⁵⁶. In brief, C2C12 cells were transfected with *Ebf3*-expressing plasmid, and *in vitro* differentiation was initiated by adding 2% horse serum in medium instead of fetal calf serum for 2 or 5 days.

CFU-F assay. Mouse bone marrow cells were harvested from E18.5 *Ebf3*^{+/+} and *Ebf3*^{-/-} mice as described above. Cell numbers were determined by using Casy cell counter (Schärfe Systems). Cells were diluted in mouse Complete MesenCult Medium (StemCell Technologies), and 10,000 cells were seeded per well in six-well plates. The cells were cultured at 37 °C in 5% CO₂ for 10 days without medium change. The medium was aspirated, and each well was washed twice with PBS thereafter. Cells were fixed with methanol for 10 min at room temperature. The methanol was removed, and each well was stained with Giemsa Staining Solution for 10 min at room temperature. The staining solution was aspirated and each well was washed with water for several times to remove unbound stain. The water was removed and the wells were allowed to air dry. Stained colonies were counted microscopically.

Electron microscopy. Mice were killed at indicated embryonic days. After fixating whole mice in fixation buffer (2.5% PFA, 2% glutaraldehyde, Sörens-buffer (pH 7.4)) for 1 h, further fixation of single organs was carried out in 2.5% glutaraldehyde at 4 °C. Samples were washed three times with cacodylate buffer

(pH 7.4, Science Services) and fixated in chromosmium acid (1.25% potassium dichromate (K₂Cr₂O₇; pH 7.2), 1% osmium tetroxide (OsO₄), 0.85% NaCl). After stepwise dehydration, samples were treated with propyleneoxide (Merck). Afterwards, samples were incubated in 1:1:1-mixture (Epon (246 mg ml⁻¹ dodecylsuccinic anhydride (Merck), 326 mg ml⁻¹ methyl-5-norbornene-1,3-dicarboxylic anhydride (Roth), 522 mg ml⁻¹ glycidyl ether 100 (Epon 812, EMS), 15 μ l ml⁻¹ 2,4,6-tris-dimethylaminomethyl-phenol (Roth) and propylene oxide (Merck)). Sections were generated using Leica Ultramicrotome and stained with haematoxylin/eosin or analysed by using a transmission-electron microscope EM 10 CR (Zeiss).

Haematoxylin/eosin staining. Sections were hydrated and afterwards incubated for at least 4 h in haematoxylin buffer (0.2 g l⁻¹ sodium iodate, 91.8 g l⁻¹ potassium alum sulphate, 50 g l⁻¹ chloralhydrate, 1 g l⁻¹ citric acid, 1 g l⁻¹ haematoxylin; Merck). Following a washing step with water, sections were stained for 20 s with Eosin (0.17% acid, 0.58% sodium acetate, 5 g l⁻¹ eosin Y; Merck) and washed again. For mounting, sections were again stepwise dehydrated, incubated with xylene and embedded with Eukitt (Kindler).

β -Galactosidase staining. Cryosections or whole embryos were perfused in phosphate buffer (23 mM sodium phosphate monobasic, 77 mM sodium phosphate dibasic, pH 7.3). After fixation (0.2% glutaraldehyde, 0.5 mM EGTA (pH 7.3), 2 mM magnesium chloride, 94 mM sodium phosphate (pH 7.3)), samples were washed three times in wash buffer (625 M magnesium chloride, 0.02% Nonidet-P40, 97.6 mM sodium phosphate, pH 7.3). Staining was carried out in staining solution (96% wash buffer as mentioned above, 4% di-methyl formamide, 10 mg ml⁻¹ X-gal (Roche), 2.12 mg potassium ferrocyanide, 1.64 mg potassium ferricyanide) for at least 16 h. Samples were washed as above, fixed with 4% PFA, washed twice in PBS and stepwise dehydrated. After incubation in xylene, sections could be mounted (DPX Mountant, Fluka). All reagents were obtained from Sigma, if not otherwise provided. Whole mounts were stained as described above, but were photographed after fixing and washing steps.

Bone histology. Analysis of bone and cartilage by alcian blue/alizarin red staining was done as described²⁷. In brief, skin of the embryo was removed and whole embryo was fixed in 95% ethanol for several days. All internal organs were removed and skeletal tissue was stained for at least 18 h using alcian blue (90% ethanol, 20% glacial acetic acid, 0.19 mg ml⁻¹ alcian blue). After washing twice with 95% ethanol, embryos were macerated in 2% potassium hydroxide. Next, embryos were stained with Alizarin Red S in 2% KOH solution. After stepwise dehydration of the embryo in KOH-glycerine solution, skeleton and cartilage were analysed. To examine calcified bone matrix, femurs and tibia from embryos were cryosectioned and stained by von Kossa solution as described²⁷.

Flow cytometry. For flow cytometry, cells were obtained from the diaphragm or the bone marrow as described above. Isolated cells were incubated with fluorochrome-conjugated antibodies according to standard procedures, measured or sorted using either a FACScalibur or a FACSAriaIII (BD Biosciences), and data were analysed using CELLQuestPro, FACSDiva Software (Becton Dickinson GmbH) and FlowJo 9.3 (TreeStar) software. For depletion of dead cells propidium iodide was used. Conjugated antibodies directed against the following markers were obtained from BD Biosciences: Mac1 (M1/70), Gr1 (RB6-8C5), B220 (RA3-6B2) and CD43 (RM4-5). Antibody CD45.2 (104) was obtained from eBioscience. All antibodies were used at a dilution of 1:250. For *Ebf3*- β -galactosidase detection, cells were isolated as described above, incubated in 1% FCS and 1 mM fluorescein digalactoside (FDG; Invitrogen) for 75 s at 37 °C and resuspended in ice-cold DPBS thereafter.

Gene expression analysis measurement by qPCR. In brief, mRNA was isolated from cells, whole organs or embryos using peqGOLD TriFast (Peqlab) according to manufacturer's instructions; organs and embryos were dispersed before using an Ultra Turrax T25 (IKA Labortechnik). cDNA was synthesized with a SuperScript II reverse transcriptase kit (Invitrogen). PCR reactions were performed in duplicate with SYBR Green I Master in a LightCycler 480II (Roche) with standard conditions: 95 °C for 10 min followed by 45 cycles of 95 °C for 10 s, 65 °C for 10 s and 72 °C for 10 s. Alternatively, 40 cycles with an annealing temperature of 63 °C were used. Primer sequences for *Atp2a1a + b*, *Atp2a 2a*, *Atp2a 2b*, *Atp2a 1 + 2*, *Atp2a 2*, *Atp2a 3*, *Sarcolipin* and *Phospholamban* are described²⁹; sequences for *MyHC- β* , *MyHC-IIA*, *MyHC-IIB*, *MyHC-IIX/D* are according to⁷, and all other sequences are listed in the Supplementary Methods. Target gene expression was normalized to *Hypoxanthine phosphoribosyltransferase (HPRT)* expression.

Cloning and site-directed mutagenesis. *Ebf3* was inserted into the mammalian expression vector pCMV_{cyto} using standard methods. CTAP-MyoD was obtained from Michael Rudnicki (University of Ottawa, Canada) as described³⁹. PCR using specific primer for genes or genomic DNA were designed with additional restriction sites as indicated below with italic letters. Subcloning was done by

digesting PCR products and relevant vectors with corresponding enzymes for at least 3 h, purified by gel extraction kit (Qiagen), and ligated for at least 16 h at 16 °C. The QuikChange site-directed mutagenesis kit (Stratagene) was used according to the manufacturer's instructions to introduce mutations into Ebf-binding sequences. Primer sequences to generate point mutations are indicated with small letters given below; binding site core palindromes are underlined. Sequencing was done for each construct to exclude errors.

Protein extraction and western blotting. Cells or organs were washed twice in ice-cold PBS and solubilised in the lysis buffer (50 mM Tris (pH 8), 150 mM NaCl, 1% NP-40, 1 $\mu\text{g ml}^{-1}$ leupeptin, 1 $\mu\text{g ml}^{-1}$ aprotinin, 100 $\mu\text{g ml}^{-1}$ PMSF) using Ultra Turrax T25. The samples were lysed for 40 min on ice. The supernatant (soluble whole-cell lysate) was fractionated on a 10–12% SDS-polyacrylamide gel and then transferred onto nitrocellulose membranes (Protran, Whatman). Membranes were first blocked in 5% milk-PBS-Tween and then incubated for 14 h at 4 °C with 5% milk-PBS-Tween containing the first antibody in a dilution recommended by the manufacturer. Membranes were washed three times with PBS-Tween, incubated with 5% milk-PBS-Tween, containing alkaline phosphatase-conjugated secondary polyclonal antibody, and then washed as mentioned above. Signals were detected using detection mixture (0.1M Tris-HCl (pH 8.6), 0.25 mg ml⁻¹ luminol, 0.11 mg ml⁻¹ para-hydroxy-conmarin acid, 0.009% H₂O₂) and Hyperfilm ECL (Amersham). The anti- β -Actin (AC-74), α -Flag (M2; F3165), α -Serca1 (adult; I1H11) and secondary α -mouse-IgG,HRP antibodies were obtained from Sigma. The anti- β -Tubulin (5H1) was obtained from BD Pharmingen and α -Serca1 (embryonic; VE121G9) antibody from Thermo Scientific. The secondary α -rat-IgG + IgM,HRP antibody was purchased from Jackson Immuno Research. Bands in western blot experiments were quantified using the open source software ImageJ (<http://rsb.info.nih.gov/ij/>; W. S. Rasband, NIH, National Institutes of Health, Bethesda, MD).

Statistics. *P*-values were determined with the Student's two-tailed *t*-test for independent samples, assuming equal variances on all experimental data sets.

EMSA. Double-stranded oligonucleotides were annealed in annealing buffer (10 mM Tris/HCl (pH 7.4), 10 mM MgCl₂, 50 mM NaCl) and labelled by filling up with Klenow enzyme, [α -P³²]-dCTP, and unlabelled dATP, dGTP and dTTP and purified using Sephadex G50 columns (Amersham Bioscience). The probes used, are listed below. Probes with mutations (small letters) in Ebf-binding sites (underlined) were synthesized as shown in Fig. 6a. EMSA was performed as following: 5 μg protein extracts from HEK293T cells (as described in protein extraction) was mixed in either binding buffer 1 (10 mM HEPES (pH 7.9), 70 mM KCl, 4% glycerol, 1 mM EDTA, 1 mM DTT, 1 \times protease-inhibitor (complete mini EDTA-free, Roche), 2 μl poly(dIdC) (1 mg ml⁻¹, Sigma), 2 μl BSA (1 mg ml⁻¹), 2.5 mM MgCl₂) or for M2-binding site in binding buffer 2 A (20 mM HEPES (pH 7.9), 75 mM NaCl, 1% glycerol, 1 $\mu\text{g ml}^{-1}$ salmon sperm DNA, 2 mM DTT, 1 \times protease-inhibitor (complete mini EDTA-free, Roche), 1 μl poly(dIdC) (1 mg ml⁻¹, Sigma) 2 μl BSA (1 mg ml⁻¹), 2 mM MgCl₂) with either wild-type or mutated probe DNA (250 ng μl^{-1}), anti-Flag M2 (F3165; Sigma) antibody or 10-fold concentrated unlabelled probe for competition as indicated. Binding complexes were fractionated on a 4% polyacrylamide gel. After drying of the gel, signals were detected using Biomax MS films (Kodak).

Chromatin Immunoprecipitation. For ChIP assay, either C2C12 cells were transiently transfected for 2 days or single-cell suspensions of 10 diaphragms of *Ebf3*^{+/+} and *Ebf3*^{-/-} mice each were pooled, resuspended in IP-Buffer (10 mM Hepes (pH 7.9), 10 mM KCl, 1.5 mM MgCl₂, 0.34 M sucrose, 10% protein inhibitors (complete mini EDTA-free, Roche) in glycerol, 0.1% Triton X-100) and partially digested in 1,000 U Mnase (NEB) for 2 min at 37 °C. Mnase was inactivated by adding 10 mM EGTA. Afterwards, 150 mM KCl and 0.2% TritonX-100 were added and immunoprecipitation was performed with α -Flag-coupled magnetic beads (M2; Sigma) or an α -MyoD specific antibody (5.8A, Santa Cruz Biotechnology) for at least 16 h at 4 °C under rotation. Then samples were washed twice with washing buffer A (50 mM Hepes (pH 7.9), 140 mM NaCl, 1 mM EDTA, 1% Triton X-100, 0.1% Na-deoxycholate, 0.1% SDS) and twice with washing buffer 2 (washing buffer 1, 500 mM NaCl) for 10 min. Precipitated complexes were eluted in elution buffer (50 mM Tris (pH 8.0), 1 mM EDTA, 1% SDS), reverse crosslinked by incubation at 65 °C for at least 16 h and purified using NucleoSpin PCR purification kit (Macherey-Nagel). DNA was used for RT-PCR as indicated above, and oligonucleotides and PCR programme are listed above. Input samples were amplified simultaneously to internal controls.

Transient transfections and reporter assay. C2C12 cells were transfected by Lipofectamine 2000 (Invitrogen) as described in manufacturer's protocol with a 1:3 ratio of DNA (μg) and Lipofectamine (μl). HEK293T cells were transfected using polyethylenimine (PEI, 1 mg ml⁻¹; Sigma) according to the standard conditions with a 1:1 ratio of DNA (μg) and PEI (μl). For reporter assays, HEK293T cells were transfected with 5 μg of plasmid DNA (composed of reporter/luciferase (pCMVcyto), activator (pBLLuc5) and β -Galactosidase (pCMVlacZ) plasmids;

5:10:1). Cells were harvested in 100 μl reporter lysis buffer (10% glycerol, 1% Triton X-100, 2 mM EDTA, 25 mM Tris (HCl; pH 7.8), 2 mM DTT) 48 h post-transfection. Measurement of luciferase activity was carried out by adding assay buffer (20 mM tricin, 1.07 mM magnesium carbonate pentahydrate, 2.67 mM MgSO₄, 33.3 mM DTT, 0.1 mM EDTA, 530 μM ATP, 270 μM acetyl-coenzyme A, 470 μM D(-)-luciferin (Roche), pH 5.8) to the sample duplicates at 560 nm in the micro-plate luminometer OrionII. β -Galactosidase activity was measured at 475 nm after adding first assay buffer (1% Tropix GalactonPlus; Applied Biosystems, 1 mM MgCl₂, 100 mM Na-P pH 8) and 20 min later activation buffer (0.2 M NaOH; 10% Tropix Emerald Enhancer; Applied Biosystems).

References

- Buckingham, M. & Vincent, S. D. Distinct and dynamic myogenic populations in the vertebrate embryo. *Curr. Opin. Genet. Dev.* **19**, 444–453 (2009).
- Relaix, F., Rocancourt, D., Mansouri, A. & Buckingham, M. A Pax3/Pax7-dependent population of skeletal muscle progenitor cells. *Nature* **435**, 948–953 (2005).
- Bismuth, K. & Relaix, F. Genetic regulation of skeletal muscle development. *Exp. Cell Res.* **316**, 3081–3086 (2010).
- Pownall, M. E., Gustafsson, M. K. & Emerson, Jr C. P. Myogenic regulatory factors and the specification of muscle progenitors in vertebrate embryos. *Annu. Rev. Cell Dev. Biol.* **18**, 747–783 (2002).
- Gordon, A. M., Homsher, E. & Regnier, M. Regulation of contraction in striated muscle. *Physiol. Rev.* **80**, 853–924 (2000).
- Squire, J. M. & Morris, E. P. A new look at thin filament regulation in vertebrate skeletal muscle. *FASEB J.* **12**, 761–771 (1998).
- Mok, G. F. & Sweetman, D. Many routes to the same destination: lessons from skeletal muscle development. *Reproduction* **141**, 301–312 (2011).
- Cao, Y. *et al.* Genome-wide MyoD binding in skeletal muscle cells: a potential for broad cellular reprogramming. *Dev. Cell* **18**, 662–674 (2010).
- Dressel, U. *et al.* A dynamic role for HDAC7 in MEF2-mediated muscle differentiation. *J. Biol. Chem.* **276**, 17007–17013 (2001).
- Puri, P. L. *et al.* Class I histone deacetylases sequentially interact with MyoD and pRb during skeletal myogenesis. *Mol. Cell* **8**, 885–897 (2001).
- Ackerman, K. G. & Greer, J. J. Development of the diaphragm and genetic mouse models of diaphragmatic defects. *Am. J. Med. Genet. C. Semin. Med. Genet.* **145C**, 109–116 (2007).
- Merrell, A. J. & Kardon, G. Development of the diaphragm—a skeletal muscle essential for mammalian respiration. *FEBS J.* **280**, 4026–4035 (2013).
- Dubois, L. & Vincent, A. The COE—Collier/Olf1/EBF-transcription factors: structural conservation and diversity of developmental functions. *Mech. Dev.* **108**, 3–12 (2001).
- Liberg, D., Sigvardsson, M. & Akerblad, P. EBF/Olf/Collier family of transcription factors: regulators of differentiation in cells originating from all three embryonal germ layers. *Cell Biol.* **22**, 8389–8397 (2002).
- Wang, S. S., Betz, A. G. & Reed, R. R. Cloning of a novel Olf-1/EBF-like gene, O/E-4, by degenerate oligo-based direct selection. *Mol. Cell Neurosci.* **20**, 404–414 (2002).
- Wang, S. S., Lewcock, J. W., Feinstein, P., Mombaerts, P. & Reed, R. R. Genetic disruptions of O/E2 and O/E3 genes reveal involvement in olfactory receptor neuron projection. *Development* **131**, 1377–1388 (2004).
- Chiara, F. *et al.* Early B-cell factors 2 and 3 (EBF2/3) regulate early migration of Cajal-Retzius cells from the cortical hem. *Dev. Biol.* **365**, 277–289 (2012).
- Garel, S. *et al.* Family of Ebf/Olf-1-related genes potentially involved in neuronal differentiation and regional specification in the central nervous system. *Dev. Dyn.* **210**, 191–205 (1997).
- Wang, S. S., Tsai, R. Y. & Reed, R. R. The characterization of the Olf-1/EBF-like HLH transcription factor family: implications in olfactory gene regulation and neuronal development. *J. Neurosci.* **17**, 4149–4158 (1997).
- Pozzoli, O., Bosetti, A., Croci, L., Consalez, G. G. & Vetter, M. L. Xebf3 is a regulator of neuronal differentiation during primary neurogenesis in *Xenopus*. *Dev. Biol.* **233**, 495–512 (2001).
- Liao, D. Emerging roles of the EBF family of transcription factors in tumor suppression. *Mol. Cancer Res.* **7**, 1893–1901 (2009).
- Zhao, L. Y. *et al.* An EBF3-mediated transcriptional program that induces cell cycle arrest and apoptosis. *Cancer Res.* **66**, 9445–9452 (2006).
- Zardo, G. *et al.* Integrated genomic and epigenomic analyses pinpoint biallelic gene inactivation in tumors. *Nat. Genet.* **32**, 453–458 (2002).
- Kim, J., Min, S. Y., Lee, H. E. & Kim, W. H. Aberrant DNA methylation and tumor suppressive activity of the EBF3 gene in gastric carcinoma. *Int. J. Cancer* **130**, 817–826 (2012).
- Agbulut, O., Noirez, P., Beaumont, F. & Butler-Browne, G. Myosin heavy chain isoforms in postnatal muscle development of mice. *Biol. Cell* **95**, 399–406 (2003).
- Pette, D. & Staron, R. S. Cellular and molecular diversities of mammalian skeletal muscle fibers. *Rev. Physiol. Biochem. Pharmacol.* **116**, 1–76 (1990).
- Kieslinger, M. *et al.* EBF2 regulates osteoblast-dependent differentiation of osteoclasts. *Dev. Cell* **9**, 757–767 (2005).

28. McCool, F. D. & Tzelepis, G. E. Dysfunction of the diaphragm. *N. Engl. J. Med.* **366**, 932–942 (2012).
29. Pan, Y. *et al.* Targeted disruption of the ATP2A1 gene encoding the sarco(endo)plasmic reticulum Ca²⁺ ATPase isoform 1 (SERCA1) impairs diaphragm function and is lethal in neonatal mice. *J. Biol. Chem.* **278**, 13367–13375 (2003).
30. Goonasekera, S. A. *et al.* Mitigation of muscular dystrophy in mice by SERCA overexpression in skeletal muscle. *J. Clin. Invest.* **121**, 1044–1052 (2011).
31. Schleef, M. *et al.* The gene encoding sarcoplasmic reticulum calcium ATPase-1 (Atp2a1) maps to distal mouse chromosome 7. *Mamm. Genome* **7**, 788 (1996).
32. Schug, J. Using TESS to predict transcription factor binding sites in DNA sequence. *Curr. Protoc. Bioinformatics* Chapter 2, Unit 2 6, doi:10.1002/0471250953.bi0206s21 (2008).
33. Hagman, J., Travis, A. & Grosschedl, R. A novel lineage-specific nuclear factor regulates mb-1 gene transcription at the early stages of B cell differentiation. *EMBO J.* **10**, 3409–3417 (1991).
34. Travis, A., Hagman, J., Hwang, L. & Grosschedl, R. Purification of early-B-cell factor and characterization of its DNA-binding specificity. *Mol. Cell Biol.* **13**, 3392–3400 (1993).
35. O’Riordan, M. & Grosschedl, R. Coordinate regulation of B cell differentiation by the transcription factors EBF and E2A. *Immunity* **11**, 21–31 (1999).
36. Sigvardsson, M., O’Riordan, M. & Grosschedl, R. EBF and E47 collaborate to induce expression of the endogenous immunoglobulin surrogate light chain genes. *Immunity* **7**, 25–36 (1997).
37. Treiber, T. *et al.* Early B cell factor 1 regulates B cell gene networks by activation, repression, and transcription-independent poising of chromatin. *Immunity* **32**, 714–725 (2010).
38. Zeller, K. I. *et al.* Global mapping of c-Myc binding sites and target gene networks in human B cells. *Proc. Natl Acad. Sci. USA* **103**, 17834–17839 (2006).
39. Soleimani, V. D. *et al.* Snail regulates MyoD binding-site occupancy to direct enhancer switching and differentiation-specific transcription in myogenesis. *Mol. Cell* **47**, 457–468 (2012).
40. MacLennan, D. H., Brandl, C. J., Korczak, B. & Green, N. M. Amino-acid sequence of a Ca²⁺ + Mg²⁺ -dependent ATPase from rabbit muscle sarcoplasmic reticulum, deduced from its complementary DNA sequence. *Nature* **316**, 696–700 (1985).
41. Liu, Y., Chu, A., Chakroun, I., Islam, U. & Blais, A. Cooperation between myogenic regulatory factors and SIX family transcription factors is important for myoblast differentiation. *Nucleic Acids Res.* **38**, 6857–6871 (2010).
42. Sigvardsson, M. Overlapping expression of early B-cell factor and basic helix-loop-helix proteins as a mechanism to dictate B-lineage-specific activity of the lambda₅ promoter. *Mol. Cell Biol.* **20**, 3640–3654 (2000).
43. Daburon, V. *et al.* The metazoan history of the COE transcription factors. Selection of a variant HLH motif by mandatory inclusion of a duplicated exon in vertebrates. *BMC Evol. Biol.* **8**, 131 (2008).
44. Krzemien, J. *et al.* Control of blood cell homeostasis in Drosophila larvae by the posterior signalling centre. *Nature* **446**, 325–328 (2007).
45. Kieslinger, M., Hiechinger, S., Dobreva, G., Consalez, G. G. & Grosschedl, R. Early B cell factor 2 regulates hematopoietic stem cell homeostasis in a cell-nonautonomous manner. *Cell Stem Cell* **7**, 496–507 (2010).
46. Crozatier, M. & Vincent, A. Requirement for the Drosophila COE transcription factor Collier in formation of an embryonic muscle: transcriptional response to notch signalling. *Development* **126**, 1495–1504 (1999).
47. Dubois, L. *et al.* Collier transcription in a single Drosophila muscle lineage: the combinatorial control of muscle identity. *Development* **134**, 4347–4355 (2007).
48. Enriquez, J., de Taffin, M., Crozatier, M., Vincent, A. & Dubois, L. Combinatorial coding of Drosophila muscle shape by Collier and Nautilus. *Dev. Biol.* **363**, 27–39 (2012).
49. Green, Y. S. & Vetter, M. L. EBF proteins participate in transcriptional regulation of Xenopus muscle development. *Dev. Biol.* **358**, 240–250 (2011).
50. Karpati, G., Charuk, J., Carpenter, S., Jablecki, C. & Holland, P. Myopathy caused by a deficiency of Ca²⁺ -adenosine triphosphatase in sarcoplasmic reticulum (Brody’s disease). *Ann. Neurol.* **20**, 38–49 (1986).
51. Odermatt, A. *et al.* Mutations in the gene-encoding SERCA1, the fast-twitch skeletal muscle sarcoplasmic reticulum Ca²⁺ ATPase, are associated with Brody disease. *Nat. Genet.* **14**, 191–194 (1996).
52. Zhang, Y. *et al.* Characterization of cDNA and genomic DNA encoding SERCA1, the Ca(2+) -ATPase of human fast-twitch skeletal muscle sarcoplasmic reticulum, and its elimination as a candidate gene for Brody disease. *Genomics* **30**, 415–424 (1995).
53. Sambrook, J., Fritsch, E. F. & Maniatis, T. *Molecular Cloning: a Laboratory Manual* 2nd edn (Cold Spring Harbor Laboratory, 1989).
54. Lallemand, Y., Luria, V., Haffner-Krausz, R. & Lonai, P. Maternally expressed PGK-Cre transgene as a tool for early and uniform activation of the Cre site-specific recombinase. *Transgenic Res.* **7**, 105–112 (1998).
55. Whitlock, C. A. & Witte, O. N. Long-term culture of B lymphocytes and their precursors from murine bone marrow. *Proc. Natl Acad. Sci. USA* **79**, 3608–3612 (1982).
56. Noh, O. J., Park, Y. H., Chung, Y. W. & Kim, I. Y. Transcriptional regulation of selenoprotein W by MyoD during early skeletal muscle differentiation. *J. Biol. Chem.* **285**, 40496–40507 (2010).
57. Sartorius, C. A. *et al.* Myosin heavy chains IIa and IIb are functionally distinct in the mouse. *J. Cell Biol.* **141**, 943–953 (1998).

Acknowledgements

We thank Michael Rudnicki for sharing information on MyoD and Myf5 binding sites, Jeffrey Molkenin for sharing the *Atp2a1*-transgenic mice, Michaela Aichler and Frauke Neff for help with histology and electron microscopy, Moritz Förderer, Tihomir Georgiev and Cornelia Weber for assistance in the analysis of muscle function and Katharina Zettl and Carolina Galgenmüller for excellent technical assistance. We also would like to thank Petra Kopp for help with experimental design and drafting of the figures and Quiongman Wang for assistance in qPCR. This work was supported by grants from the German Research Foundation (DFG, TRR54; FOR1586; FOR2033) and by a stipend of the Max Planck Society.

Author contributions

Performed experiments: S.J., J.K. and T.W. Pathology: T.K.-R., I.E. Electrophysiology and force measurements: M.M., R.F. Generation of *Ebf3* knock-out mice: M.G.-D., P.C. Contributed to data analysis and writing: L.C.H. Designed the study and wrote the manuscript: M.K.

Additional information

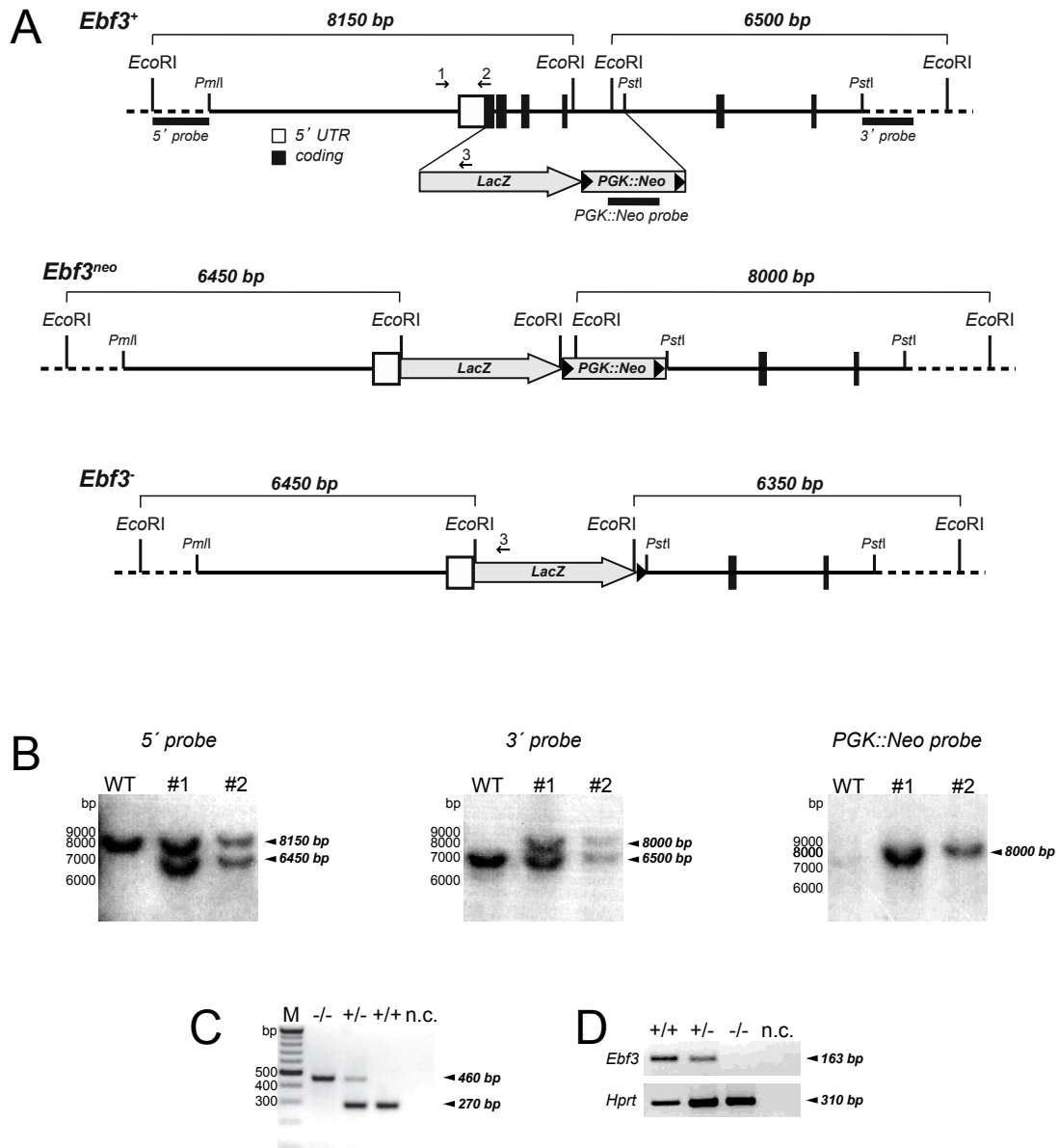
Supplementary Information accompanies this paper at <http://www.nature.com/naturecommunications>

Competing financial interests: The authors declare no competing financial interests.

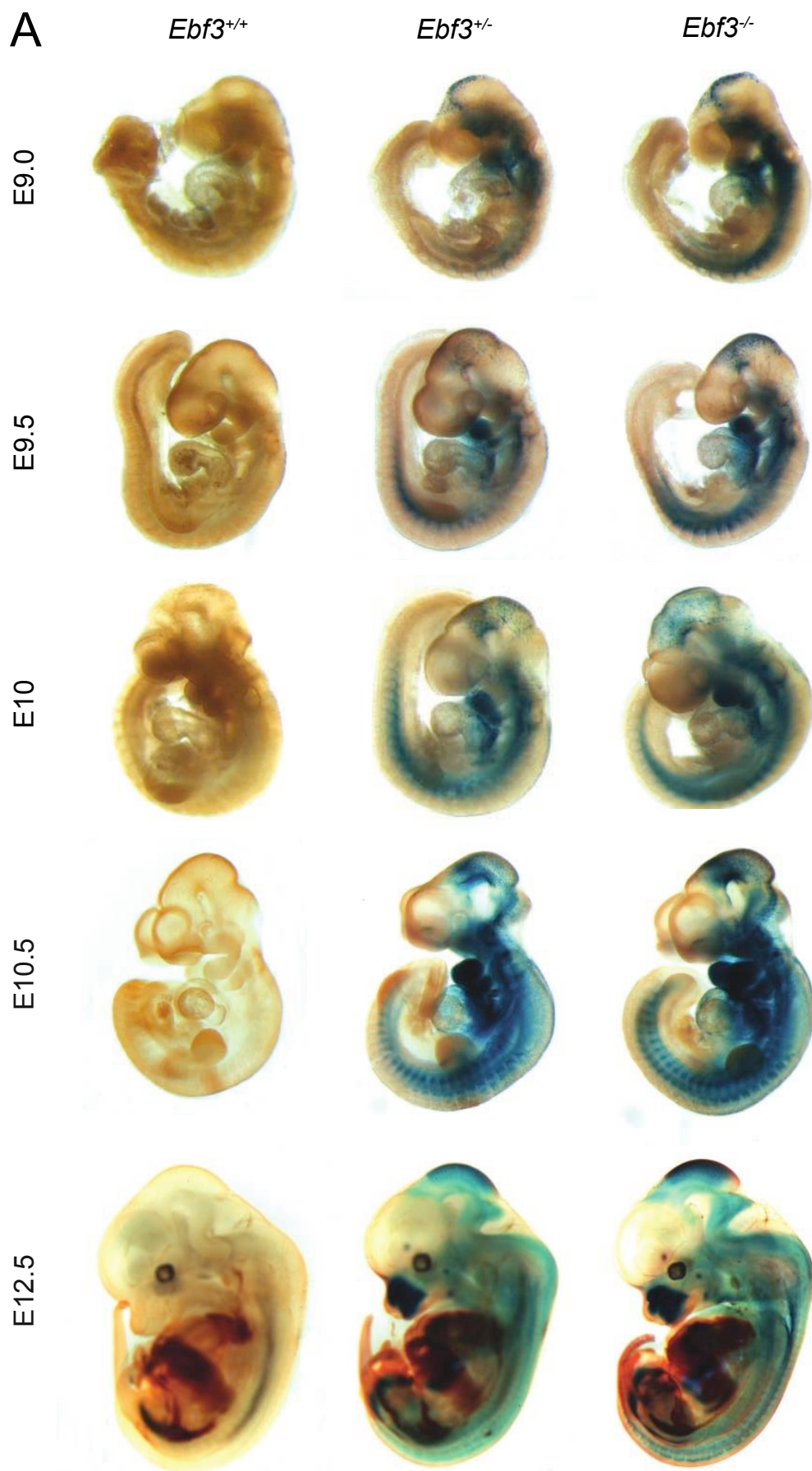
Reprints and permission information is available online at <http://npg.nature.com/reprintsandpermissions/>

How to cite this article: Jin, S. *et al.* Ebf factors and MyoD cooperate to regulate muscle relaxation via *Atp2a1*. *Nat. Commun.* **5**:3793 doi: 10.1038/ncomms4793 (2014).

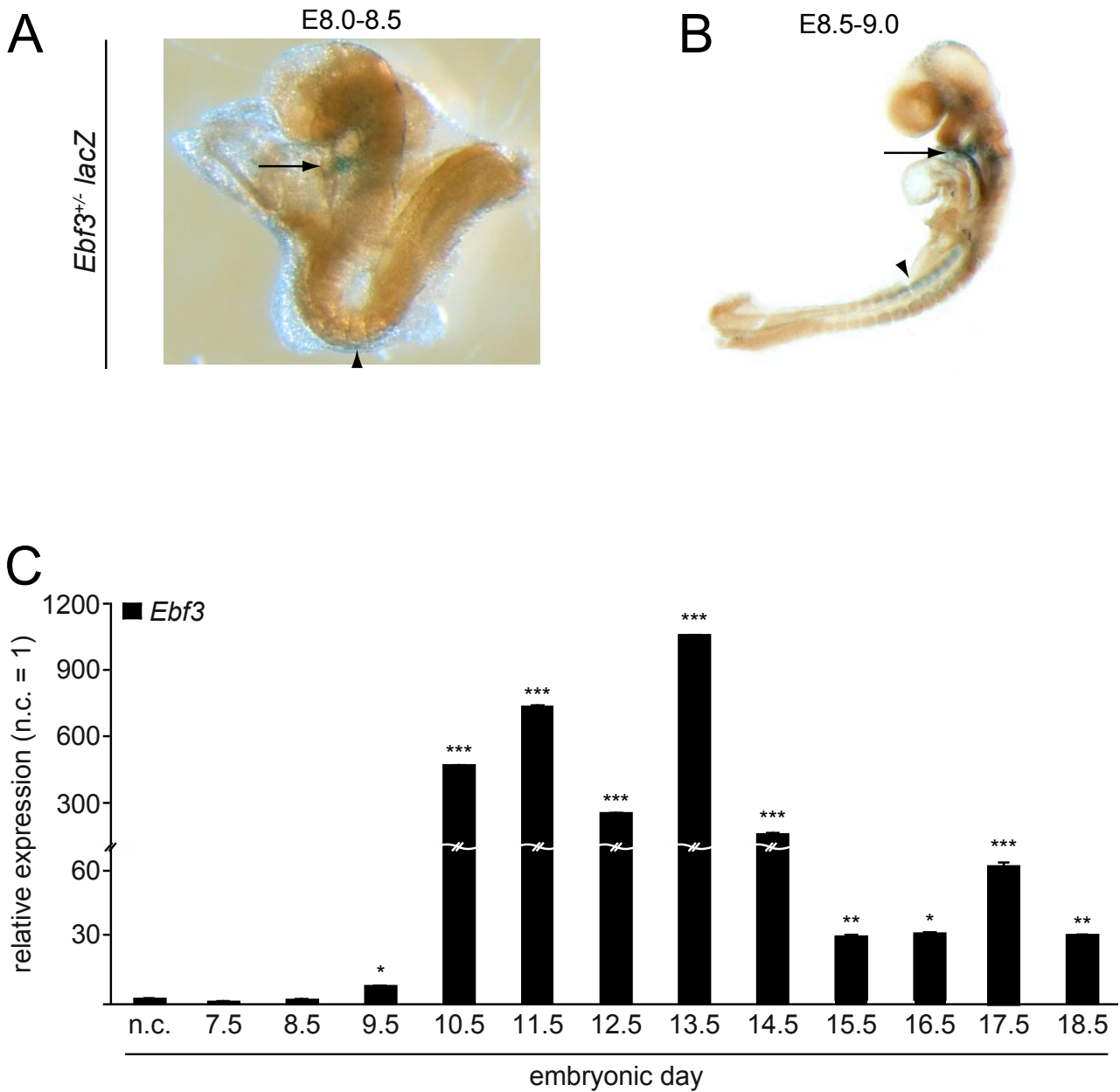
SUPPLEMENTARY FIGURES



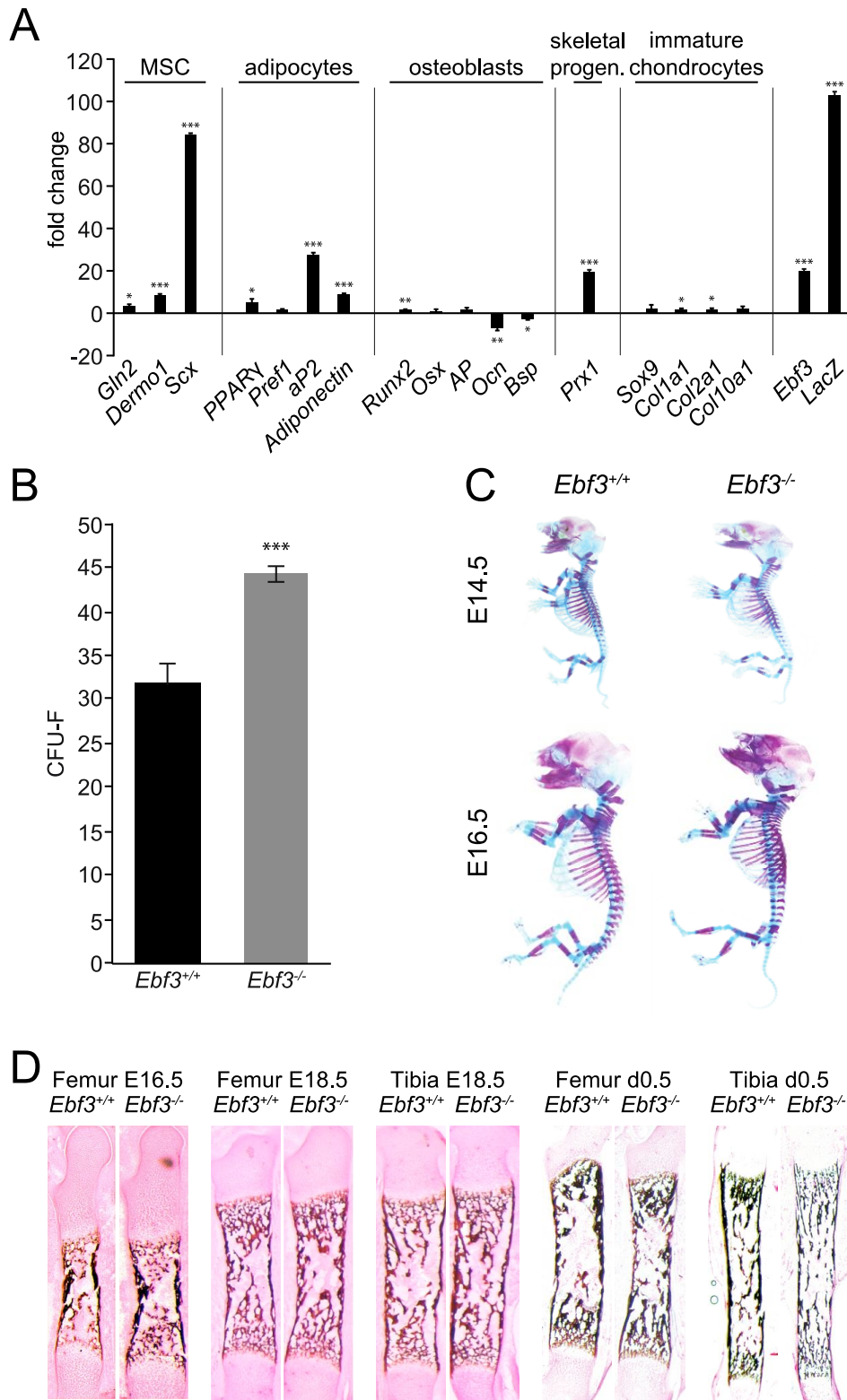
Supplementary Figure 1 Generation of *Ebf3*-Deficient Mice. (A) Schematic representation of *Ebf3* wild-type (*Ebf3*⁺) and mutant (*Ebf3*⁻) alleles. A solid line represents regions involved in the targeting construct, while a dashed line depicts genomic regions beyond the targeting construct. The targeting strategy consists of replacing *Ebf3* genomic DNA from the translation start codon to a *PstI* site in intron 4, corresponding to part of the DNA binding domain, by an in frame *NLS-LacZ* gene followed by a *PGK::Neo* cassette flanked by *loxP* sites indicated by two arrowheads. Boxes in the schema represent exons. The white box corresponds to the 5' untranslated region, while black boxes indicate coding regions. Southern blot probes corresponding to 5' and 3' regions, and to a fragment of the *PGK::Neo* cassette are shown. Small arrows with numbers 1-3 indicate the position of primers used for genotyping. The lower two panels represent the *Ebf3* locus after recombination with the targeting vector (*Ebf3*^{neo}) and after removal of the *PGK::Neo* cassette via *PGK-Cre* mediated recombination (*Ebf3*). (B) Southern blot using 5' probe (left), 3' probe (middle) and *PGK::Neo* probe (right) as indicated in A with genomic DNA of wild-type and two mutant ES cell clones after *EcoRI* digestion. (C) Example of genotyping genomic DNA from tails of wild-type (+/+), *Ebf3*-heterozygous (+/-) and *Ebf3*-deficient (-/-) mice by PCR using primers 1, 2 and 3 as indicated in A. No template is used as negative control. (D) Expression of *Ebf3* is analysed in bones of E18.5 mice of the indicated genotypes (see above) by RT-PCR using 27 cycles.



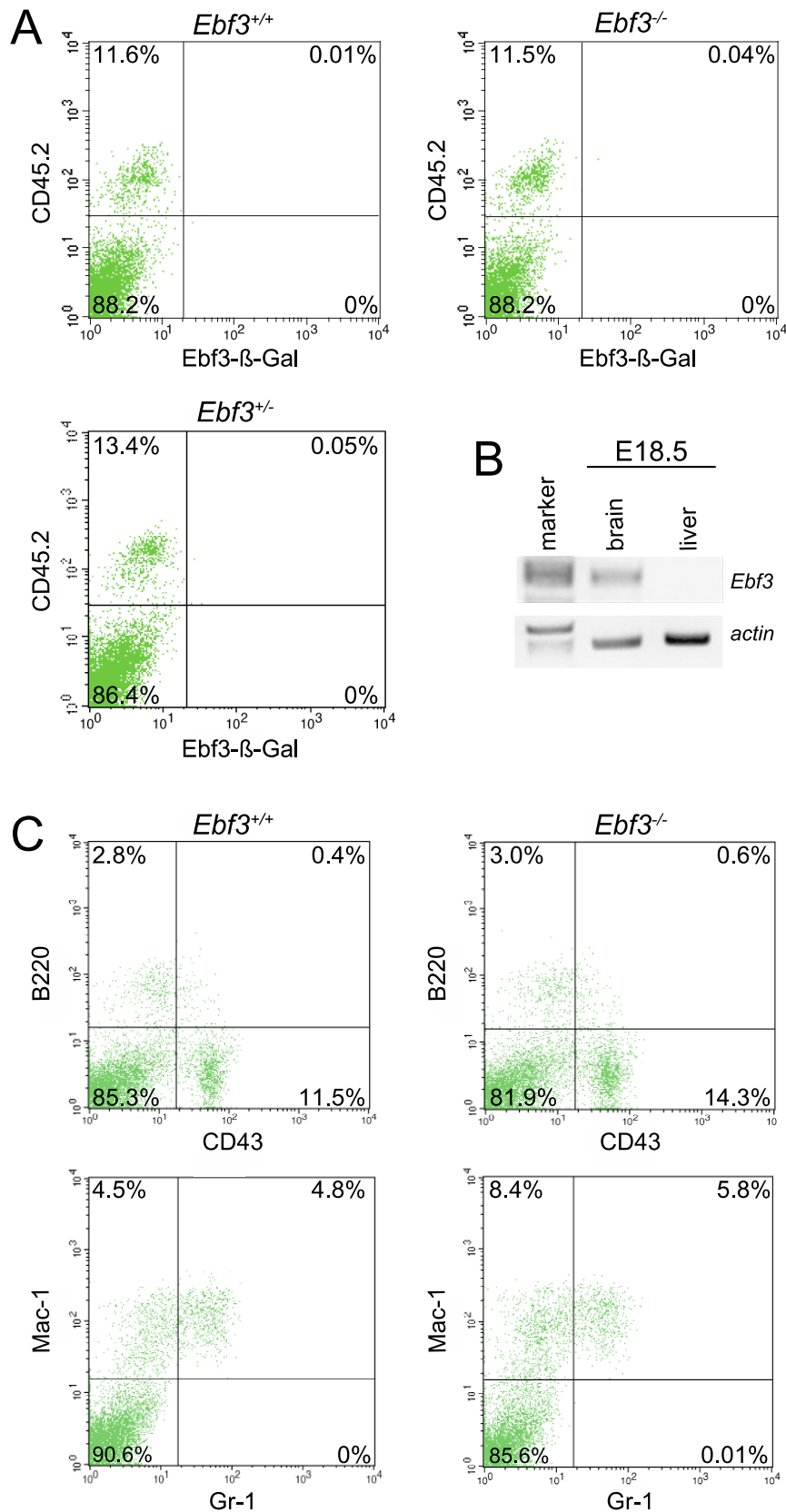
Supplementary Figure 2 Expression of *Ebf3* During Embryogenesis. Whole-mount *Ebf3*- β -galactosidase staining of wild-type (left row), *Ebf3*^{+/-} (middle row) and *Ebf3*^{-/-} (right row) embryos from E9.5 to E12.5 as indicated.



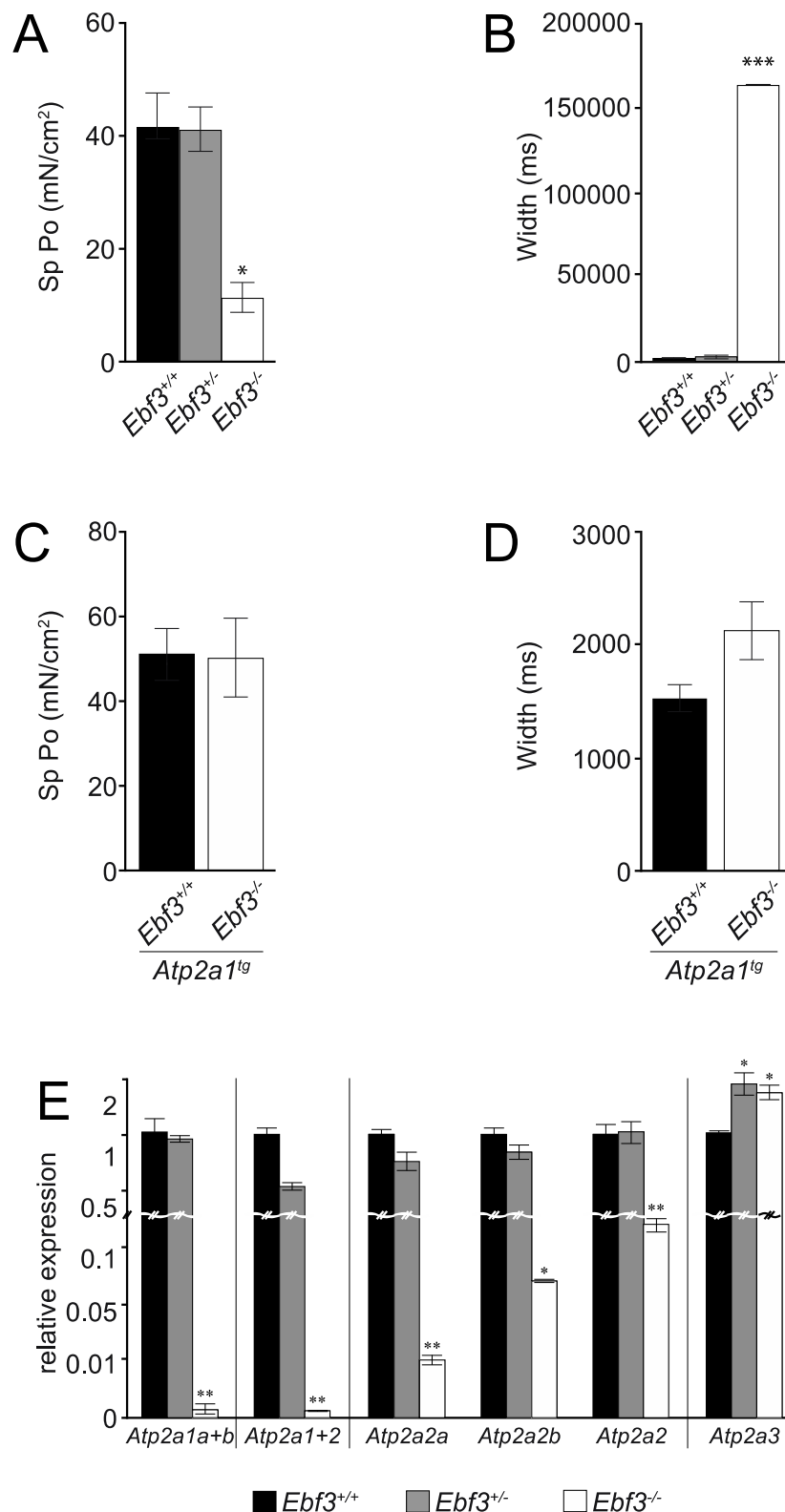
Supplementary Figure 3 Embryonic and Cell Type Specific Expression of *Ebf3*. (A-B) Whole mount β -gal staining of *Ebf3*^{+/-} embryos at E8.0 to 8.5 (A) and E8.5 to 9.0 (B). Somites are indicated by an arrowhead, branchial arches by an arrow. (C) Quantitative PCR analysis of the expression of *Ebf3* in whole embryos from E7.5 to E18.5 as indicated. The pro-B cell line Ba/F3 were used as a negative control and set to 1. n=3; error bars=SD; * p<0.05, ** p<0.01, *** p<0.001.



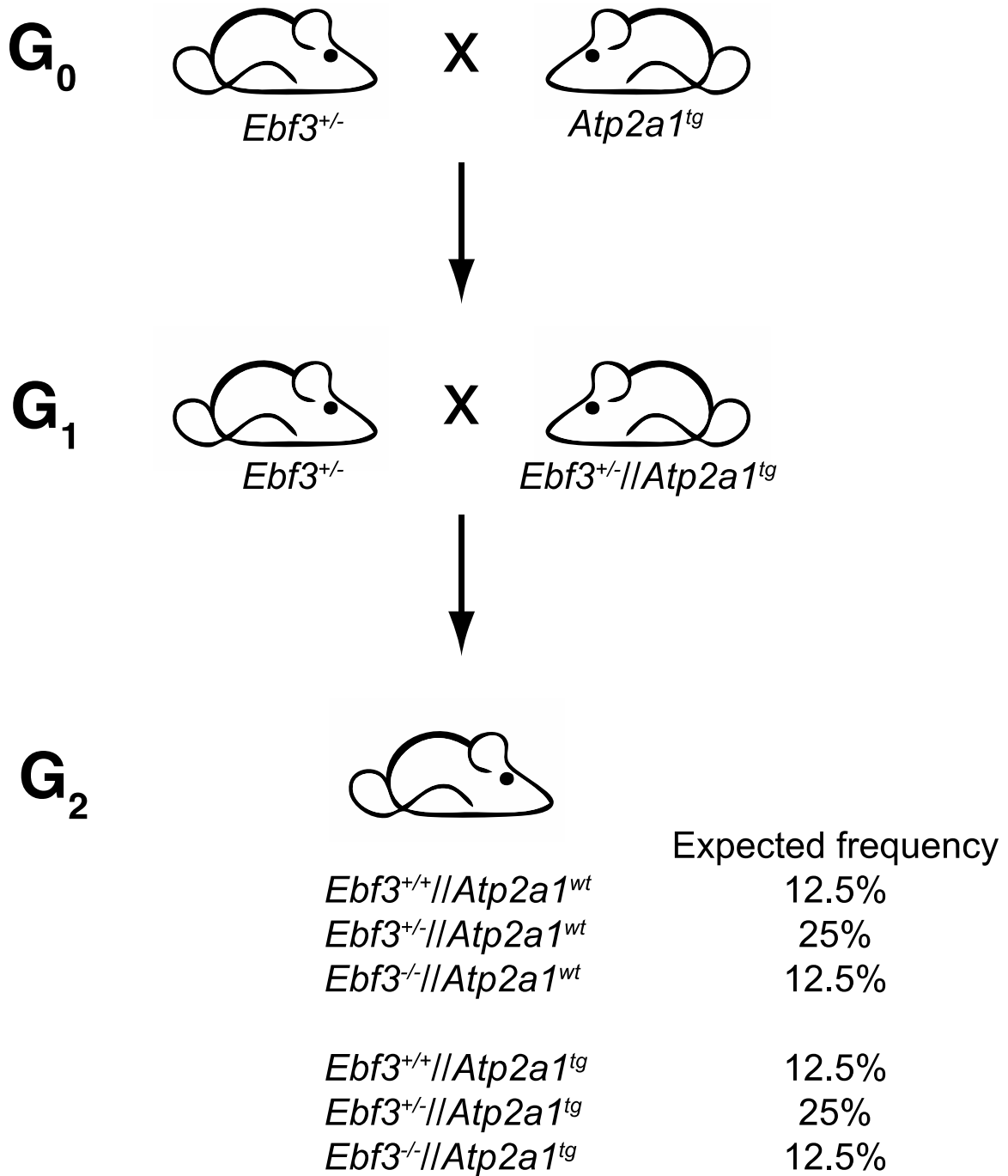
Supplementary Figure 4 *Ebf3* is Expressed by Immature Mesenchymal Cells, but is not Required for Normal Bone Formation. (A) *Ebf3*- β -gal expressing and non-expressing cells were sorted from the bone marrow of E18.5 *Ebf3*^{+/+} embryos and subjected to qPCR analysis. Marker genes for different developmental stages of various mesenchymal cell lineages are indicated. The fold change in the expression between *Ebf3*- β -gal positive and *Ebf3*- β -gal negative cells is shown. n=5, error bars=SD. * p<0.05, ** p<0.01, *** p<0.001. (B) Determination of CFU-F frequency from the bone marrow of E18.5 *Ebf3*^{+/+} and *Ebf3*^{-/-} mice. n=3 (*Ebf3*^{-/-}) to 4 (*Ebf3*^{+/+}); error bars=SD; ***p<0.001. (C) Alcian blue / alizarin red staining of cartilage and bone of wild-type or *Ebf3*^{-/-} skeletons at E14.5 and E16.5. (D) Von Kossa and nuclear fast red staining of longitudinal sections of tibia and femur of *Ebf3*^{+/+} and *Ebf3*^{-/-} embryos from E16.5 to D0.5 as indicated.



Supplementary Figure 5 *Ebf3* is Not Expressed in the Fetal Liver and is Not Required for Normal Embryonic Hematopoiesis. (A) Analysis of fetal liver cells from E18.5 *Ebf3*^{+/+}, *Ebf3*^{+/-} and *Ebf3*^{-/-} embryos for the expression of *Ebf3*-β-gal and CD45.2 by flow cytometry. n=5. (B) Semi-quantitative RT-PCR for the expression of *Ebf3* in liver and brain of wild-type E18.5 embryos. Primers specific for β-actin are used as control. n=3. (C) Representative examples of fetal liver cells analysed by flow cytometry for the percentage of B220/CD43 and Mac1/Gr1 from E18.5 wild-type and *Ebf3*^{-/-} embryos. n=3.



Supplementary Figure 6 (A-D) Tetanus stimulation (50V, 1ms, 120 Hz for 500ms) of diaphragm muscle from newborn mice of the indicated genotypes. (A) Measurement of force produced in response to tetanus stimulation normalised to the cross sectional area. (B) Total duration of muscle contraction after tetanus stimulation. n=5 *Ebf3*^{+/+}, n=7 *Ebf3*^{+/-}, n=4 *Ebf3*^{-/-}; error bars = SD; * p<0.05, ** p<0.01, *** p<0.001. (C) Measurement of force produced in response to tetanus stimulation normalised to the cross sectional area. (D) Total duration of muscle contraction after tetanus stimulation. n=3; error bars = SD. (E) Analysis of the expression of various splice variants of the *Atp2a1*, *Atp2a2* and *Atp2a3* genes in E18.5 embryonic diaphragm of the indicated genotypes; n=3, *p<0.05, **p<0.01.



Supplementary Figure 7 Indication of the breeding scheme used to generate *Ebf3/Atp2a1* double mutant mice. A breeding scheme involving three generations was followed (G₀-G₂), in which the mating of *Ebf3^{+/-}* to *Ebf3^{+/-}//Atp2a1^{tg}* mice in G₁ results in a 50% distribution of the *Atp2a1* transgene in G₂. Within these 50%, a Mendelian distribution of the wild-type and the mutant *Ebf3* allele should be observed in case *Ebf3* and the *Atp2a1* transgene segregate independently of each other. The expected frequencies for independent segregation are indicated.

SUPPLEMENTARY METHODS

Primers used in Gene Expression Analysis Measurement by qPCR

<i>Hprt</i> fwd	5'-TGCTGGTGAAAAGGACCTCTCG-3'
<i>Hprt</i> rev	5'-TCTGGGGACGCAGCAACTGA-3'
<i>Ebf3</i> fwd	5'-AGAGCCGAACAACGAGAAAA-3'
<i>Ebf3</i> rev	5'-GCACATCTCCGGATTCTTGT-3'
<i>Atp2a1</i> fwd	5'-ACACAGACCCTGTCCCTGAC-3'
<i>Atp2a1</i> rev	5'-TGCAGTGGAGTCTTGTCCTG-3'
<i>Prx1</i> fwd	5'-AGGCCAGAGTGCAGGTGTGGT-3'
<i>Prx1</i> rev	5'-TGGATGGCTGGGGAGCGTGT-3'
<i>Scx</i> fwd	5'-CTGTGGCGACGGGCAACCAT-3'
<i>Scx</i> rev	5'-GGCCTGGGTCAAGTGTTCGGC-3'
<i>Dermo1</i> fwd	5'-CAGCGCACCCAGTCGCTCAA-3'
<i>Dermo1</i> rev	5'-CAGGTGGGTCTGGCTTGCG-3'
<i>aP2</i> fwd	5'-GAAGTGGGAGTGGGCTTTGCCA-3'
<i>aP2</i> rev	5'-GGGCCCCGCCATCTAGGGTT-3'
<i>Adiponectin</i> fwd	5'-CACACCAGGCCGTGATGGCA-3'
<i>Adiponectin</i> rev	5'-CGGGTCTCCAGCCCCACACT-3'
<i>Pref-1</i> fwd	5'-CCATCGTGCGCAGAAGCCCA-3'
<i>Pref-1</i> rev	5'-GCCGAAAGCCAGCAGGAGCA-3'
<i>Col10a1</i> fwd	5'-ACCCCAAGGACCTAAAGGAA-3'
<i>Col10a1</i> rev	5'-CCCCAGGATACCCTGTTTTT-3'
<i>PPAR-gamma</i> fwd	5'-GATGGAAGACCACTCGCATT-3'
<i>PPAR-gamma</i> rev	5'-GGATCCGGCAGTTAAGATCA-3'
<i>Col1a1</i> fwd	5'-CACCTCAAGAGCCTGAGTC-3'
<i>Col1a1</i> rev	5'-GTTCCGGGCTGATGTACCAGT-3'
<i>Runx2</i> fwd	5'-TTTAGGGCGCATTTCCTCATC-3'
<i>Runx2</i> rev	5'-TGTCCTTGTGGATTAAGACTTG-3'
<i>Osx</i> fwd	5'-ACTCATCCCTATGGCTCGTG-3'
<i>Osx</i> rev	5'-GGTAGGGAGCTGGGTTAAGG-3'
<i>AP</i> fwd	5'-CACGCGATGCAACACCACTCAGG-3'
<i>AP</i> rev	5'-GCATGTCCCCGGGCTCAAAGA-3'
<i>Ocn</i> fwd	5'-ACCCTGGCTGCGCTCTGTCTCT-3'
<i>Ocn</i> rev	5'-GATGCGTTTGTAGGCGGTCTTCA-3'
<i>Bsp</i> fwd	5'-TACCGGCCACGCTACTTTCTTTAT-3'
<i>Bsp</i> rev	5'-GACCGCCAGCTCGTTTTTCATCC-3'
<i>Sox9</i> fwd	5'-CTGAAGGGCTACGACTGGAC-3'
<i>Sox9</i> rev	5'-TACTGGTCTGCCAGCTTCCT-3'
<i>Col2a1</i> fwd	5'-GCCAAGACCTGAAACTCTGC-3'
<i>Col2a1</i> rev	5'-CTTGCCCCACTTACCAGTGT-3'
β -Actin fwd	5'-GACGACATGGAGAAGATCTGG-3'

<i>β-Actin rev</i>	5-TGTGGTGGTGAAGCTGTAGC-3'
ChIP M1 fwd	5'-TGTCCCCTTTTCTCCATACC-3'
ChIP M1 rev	5'-CCCAAGCCAGTGAAGTACTGAGAG-3'
ChIP M2 fwd	5'-TAAGGGCCAAGAGGGCTTAT-3'
ChIP M2 rev	5'-CCCAGTTGCCTCAACTTCTC-3'
ChIP E1 fwd	5'-TGTTGCATCAGGGTGAGAGT-3'
ChIP E1 rev	5'-GCAGGGGGAGTAAGGATCTC-3'
ChIP E2 fwd	5'-GACACTAAATCCCTTGTTGATGG-3'
ChIP E2 rev	5'-GGGGACAGTGCAGATGGTAA-3'
<i>Ebf1 fwd</i>	5'-CATGTCCTGGCAGTCTCTGA-3'
<i>Ebf1 rev</i>	5'-CAACTCACTCCAGACCAGCA-3'
<i>Ebf2 fwd</i>	5'-TGGAGAATGACAAAGAGCAAG-3'
<i>Ebf2 rev</i>	5'-GGGTTTCCCGCTGTTTTCAA-3'
<i>Ebf4 fwd</i>	5'-TTGACTCCATGTGGAAGCAG-3'
<i>Ebf4 rev</i>	5'-GCAGTTCTGGTTGCATTTGA-3'
<i>Tpm1 fwd</i>	5'-TGAGCAAGCGGAGGCTGATAAG-3'
<i>Tpm1 rev</i>	5'-GCATCTTTGAGAGCCTCGGAGT-3'
<i>Eno3 fwd</i>	5'-CTGCTCCTGAAGGTCAACCAGA-3'
<i>Eno3 rev</i>	5'-GTCAGCGATGAAAGTGTCTTCGG-3'
<i>MyBP-C fwd</i>	5'-GAAGGAACTGGTGCCTGACAAC-3'
<i>MyBP-C rev</i>	5'-CTGTAGTCAGCCTCATCAGCAG-3'
<i>M-cadherin fwd</i>	5'-AGGACGAGCATAGCTGAAGGAG-3'
<i>M-cadherin rev</i>	5'-GTCCACTTGCAGCCAGTCTTCT-3'
<i>Rbm24 fwd</i>	5'-GTGAATCTGGCATACTTGGGAGC-3'
<i>Rbm24 rev</i>	5'-ATGACCACTCCAGGCTGCACAA-3'
<i>Tnnc1 fwd</i>	5'-GATGGTTCGGTGCATGAAGGAC-3'
<i>Tnnc1 rev</i>	5'-CTTCCGTAATGGTCTCACCTGTG-3'
<i>MyHC-EMB fwd</i>	5'-CTGGCTAAGTCGGAGGCAAAGA-3'
<i>MyHC-EMB rev</i>	5'-TCGCATCGTTCCTCAGCATCCA-3'
<i>MyHC-PN fwd</i>	5'-GGAGGACAAAGTCAACACCCTG-3'
<i>MyHC-PN rev</i>	5'-CCTCCAGTTTCTCTTGGCTCT-3'
<i>Mlc1f fwd</i>	5'-TTCGTTGAGGGTCTGCGTGTCT-3'
<i>Mlc1f rev</i>	5'-CAGCAACGCTTCTACCTCTTCC-3'
<i>Tnni2 fwd</i>	5'-GGCTCTAAGCACAAGGTGTGCA-3'
<i>Tnni2 rev</i>	5'-ATTCTTCTCCAGTCACCCACG-3'
<i>skeletal α-actin fwd</i>	5'-ACCATCGGCAATGAGCGTTTCC-3'
<i>skeletal α-actin rev</i>	5'-GCTGTTGTAGGTGGTCTCATGG-3'

Primers used for cloning and site-directed mutagenesis

<i>Ebf3</i> Luc fwd	5'-GTCGACATGTTTGGGATTTCAGGAGAA-3'
<i>Ebf3</i> Luc rev	5'-CTCGAGTCACATGGGCGGGAC-3'
<i>Atp2a1</i> pr.1 fwd	5'-AAGCTTGTGCTCTTTGCTCCCAACTC-3'
<i>Atp2a1</i> pr.1 rev	5'-GGATCCGACCCCAGTCCTACTTGCGC-3'
Δ M1 fwd	5'-GCTTCATCCAGCCTCAGccGTCCTGCTCTCAG-3'
Δ M1 rev	5'-CTGAGAGCAGGACcggCTGAGGCTGGATGAAGC-3'
Δ M2 fwd	5'-TGGAAAGATCTGCTCAGccGTGGGCTTGGAAGT-3'
Δ M2 rev	5'-CAGTTCCAAGCCCACcggCTGAGCAGATCTTTCCA-3'
Δ E1 fwd	5'-GGGGGTACCATGAAGaatTAGGGTTGAAGGCTAGTG-3'
Δ E1 rev	5'-CACTAGCCTTCAACCCTAattCTTCATGGTGACCCCC-3'
Δ E2 fwd	5'-GGCTGCAGCAACCCCTaatTAGGGTAAGGTTACCATCTG-3'
Δ E2 rev	5'-CAGATGGTAACCTTACCCTAattAGGGGTTGCTGCAGCC-3'
Δ X1 fwd	5'-CCCCGGCTGCTCCTCCTCCAGttacgaCTTGGGTGGAAATCAAAGATACCCC-3'
Δ X1 rev	5'-GGGGTATCTTTTGATTTCCACCCAAGtcgtaaCTGGAGGAGGAGCAGCCGGGG-3'
Δ X2 fwd	5'-GGGTTACCTGGCctatgtaGTGTCCCATTTC-3'
Δ X2 rev	5'-GAAAATGGGACACtacatagGCCAGGTAACCC-3'
Δ X3 fwd	5'-CTAGGGTAAGGTTACcaaaaGCACTGTCCCCTTGACT-3'
Δ X3 rev	5'-GTCAAGGGGACAGTGcttttGGTAAGCTTACCCTAG-3'
Δ X4 fwd	5'-GGAGAAGTTGAGGttacgaGGGGTGGGG-3'
Δ X4 rev	5'-CCCCACCCctcgtaaCCTCAACTTCTCC-3'
Δ X5 fwd	5'-CTCCCTCATAAGGACCcaaaaGGGGGCTGGG-3'
Δ X5 rev	5'-CAGCCCCcttttGGTCCTTATGAGGGAGTG-3'

Primers used in EMSA

<i>Atp2a1</i> M1 fwd	5'-GATGGCTGCCATCCAGCCTCAGGGGTCCTGCTC-3'
<i>Atp2a1</i> M1 rev	5'-CAGTGCAGATGGAGCAGGACCCCTGAGGCTGGATG-3'
<i>Atp2a1</i> Δ M1 fwd	5'-GATGGCTGCCATCCAGCCTCAGccGTCCTGCTC-3'
<i>Atp2a1</i> Δ M1 rev	5'-CAGTGCAGATGGAGCAGGACcggCTGAGGCTGGATG-3'
<i>Atp2a1</i> M2 fwd	5'-GATGGCTGCGAAAGATCTGCTCAGGGGTGGGCTTG-3'
<i>Atp2a1</i> M2 rev	5'-CAGTGCAGATGCAAGCCCACCCCTGAGCAGATCTTTTC-3'
<i>Atp2a1</i> Δ M2 fwd	5'-GATGGCTGCGAAAGATCTGCTCAGccGTGGGCTTG-3'
<i>Atp2a1</i> Δ M2 rev	5'-CAGTGCAGATGCAAGCCCACcggCTGAGCAGATCTTTTC-3'
<i>Atp2a1</i> E1 fwd	5'-GATGGCTGCCATGAAGCCCTAGGGTTGAAGG-3'
<i>Atp2a1</i> E1 rev	5'-CAGTGCAGATGCCTTCAACCCTAGGGCTTCATGG-3'
<i>Atp2a1</i> Δ E1 fwd	5'-GATGGCTGCCATGAAGaatTAGGGTTGAAGG-3'
<i>Atp2a1</i> Δ E1 rev	5'-CAGTGCAGATGCCTTCAACCCTAattCTTCATGG-3'
<i>Atp2a1</i> E2 fwd	5'-GATGGCTGCGCAGCAACCCCTCCCTAGGGTAAGGTTAC-3'
<i>Atp2a1</i> E2 rev	5'-CAGTGCAGATGGTAACCTTACCCTAGGGAGGGGTTGCTGC-3'
<i>Atp2a1</i> Δ E2 fwd	5'-GATGGCTGCGCAGCAACCCCTaatTAGGGTAAGGTTAC-3'
<i>Atp2a1</i> Δ E2 rev	5'-CAGTGCAGATGGTAACCTTACCCTAattAGGGGTTGCTGC-3'

7. Discussion

7.1. Generation of the *EbfmiRNA* mouse line

Ebf transcription factors are highly homologous and each member's contribution to a biological process is likely compensated for by their co-expression. Therefore, genetic redundancy is an important aspect when studying the biological role of single *Ebf* genes (Dubois & Vincent, 2001; Liberg et al., 2002; Wang et al., 2004).

To overcome a potential redundancy between *Ebf* factors in the support of hematopoietic stem cells, a new RNAi construct was generated with three concatemerized shRNA sequences against *Ebf1*, *Ebf2* and *Ebf3* incorporated into a polycistronic expression vector for RNA polymerase II (Chung et al., 2006; Kieslinger et al., 2010). In cultured cells, this RNAi construct shows high efficiency for down-regulating the targeted *Ebf* factors simultaneously (Kieslinger et al., 2010). To overcome the limitations of cell culture approaches, we wanted to develop the RNAi system for use *in vivo*.

In a newly generated *EbfmiRNA* transgenic mouse line, the miRNA cassette including the *Gfp* marker gene is inserted into a targeting vector for the *Rosa26* locus. The *Rosa26* locus provides reproducible and ubiquitous transgene expression of inserted constructs (Backman et al., 2009; Kleinhammer et al., 2011). It has been used to knock-in a variety of transgenes including cDNA, reporters and noncoding RNAs without causing phenotypic changes due to the disruption of the *Rosa26* locus (Casola, 2010).

Furthermore, the synthetic CAG promoter, which has stronger transcriptional activity than the endogenous promoter activity of the *Rosa26* locus is used to induce high expression of the transgene (Alexopoulou et al., 2008; Niwa et al., 1991). Downstream of the CAG promoter, *loxP* sites flank a transcriptional Stop site and a *PGK/Neo* resistance cassette. The *loxP* sites are deleted when Cre recombinase is expressed, thereby allowing tissue-specific expression of the RNAi construct together with *Gfp*.

Ebf1 is the only *Ebf* family member expressed in B-lymphocytes and its deletion completely blocks early B cell development. Specifically, *Ebf1*-deficient mice show strongly reduced numbers of early B cells (fraction B and C) in the bone marrow (Lin

& Grosschedl, 1995; Hardy, 2001; Fig. 8). In case our RNAi construct is effective in down-regulating *Ebf* transcription factors, an inhibition of early B cell differentiation is expected upon induction of the transgene.

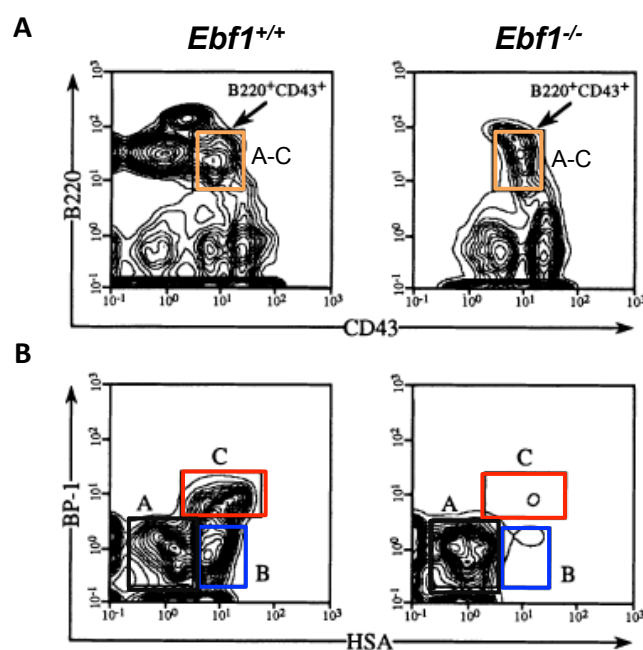


Figure 8. B-lymphocyte differentiation in *Ebf1*-deficient mice.

(A) The expression of B220 and CD43 identifies early B-lymphocytes of fraction A-C (orange gate). B220⁺CD43⁺ cells were further analyzed for the expression of BP-1 and HSA (CD24) (B) Fraction A, B and C of pro-B cells are indicated as black, blue and red gate. In both wild-type and *Ebf1*-deficient mice, fraction A cells represent as 0.5% and 0.6% of total bone marrow cells. *Ebf1*-deficient mice lack cells in fractions B and C (figure modified from Lin & Grosschedl, 1995).

Therefore, the hematopoietic system was chosen to test the efficiency of our RNAi system *in vivo*. Additionally, since a precise functioning of the RNAi pathway is required for T cell development, we are also able to test the specificity of the transgene.

The Vav-iCre mouse line was considered as an ideal way to examine the efficiency and specificity of our RNAi system *in vivo* (Kuhn et al., 1995; de Boer et al., 2003; Ventura et al., 2004). The *Vav* gene is expressed in immature hematopoietic cells, including hematopoietic stem cells. Therefore, the Cre-*loxP* recombination strategy

will induce expression of the transgenic RNAi construct and the *Gfp* marker gene in all hematopoietic cells (Ogilvy et al., 1999; de Boer et al., 2003; Fig. 9).

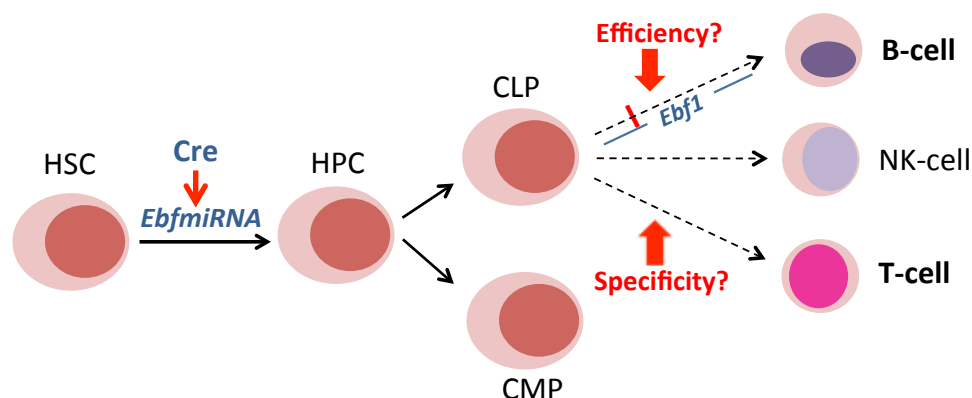


Figure 9. Hematopoietic system and Ebf/RNAi test strategy.

Expression of the Cre recombinase starts in HSC and leads the deletion of the *loxP*-flanked transcriptional Stop site in all hematopoietic cells. Efficiency of the RNAi-based transgene can be analyzed in the B-cell lineage, as *Ebf1* is essential for early B cell development. Also, as T-cell development requires a precisely regulated RNAi pathway, specificity of the transgene can be tested in this cell lineage. HPC, hematopoietic progenitor cell; CLP, common lymphoid progenitor; CMP, common myeloid progenitor (figure modified from Metcalf, 2007).

7.2. RNAi and RNA polymerase II driven shRNA

RNAi, mostly by virtue of short-hairpin RNAs (shRNA), has been developed as an efficient tool to silence the expression of single target genes for studying specific gene function (Kunath et al., 2003; Ventura et al., 2004; Kleinhammer et al., 2011).

The shRNA includes a short loop of 4-11 nucleotides, forming a hairpin structure and can be transcribed using RNA polymerase III (pol III)- or RNA polymerase II (pol II)-dependent promoters (Kunath et al., 2003; Ambros et al., 2004). Initially, RNA pol III-dependent promoters were used for expressing a single shRNA. However, the use of RNA pol III has several disadvantages. For example, it lacks the possibility for tissue-specific expression, the expression levels cannot be controlled and reporter genes cannot be co-transcribed (Yu et al., 2002; Jazag et al., 2005). In fact, most if not all miRNA genes are synthesized by RNA pol II (Cai et al., 2004; Lee et al., 2004). Also,

the pri-mRNA transcripts, which are generated by RNA pol II, contain poly (A) tails and are spliced occasionally (Lee et al., 2004).

BIC is a murine non-coding RNA that contains the stem-loop miR-155 miRNA precursor (Lagos-Quintana et al., 2002). Because the mouse BIC gene is functionally efficient to produce the miR-155 precursor in mammalian cells, miR-155/BIC represents a good framework for pol II-based RNAi vectors (Chung et al., 2006).

Importantly, miR-155/BIC has successfully been used to concatemerize several sequences with flanking regions that are recognized and cleaved by the RNase III enzyme Drosha (Chung et al., 2006). Therefore, combining the SIBR (synthetic inhibitory BIC-derived RNA) vector and the miR-155 based construct was considered as a new and promising approach to down regulate three *Ebf* genes simultaneously *in vivo*.

7.3. RNAi expression *in vivo*

According to direct measurement of *Gfp* via flow cytometry and deletion of the RNAi sequences by qPCR, I confirmed that the expression of our RNAi construct was inducible at high levels in hematopoietic cells. However, no significant defects were observed in B cell development *in vivo* such as differences in the percentage of early B cells (fraction A-C).

To explain this discrepancy between *in vitro* and *in vivo* experiments with the same RNAi constructs, three different possibilities are proposed: The expression level, the complexity of the transgene and the efficiency of the RNAi sequences.

Firstly, the expression level of the RNAi construct *in vivo* has to be considered. To achieve a high and stable expression level, the pol II-driven synthetic CAG promoter (CMV early enhancer/ chicken β -actin) was chosen. This promoter facilitates long-term and stronger expression of transgenes compared to CMV and β -actin promoters (Alexopoulou et al., 2008). It also allows the co-expression of a marker gene such as *Gfp*. Indeed, I was able to demonstrate that this promoter strongly induces the expression of the RNAi construct and *Gfp* in all hematopoietic cells.

To determine a potential influence of expression levels, we wanted to separate cells according to their expression level of the transgene. To this end, I found and isolated three distinct population of *Gfp*-expressing cells from high to low level by flow

cytometry. Together with co-authors, I confirmed the correlation between the expression of *Gfp* and the miRNA construct by qPCR. The expression of *Gfp* was higher in homozygous transgenic mice than homozygous transgenic mice and the expression of the transgene corresponds to *Gfp*. However, both in hetero-, and homozygous transgenic mice, the Ebf protein levels in the high, middle or low expressing cells were comparable. Therefore, an insufficiency of expression of the transgene alone is unlikely to provide an explanation for the discrepancy in the effectiveness of the RNAi construct *in vivo*.

Secondly, the complexity of the polycistronic mRNA sequences may impair their processing *in vivo*. In our group's previous experiments, the combination of four shRNA sequences that target all four *Ebf* family members resulted in a strongly reduced down-regulation efficiency (data now shown). The artificial RNAi constructs likely pose more problems of correct processing due to their structural complexity. Therefore, it is likely that mir155-based RNAi constructs with three concatemerized shRNA sequences reach the maximum level of complexity for processing in the RNAi pathway.

Finally, finding the appropriate RNAi sequences is one of the most important determinants to generate efficient RNAi constructs *in vivo* as well as *in vitro*. The RNAi constructs in this study were designed using state-of-the-art computer predictions and underwent biochemical testing before the best sequence combination against *Ebf1*, *Ebf2*, and *Ebf3* was selected. These constructs have shown a high efficiency in the down-regulation of *Ebf1*, *Ebf2*, and *Ebf3* in cell culture as demonstrated by us and other groups (Kieslinger et al., 2010; Croci et al., 2011; Chiara et al., 2012).

However, it was later found that sequences predicted by such computer programs work efficiently in only a small percentage *in vivo* (Dow et al., 2012). In addition, the expression of RNAi transcripts is derived from multiple integration sites in cultured cells, whereas the transgenic mice express it from a single genomic locus. Therefore, it is necessary to consider more carefully this different aspect between *in vitro* and *in vivo* to design precise RNAi sequences. New methods have been established such as the massively parallel sensor assay to develop highly efficient RNAi sequences which are also suitable for use *in vivo* (Fellmann et al., 2011).

7.4. *Ebf3* in muscle function

Ebf3 has been known as an important regulatory factor in neuronal differentiation (Garel et al., 1997; Wang et al., 2004; Chiara et al., 2012). However, the biological role of *Ebf3* outside of the neuronal system is poorly characterized. Here, in the second publication (*Nature Comm.*, 2014), *Ebf3* expression during mouse embryonic development was examined, and *Ebf3* was identified as an important regulator for the function of a specific muscle by analyzing *Ebf3*-deficient mice.

To generate *Ebf3*^{-/-} mice, the first four exons (exons 2-5) after the translational start site, which encode for essential parts of the DNA binding domain, are replaced by the *NLS-LacZ* gene and a *PGK/Neo* cassette. Thereby, the expression of β -galactosidase is under control of the endogenous *Ebf3* promoter and recapitulates the expression of *Ebf3*.

Staining for β -galactosidase in mouse embryos demonstrates that *Ebf3* is strongly expressed in the olfactory epithelium, neuronal tissues, adipocytes and skeletal muscles, particularly the diaphragm. However, *Ebf3* is not expressed in lung, which is an important clue for supporting our hypothesis on the biological function of *Ebf3*.

Deficiency of *Ebf3* did not result in any morphological difference during embryonic development. However, *Ebf3*^{-/-} mice showed gasping respiration and cyanosis after birth. Eventually, all *Ebf3*^{-/-} mice died within a few hours after birth because of respiratory failure, raising the question for the reason of this phenotype.

Unfolding of the lung at birth is important to facilitate normal breathing and delivery of oxygen to the body. *Ebf3*^{-/-} mice have a defect in the unfolding of the lung, preventing a normal oxygen uptake, and explaining the postnatal cyanosis. However, this cannot be a defect intrinsic to the lung, as it does not express *Ebf3* and unfolding at birth is not achieved by the lung itself. The diaphragm and the rib cage are the main structures required for the unfolding at birth and a normal breathing process. Since the formation of bone and cartilage are unaffected by the loss of *Ebf3*, the expression and function of *Ebf3* in diaphragm and muscle were analyzed to potentially explain this respiratory failure.

7.5. Biochemical mechanisms of muscle function

Skeletal muscles consist of bundles of muscle fibers, and the sliding of two sets of fibers, which are thin actin filament and thick myosin filament, produces force and movement (Herzog, 2013). The molecular mechanism of muscle function is summarized in the cross-bridge cycle, which is explained below (Fig. 10).

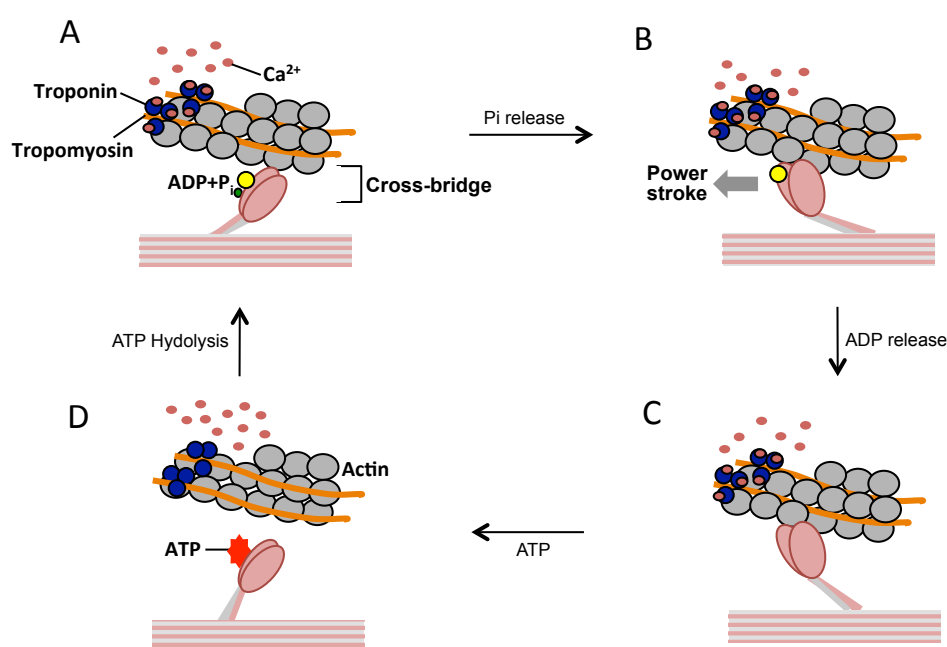


Figure 10. The cross-bridge cycle of muscle filaments.

The cross-bridge cycle is mainly divided into four steps. (A) Formation of the cross-bridge. Ca^{2+} binding to troponin induces the dissociation of troponin and tropomyosin, allowing actin-myosin cross-bridge formation. (B) Power stroke. After ATP hydrolysis, the cross-bridge generates the power stroke by release of P_i inducing the sliding myosin along the actin filament towards the center of the sarcomere. (C) ADP release. After the power stroke, ADP is released from the myosin head. (D) Detachment of cross-bridge. Another ATP binds to the myosin head thereby detaching it from actin (figure modified from Coirault et al., 1999b).

The formation of the cross-bridge is initiated when calcium ions are released from the SR and bind to the troponin associated with tropomyosin. This causes tropomyosin to dissociate from actin allowing activated myosin heads to attach to the binding site in actin. The hydrolysis of ATP into ADP and an inorganic phosphate (P_i) initiates the tight cross-bridge bond between actin and myosin. By release of P_i from the myosin head, the power stroke generates force to slide actin filaments towards the center of

the sarcomere. After the power stroke, the release of ADP allows new ATP binding to the myosin head causing rapid detachment of myosin from the actin. This cross-bridge cycle induces muscle contraction, contrarily muscle relaxation occurs by dissociation of calcium ions from troponin (Coirault et al., 1999a, 1999b; Berchtold et al., 2000; Fig. 10). Thereby, decreasing the Ca^{2+} concentration is essential to mediate muscle relaxation. When Ca^{2+} is removed, troponin and tropomyosin associate again resulting in the inhibition of the cross-bridge formation due to blocking of the binding site for activated myosin heads (Davis and Tikunova, 2008). Taken together, the main trigger of muscle contraction and relaxation is the directed transport of Ca^{2+} between the cytoplasm and its cellular storage compartment, the sarcoplasmic reticulum.

The calcium-transport processes are performed by two key molecular mediators, ryanodine receptor and SERCA proteins (James et al., 2011).

The ryanodine receptor plays a role as the sarcoplasmic reticulum calcium channel which releases Ca^{2+} for inducing muscle contraction. Increasing density of ryanodine receptors in muscle cells is an important determinant of strength and endurance of muscle contraction (Anttila et al., 2008; James et al., 2011).

SERCA proteins, which are sarcoplasmic reticulum Ca^{2+} pumps, are responsible for the transport of Ca^{2+} from the cytoplasm to the SR to allow muscle relaxation. They are regulated by ATP supply and the phosphorylation of phospholamban (Coirault et al., 1999b; Berchtold et al., 2000). Unphosphorylated phospholamban binds to SERCA proteins and decreases their affinity to Ca^{2+} . Two different isoforms of SERCA, SERCA1 and SERCA2a1, are expressed in fast-twitch and slow-twitch muscle fibers. The SERCA1 has a higher capacity of SR Ca^{2+} uptake than SERCA2a1, which is associated with a higher frequency of muscle relaxation (Coirault et al., 1999b).

In the second publication (*Nature Comm.*, 2014), the expression of various important genes implicated in muscle contraction and relaxation were analyzed. For example, *Tnnc1* (troponin C type I), *Tpm1* (tropomyosin 1), *MyBP-C* (myosin binding protein C) and myosin heavy chain isoforms do not show differences in expression in *Ebf3*-deficient diaphragm. However, the expression of *Atp2a1* encoding for SERCA1 is significantly reduced in absence of *Ebf3*.

Interestingly, the loss of *Ebf3* and *Atp2a1* results in similar phenotypic defects. Expression of *Atp2a1* can rescue the respiratory failure of *Ebf3*-deficient mice demonstrating the importance of *Atp2a1* as an *Ebf3* target gene in muscle relaxation.

Furthermore, *Ebf3* binds to consensus sites in the promoter of *Atp2a1* as shown by EMSA and ChIP assay, and that it can transactivate the *Atp2a1* promoter via these binding sites. Moreover, *Ebf3* alone is not enough to induce the expression of endogenous *Atp2a1* but together with *MyoD* it shows strong synergy to induce *Atp2a1*. Likewise, *MyoD* can bind to its consensus site in the *Atp2a1* promoter in the absence of *Ebf3*, demonstrating its pioneering activity in this cellular and molecular context. In summary, we uncovered a new role for *Ebf3* in muscle biology and were able to describe the molecular mechanism.

In the *Ebf3*-deficient mice, SERCA1 is barely detectable in the diaphragm. Interestingly, however, its expression level does not change in other skeletal muscles. Other *Ebf* family factors in both diaphragm and skeletal muscle were tested for potential co-expression, and *Ebf1* was found to be strongly expressed in other skeletal muscles. Moreover, the down-regulation of *Ebf1* causes a reduction of *Atp2a1* expression in skeletal muscle. Because *Ebf1* is a member of the highly homologous *Ebf* gene family, the genetic redundancy between *Ebf1* and *Ebf3* might explain the lack of phenotype in other skeletal muscles. Although diaphragm is a skeletal muscle, the mechanisms leading to different levels of *Ebf* expression between the diaphragm and other skeletal muscles are not clear.

8. Outlook

I. A new strategy for genomic manipulation

Since RNA interference (RNAi) has been discovered in *C. elegans* for regulating gene expression, RNAi-based mechanisms have been widely used as a powerful tool to study gene function in a variety of organisms and cells (Kim & Rossi, 2008; Boutros and Ahringer, 2008).

However, even if applied successfully, inherent problems of this technology remain. The most severe among those are the difficulties to control for off-target effects and the fact that it is a down-regulation, not a complete genomic loss. Therefore, when analyzing phenotypes from an RNAi-based down-regulation, it is virtually impossible to determine if the remaining protein prevents the manifestation of a complete phenotype or if off-target effects contribute. This situation is even more complicated *in vivo* as it requires the generation of several control mouse strains, increasing the financial and time burden. Therefore, such studies would benefit greatly from a genetically clearly defined situation.

To overcome intrinsic limitations of RNAi, the newly discovered CRISPR-Cas9 system offers big advantages in manipulating the genome. Cas9 is a RNA-guided endonuclease that can perform site-specific DNA-targeting and cleaving based on a complementary sequence. CRISPRs are clustered, regularly interspaced, short palindromic repeats of RNA that function as guiding RNAs for Cas9 (Sander & Joung, 2014). This nuclease-based method offers an easy, rapid and efficient way of modifying or deleting endogenous genes, greatly improving the manipulation of the genome of cells or organisms (Baker, 2014; Jia et al., 2014). Therefore, rather than trying to improve the RNAi-based approach, we would suggest to apply this new technology to delete several *Ebf* genes in a tissue-specific manner.

II. Brody's disease and Ebf protein family

Brody disease is a rare genetic myopathy that shows functional impairments of skeletal muscle like a delay in muscle relaxation after contraction and cramped muscles (Brody, 1969). Some cases of this disease are due to the mutation of

ATP2A1 that reduce SERCA1 activity or expression (Taylor et al., 1988; Voermans et al., 2012). However, not all Brody's patients have defects in the *ATP2A1* gene even though they show loss of SERCA1 activity or expression (Odermatt et al. 1996; Zhang et al., 1995). These patients, without *ATP2A1* mutations, are classified as Brody syndrome and it is estimated that they constitute approximately 50% of all Brody's cases (Karpati et al., 1986; Voermans et al., 2012). In the second publication (*Nature Comm*, 2014), we demonstrate a significant reduction of Serca1 expression in the diaphragm of *Ebf3*-deficient mice resulting in an impairment of muscle relaxation. Since binding sites for Ebf proteins are also present in the promoter of human *Atp2a1*, we propose *Ebf3* as a potential factor involved in the development of Brody syndrome. Therefore, samples from Brody's patients should be analyzed for potential mutations of their *Ebf* binding sites.

Furthermore, we show that *Ebf3* directly regulates the expression of *Atp2a1* in the diaphragm. While *Ebf3* shows the strongest expression in diaphragm, in other skeletal muscles, *Ebf1* is the most significantly expressed *Ebf* member. Moreover, *Ebf1*-deficient mice also show down-regulation of *Atp2a1* in skeletal muscle. Taken together, this raises the question why the expression patterns of *Ebf* family members are different between diaphragm and other skeletal muscles.

Therefore, we suggest testing cells from *Ebf3*^{-/-} mice with an *Ebf1* retroviral approach or analyzing *Ebf1* and *Ebf3* double knock-out transgenic mice whether the functional damage of *Ebf3*^{-/-} diaphragm can be rescued or is synergistic.

9. References

- Ackerman, K. G. and J. J. Greer (2007). "Development of the diaphragm and genetic mouse models of diaphragmatic defects." Am J Med Genet C Semin Med Genet **145C**(2): 109-116.
- Alexopoulou, A. N., et al. (2008). "The CMV early enhancer/chicken beta actin (CAG) promoter can be used to drive transgene expression during the differentiation of murine embryonic stem cells into vascular progenitors." BMC Cell Biol **9**: 2.
- Ambros, V. (2004). "The functions of animal microRNAs." Nature **431**(7006): 350-355.
- Ambros, V., et al. (2003). "MicroRNAs and other tiny endogenous RNAs in *C. elegans*." Curr Biol **13**(10): 807-818.
- Anger, M., et al. (1995). "Sarcoplasmic reticulum Ca²⁺ pumps in heart and diaphragm of cardiomyopathic hamster: effects of perindopril." Am J Physiol **268**(5 Pt 2): H1947-1953.
- Anttila, K., et al. (2008). "The swimming performance of brown trout and whitefish: the effects of exercise on Ca²⁺ handling and oxidative capacity of swimming muscles." J Comp Physiol B **178**(4): 465-475.
- Aravind, L. and E. V. Koonin (1999). "Gleaning non-trivial structural, functional and evolutionary information about proteins by iterative database searches." J Mol Biol **287**(5): 1023-1040.
- Backman, C. M., et al. (2009). "Generalized tetracycline induced Cre recombinase expression through the ROSA26 locus of recombinant mice." J Neurosci Methods **176**(1): 16-23.
- Baker, M. (2014). "Gene editing at CRISPR speed." Nat Biotechnol **32**(4): 309-312.
- Bally-Cuif, L., et al. (1998). "Molecular cloning of *Zco2*, the zebrafish homolog of *Xenopus Xco2* and mouse *EBF-2*, and its expression during primary neurogenesis." Mech Dev **77**(1): 85-90.
- Barbaric, I., et al. (2007). "Appearances can be deceiving: phenotypes of knockout mice." Brief Funct Genomic Proteomic **6**(2): 91-103.
- Bartel, D. P. (2004). "MicroRNAs: genomics, biogenesis, mechanism, and function." Cell **116**(2): 281-297.
- Berchtold, M. W., et al. (2000). "Calcium ion in skeletal muscle: its crucial role for muscle function, plasticity, and disease." Physiol Rev **80**(3): 1215-1265.
- Berkes, C. A. and S. J. Tapscott (2005). "MyoD and the transcriptional control of myogenesis." Semin Cell Dev Biol **16**(4-5): 585-595.
- Bernstein, E., et al. (2001). "The rest is silence." RNA **7**(11): 1509-1521.

- Birchmeier, C. and H. Brohmann (2000). "Genes that control the development of migrating muscle precursor cells." Curr Opin Cell Biol **12**(6): 725-730.
- Biressi, S., et al. (2007). "Cellular heterogeneity during vertebrate skeletal muscle development." Dev Biol **308**(2): 281-293.
- Braun, T., et al. (1992). "Targeted inactivation of the muscle regulatory gene Myf-5 results in abnormal rib development and perinatal death." Cell **71**(3): 369-382.
- Brody, I. A. (1969). "Muscle contracture induced by exercise. A syndrome attributable to decreased relaxing factor." N Engl J Med **281**(4): 187-192.
- Brooks, N. E. and K. H. Myburgh (2014). "Skeletal muscle wasting with disuse atrophy is multi-dimensional: the response and interaction of myonuclei, satellite cells and signaling pathways." Front Physiol **5**: 99.
- Buckingham, M. and S. D. Vincent (2009). "Distinct and dynamic myogenic populations in the vertebrate embryo." Curr Opin Genet Dev **19**(5): 444-453.
- Cai, X., et al. (2004). "Human microRNAs are processed from capped, polyadenylated transcripts that can also function as mRNAs." RNA **10**(12): 1957-1966.
- Calvi, L. M., et al. (2003). "Osteoblastic cells regulate the haematopoietic stem cell niche." Nature **425**(6960): 841-846.
- Carafoli, E. (2002). "Calcium signaling: a tale for all seasons." Proc Natl Acad Sci U S A **99**(3): 1115-1122.
- Casola, S. (2010). "Mouse models for miRNA expression: the ROSA26 locus." Methods Mol Biol **667**: 145-163.
- Chalfie, M. and E. M. Jorgensen (1998). "C. elegans neuroscience: genetics to genome." Trends Genet **14**(12): 506-512.
- Chalmers, G. R. and B. S. Row (2011). "Common errors in textbook descriptions of muscle fiber size in nontrained humans." Sports Biomech **10**(3): 254-268.
- Chiara, F., et al. (2012). "Early B-cell factors 2 and 3 (EBF2/3) regulate early migration of Cajal-Retzius cells from the cortical hem." Dev Biol **365**(1): 277-289.
- Chung, K. H., et al. (2006). "Polycistronic RNA polymerase II expression vectors for RNA interference based on BIC/miR-155." Nucleic Acids Res **34**(7): e53.
- Clapham, D. E. (2007). "Calcium signaling." Cell **131**(6): 1047-1058.
- Coirault, C., et al. (1999a). "Cross-bridge kinetics in fatigued mouse diaphragm." Eur Respir J **13**(5): 1055-1061.
- Coirault, C., et al. (1999b). "Relaxation of diaphragm muscle." J Appl Physiol (1985) **87**(4): 1243-1252.
- Coirault, C., et al. (1997). "Relaxation is impaired in the diaphragm muscle of the cardiomyopathic Syrian hamster." Am J Respir Crit Care Med **155**(5): 1575-1582.

- Cooke, J., et al. (1997). "Evolutionary origins and maintenance of redundant gene expression during metazoan development." *Trends Genet* **13**(9): 360-364.
- Corradi, A., et al. (2003). "Hypogonadotropic hypogonadism and peripheral neuropathy in Ebf2-null mice." *Development* **130**(2): 401-410.
- Croci, L., et al. (2011). "Local insulin-like growth factor I expression is essential for Purkinje neuron survival at birth." *Cell Death Differ* **18**(1): 48-59.
- Crozatier, M., et al. (1996). "Collier, a novel regulator of Drosophila head development, is expressed in a single mitotic domain." *Curr Biol* **6**(6): 707-718.
- Crozatier, M. and A. Vincent (1999). "Requirement for the Drosophila COE transcription factor Collier in formation of an embryonic muscle: transcriptional response to notch signalling." *Development* **126**(7): 1495-1504.
- Davis, J. P. and S. B. Tikunova (2008). "Ca(2+) exchange with troponin C and cardiac muscle dynamics." *Cardiovasc Res* **77**(4): 619-626.
- Dubinska-Magiera, M., et al. (2013). "Muscle development, regeneration and laminopathies: how lamins or lamina-associated proteins can contribute to muscle development, regeneration and disease." *Cell Mol Life Sci* **70**(15): 2713-2741.
- de Boer, J., et al. (2003). "Transgenic mice with hematopoietic and lymphoid specific expression of Cre." *Eur J Immunol* **33**(2): 314-325.
- Dow, L. E., et al. (2012). "A pipeline for the generation of shRNA transgenic mice." *Nat Protoc* **7**(2): 374-393.
- Dubois, L. and A. Vincent (2001). "The COE--Collier/Olf1/EBF--transcription factors: structural conservation and diversity of developmental functions." *Mech Dev* **108**(1-2): 3-12.
- Ehlers, M. L., et al. (2014). "NFATc1 controls skeletal muscle fiber type and is a negative regulator of MyoD activity." *Cell Rep* **8**(6): 1639-1648.
- Elbashir, S. M., et al. (2001). "RNA interference is mediated by 21- and 22-nucleotide RNAs." *Genes Dev* **15**(2): 188-200.
- Esau, S. A., et al. (1983). "Changes in rate of relaxation of sniffs with diaphragmatic fatigue in humans." *J Appl Physiol Respir Environ Exerc Physiol* **55**(3): 731-735.
- Fellmann, C., et al. (2011). "Functional identification of optimized RNAi triggers using a massively parallel sensor assay." *Mol Cell* **41**(6): 733-746.
- Fields, S., et al. (2008). "The 'zinc knuckle' motif of Early B cell Factor is required for transcriptional activation of B cell-specific genes." *Mol Immunol* **45**(14): 3786-3796.
- Fire, A., et al. (1998). "Potent and specific genetic interference by double-stranded RNA in *Caenorhabditis elegans*." *Nature* **391**(6669): 806-811.
- Garel, S., et al. (2000). "Control of the migratory pathway of facial branchiomotor neurones." *Development* **127**(24): 5297-5307.

Garel, S., et al. (1999). "Ebf1 controls early cell differentiation in the embryonic striatum." Development **126**(23): 5285-5294.

Garel, S., et al. (1997). "Family of Ebf/Olf-1-related genes potentially involved in neuronal differentiation and regional specification in the central nervous system." Dev Dyn **210**(3): 191-205.

Green, Y. S. and M. L. Vetter (2011). "EBF proteins participate in transcriptional regulation of *Xenopus* muscle development." Dev Biol **358**(1): 240-250.

Grishok, A., et al. (2001). "Genes and mechanisms related to RNA interference regulate expression of the small temporal RNAs that control *C. elegans* developmental timing." Cell **106**(1): 23-34.

Hagman, J., et al. (1993). "Cloning and functional characterization of early B-cell factor, a regulator of lymphocyte-specific gene expression." Genes Dev **7**: 760-773.

Hagman, J., et al. (1995). "EBF contains a novel zinc coordination motif and multiple dimerization and transcriptional activation domains." EMBO J **14**(12): 2907-2916.

Hamilton, A. J. and D. C. Baulcombe (1999). "A species of small antisense RNA in posttranscriptional gene silencing in plants." Science **286**(5441): 950-952.

Hardy, C. L. (2001). "Specificity of Hematopoietic Stem and Progenitor Cell Homing to Bone Marrow: A Perspective; Subject Heading." Hematology **5**(5): 391-401.

Hardy, R. R. and K. Hayakawa (1995). "B-lineage differentiation stages resolved by multiparameter flow cytometry." Ann N Y Acad Sci **764**: 19-24.

Herzog, W. (2014). "Mechanisms of enhanced force production in lengthening (eccentric) muscle contractions." J Appl Physiol (1985) **116**(11): 1407-1417.

Hutvagner, G., et al. (2001). "A cellular function for the RNA-interference enzyme Dicer in the maturation of the let-7 small temporal RNA." Science **293**(5531): 834-838.

Inesi, G. and F. Tadini-Buoninsegni (2014). "Ca²⁺/H⁺ exchange, luminal Ca²⁺ release and Ca²⁺/ATP coupling ratios in the sarcoplasmic reticulum ATPase." J Cell Commun Signal **8**(1): 5-11.

James, R. S., et al. (2011). "Variation in expression of calcium-handling proteins is associated with inter-individual differences in mechanical performance of rat (*Rattus norvegicus*) skeletal muscle." J Exp Biol **214**(Pt 21): 3542-3548.

Jazag, A., et al. (2005). "Single small-interfering RNA expression vector for silencing multiple transforming growth factor-beta pathway components." Nucleic Acids Res **33**(15): e131.

Jia, H., et al. (2014). "Multistage Regulator Based on Tandem Promoters and CRISPR/Cas." ACS Synth Biol **3**(12): 1007-1010.

Kablar, B., et al. (2003). "Myf5 and MyoD activation define independent myogenic compartments during embryonic development." Dev Biol **258**(2): 307-318.

- Kafri, R., et al. (2009). "Genetic redundancy: new tricks for old genes." *Cell* **136**(3): 389-392.
- Karpati, G., et al. (1986). "Myopathy caused by a deficiency of Ca²⁺-adenosine triphosphatase in sarcoplasmic reticulum (Brody's disease)." *Ann Neurol* **20**(1): 38-49.
- Kennerdell, J. R. and R. W. Carthew (1998). "Use of dsRNA-mediated genetic interference to demonstrate that frizzled and frizzled 2 act in the wingless pathway." *Cell* **95**(7): 1017-1026.
- Kieslinger, M., et al. (2005). "EBF2 regulates osteoblast-dependent differentiation of osteoclasts." *Dev Cell* **9**(6): 757-767.
- Kieslinger, M., et al. (2010). "Early B cell factor 2 regulates hematopoietic stem cell homeostasis in a cell-nonautonomous manner." *Cell Stem Cell* **7**(4): 496-507.
- Kim, J., et al. (2012). "Aberrant DNA methylation and tumor suppressive activity of the EBF3 gene in gastric carcinoma." *Int J Cancer* **130**(4): 817-826.
- Kim, V. N. (2003). "RNA interference in functional genomics and medicine." *J Korean Med Sci* **18**(3): 309-318.
- Kim, V. N. (2004). "MicroRNA precursors in motion: exportin-5 mediates their nuclear export." *Trends Cell Biol* **14**(4): 156-159.
- Kim, V. N. (2005). "MicroRNA biogenesis: coordinated cropping and dicing." *Nat Rev Mol Cell Biol* **6**(5): 376-385.
- Kleinhammer, A., et al. (2011). "Constitutive and conditional RNAi transgenesis in mice." *Methods* **53**(4): 430-436.
- Kuhn, R., et al. (1995). "Inducible gene targeting in mice." *Science* **269**: 1427-1429.
- Kunath, T., et al. (2003). "Transgenic RNA interference in ES cell-derived embryos recapitulates a genetic null phenotype." *Nat Biotechnol* **21**(5): 559-561.
- Lagos-Quintana, M., et al. (2002). "Identification of tissue-specific microRNAs from mouse." *Curr Biol* **12**(9): 735-739.
- Lecarpentier, Y., et al. (1999). "Impaired load dependence of diaphragm relaxation during congestive heart failure in the rabbit." *J Appl Physiol* (1985) **87**(4): 1339-1345.
- Lee, N. S., et al. (2002). "Expression of small interfering RNAs targeted against HIV-1 rev transcripts in human cells." *Nat Biotechnol* **20**(5): 500-505.
- Lee, R. C., et al. (1993). "The *C. elegans* heterochronic gene *lin-4* encodes small RNAs with antisense complementarity to *lin-14*." *Cell* **75**(5): 843-854.
- Lee, Y., et al. (2004). "MicroRNA genes are transcribed by RNA polymerase II." *EMBO J* **23**(20): 4051-4060.
- Liao, D. (2009). "Emerging roles of the EBF family of transcription factors in tumor suppression." *Mol Cancer Res* **7**(12): 1893-1901.

- Liberg, D., et al. (2002). "EBF/Olf/Collier family of transcription factors: regulators of differentiation in cells originating from all three embryonal germ layers." *Cell Biol.* **22**: 8389-8397.
- Lin, H. and R. Grosschedl (1995). "Failure of B-cell differentiation in mice lacking the transcription factor EBF." *Nature* **376**: 263-267.
- Lukin, K., et al. (2008). "Early B cell factor: Regulator of B lineage specification and commitment." *Semin Immunol* **20**(4): 221-227.
- Lund, E., et al. (2004). "Nuclear export of microRNA precursors." *Science* **303**(5654): 95-98.
- Lytton, J., et al. (1992). "Functional comparisons between isoforms of the sarcoplasmic or endoplasmic reticulum family of calcium pumps." *J Biol Chem* **267**(20): 14483-14489.
- Mack, G. S. (2007). "MicroRNA gets down to business." *Nat Biotechnol* **25**(6): 631-638.
- MacLennan, D. H. (2000). "Ca²⁺ signalling and muscle disease." *Eur J Biochem* **267**(17): 5291-5297.
- MacLennan, D. H., et al. (1992). "Structure-function relationships in sarcoplasmic or endoplasmic reticulum type Ca²⁺ pumps." *Ann N Y Acad Sci* **671**: 1-10.
- Merrell, A. J. and G. Kardon (2013). "Development of the diaphragm -- a skeletal muscle essential for mammalian respiration." *FEBS J* **280**(17): 4026-4035.
- Metcalf, D. (2007). "On hematopoietic stem cell fate." *Immunity* **26**(6): 669-673.
- Mok, G. F. and D. Sweetman (2011). "Many routes to the same destination: lessons from skeletal muscle development." *Reproduction* **141**(3): 301-312.
- Moore, K. A. and I. R. Lemischka (2006). "Stem cells and their niches." *Science* **311**(5769): 1880-1885.
- Murchison, E. P. and G. J. Hannon (2004). "miRNAs on the move: miRNA biogenesis and the RNAi machinery." *Curr Opin Cell Biol* **16**(3): 223-229.
- Niwa, H., et al. (1991). "Efficient selection for high-expression transfectants with a novel eukaryotic vector." *Gene* **108**(2): 193-199.
- Nowak, M. A., et al. (1997). "Evolution of genetic redundancy." *Nature* **388**(6638): 167-171.
- Odermatt, A., et al. (1996). "Mutations in the gene-encoding SERCA1, the fast-twitch skeletal muscle sarcoplasmic reticulum Ca²⁺ ATPase, are associated with Brody disease." *Nat Genet* **14**(2): 191-194.
- Ogilvy, S., et al. (1999). "Promoter elements of vav drive transgene expression in vivo throughout the hematopoietic compartment." *Blood* **94**(6): 1855-1863.

- Olson, M. L., et al. (2010). "Mitochondrial Ca²⁺ uptake increases Ca²⁺ release from inositol 1,4,5-trisphosphate receptor clusters in smooth muscle cells." *J Biol Chem* **285**(3): 2040-2050.
- Pan, Y., et al. (2003). "Targeted disruption of the ATP2A1 gene encoding the sarco(endo)plasmic reticulum Ca²⁺ ATPase isoform 1 (SERCA1) impairs diaphragm function and is lethal in neonatal mice." *J Biol Chem* **278**(15): 13367-13375.
- Pozzoli, O., et al. (2001). "Xebf3 is a regulator of neuronal differentiation during primary neurogenesis in *Xenopus*." *Dev Biol* **233**(2): 495-512.
- Prasad, B. C., et al. (1998). "unc-3, a gene required for axonal guidance in *Caenorhabditis elegans*, encodes a member of the O/E family of transcription factors." *Development* **125**(8): 1561-1568.
- Relaix, F., et al. (2005). "A Pax3/Pax7-dependent population of skeletal muscle progenitor cells." *Nature* **435**(7044): 948-953.
- Rudnicki, M. A., et al. (1992). "Inactivation of MyoD in mice leads to up-regulation of the myogenic HLH gene Myf-5 and results in apparently normal muscle development." *Cell* **71**(3): 383-390.
- Rudnicki, M. A., et al. (1993). "MyoD or Myf-5 is required for the formation of skeletal muscle." *Cell* **75**(7): 1351-1359.
- Sander, J. D. and J. K. Joung (2014). "CRISPR-Cas systems for editing, regulating and targeting genomes." *Nat Biotechnol* **32**(4): 347-355.
- Sato, T., et al. (2010). "A Pax3/Dmrt2/Myf5 regulatory cascade functions at the onset of myogenesis." *PLoS Genet* **6**(4): e1000897.
- Sayen, M. R., et al. (1992). "Thyroid hormone response of slow and fast sarcoplasmic reticulum Ca²⁺ ATPase mRNA in striated muscle." *Mol Cell Endocrinol* **87**(1-3): 87-93.
- Schiaffino, S. and C. Reggiani (2011). "Fiber types in mammalian skeletal muscles." *Physiol Rev* **91**(4): 1447-1531.
- Schiaffino, S. (2012). "Tubular aggregates in skeletal muscle: just a special type of protein aggregates?" *Neuromuscul Disord* **22**(3): 199-207.
- Siponen, M. I., et al. (2010). "Structural determination of functional domains in early B-cell factor (EBF) family of transcription factors reveals similarities to Rel DNA-binding proteins and a novel dimerization motif." *J Biol Chem* **285**(34): 25875-25879.
- Stubbings, A. K., et al. (2008). "Physiological properties of human diaphragm muscle fibres and the effect of chronic obstructive pulmonary disease." *J Physiol* **586**(10): 2637-2650.
- Sweeney, H. L. (1998). "Regulation and tuning of smooth muscle myosin." *Am J Respir Crit Care Med* **158**(5 Pt 3): S95-99.
- Taylor, D. J., et al. (1988). "Ca²⁺-ATPase deficiency in a patient with an exertional muscle pain syndrome." *J Neurol Neurosurg Psychiatry* **51**(11): 1425-1433.

- Travis, A., et al. (1993). "Purification of early-B-cell factor and characterization of its DNA-binding specificity." *Mol. Cell Biol.* **13**: 3392-3400.
- Treiber, N., et al. (2010). "Structure of an Ebf1:DNA complex reveals unusual DNA recognition and structural homology with Rel proteins." *Genes Dev* **24**(20): 2270-2275.
- Vasyutina, E. and C. Birchmeier (2006). "The development of migrating muscle precursor cells." *Anat Embryol (Berl)* **211 Suppl 1**: 37-41.
- Ventura, A., et al. (2004). "Cre-lox-regulated conditional RNA interference from transgenes." *Proc Natl Acad Sci U S A* **101**(28): 10380-10385.
- Ventura, B. (2004). "Is siRNA the tool of the future for in vivo mammalian gene research? The experts speak out." *Physiol Genomics* **18**(3): 252-254.
- Vervoort, M., et al. (1999). "The COE transcription factor Collier is a mediator of short-range Hedgehog-induced patterning of the *Drosophila* wing." *Curr Biol* **9**(12): 632-639.
- Voermans, N. C., et al. (2012). "Brody syndrome: a clinically heterogeneous entity distinct from Brody disease: a review of literature and a cross-sectional clinical study in 17 patients." *Neuromuscul Disord* **22**(11): 944-954.
- Wang, M. M. and R. R. Reed (1993). "Molecular cloning of the olfactory neuronal transcription factor Olf-1 by genetic selection in yeast." *Nature* **364**(6433): 121-126.
- Wang, S. S., et al. (2002). "Cloning of a novel Olf-1/EBF-like gene, O/E-4, by degenerate oligo-based direct selection." *Mol Cell Neurosci* **20**(3): 404-414.
- Wang, S. S., et al. (2004). "Genetic disruptions of O/E2 and O/E3 genes reveal involvement in olfactory receptor neuron projection." *Development* **131**(6): 1377-1388.
- Wang, S. S., et al. (1997). "The characterization of the Olf-1/EBF-like HLH transcription factor family: implications in olfactory gene regulation and neuronal development." *J Neurosci* **17**(11): 4149-4158.
- Wang, Y., et al. (1996). "Functional redundancy of the muscle-specific transcription factors Myf5 and myogenin." *Nature* **379**(6568): 823-825.
- Wianny, F. and M. Zernicka-Goetz (2000). "Specific interference with gene function by double-stranded RNA in early mouse development." *Nat Cell Biol* **2**(2): 70-75.
- Yi, R., et al. (2003). "Exportin-5 mediates the nuclear export of pre-microRNAs and short hairpin RNAs." *Genes Dev* **17**(24): 3011-3016.
- Yu, J. Y., et al. (2002). "RNA interference by expression of short-interfering RNAs and hairpin RNAs in mammalian cells." *Proc Natl Acad Sci U S A* **99**(9): 6047-6052.
- Zhang, Y., et al. (1995). "Characterization of cDNA and genomic DNA encoding SERCA1, the Ca(2+)-ATPase of human fast-twitch skeletal muscle sarcoplasmic reticulum, and its elimination as a candidate gene for Brody disease." *Genomics* **30**(3): 415-424.
- Zhang, J., et al. (2003). "Identification of the haematopoietic stem cell niche and control of the niche size." *Nature* **425**(6960): 836-841.

10. Acknowledgement

First of all, I would like to express my special appreciation and thanks to my advisor Dr. Matthias Kieslinger, who has been a good advisor for me to finish my all PhD projects successfully. I would like to thank him for teaching and encouraging me with my research so that I could explore many scientific questions and curiosities. Without his guidance and help, it would not have been possible.

I would also like to thank my Ph.D. supervisor, Professor Barbara Conradt for being my major advisors. She has been a great mentor for me through all three years of my Ph.D. study. I was always happy to discuss with her, and she guided me with a great care.

Also, I would like to express my deepest appreciation to Professor Bettina Kempkes for her mentorship and support. She gave me a great opportunity to join her group for my last several months of Ph.D. She has also been a great counselor for me who helped with truly helpful suggestions.

I would also like to thank all of my committee members, Professor Elisabeth Weiss, Professor Marc Bramkamp, Professor Angelika Böttger, and Professor Peter Geigenberger at L.M.U. for serving as my committee members and reviewing my thesis.

Additionally, I would like to thank Sylvia Donhauser, Sylvia Manglkammer, and Dr. Gerhard Laux at Helmholtz Zentrum München. All of them have been there when I need a help to settle my living and working condition. I also want to thank my friends and fellows in my lab, Joan and Torsten, and Dr. Kempkes' group members who share a friendly working environment with me. I was happy to study with all of them during my Ph.D. study in Germany.

A special thanks to my family: Jung-bong Kim, Hyun-ja Min, and Hyun-hee Kim. They always pray for me and support endless love that helped me to stay me strong and to follow my dream. Without their belief and encouragement, it might have been impossible to finish my Ph.D. in Germany.

Especially, I would like to dedicate this thesis to my mother.

Theresienstr.81E, Munich 80333, Germany
Mobil. +49 174 9 30 97 31
E-mail. jeeheeminkim@hotmail.com
jeehee.kim@helmholtz-muenchen.de

Education

- Ludwig Maximilian University of Munich, Dep. of Biology
Munich, Germany
Ph.D. (2015)
- Yale University School of Medicine, Dep. of Genetics
New Haven, CT, USA
Post-graduated associate (2011)
- Seoul National University School of Dentistry, Dep. of Cell & Developmental Biology
Seoul, South Korea
M.S. (2009)
- Sang-Myung University, Dep. of Biotechnology in Life Science
Seoul, South Korea
B.S. (2005)

Professional Profile

Publications

- Jin S, Kim J, Willert T, Klein-Rodewald T, Garcia-Dominguez M, Mosqueira M, Fink R, Esposito I, Hofbauer LC, Charnay P, Kieslinger M. Ebf Factors and MyoD Cooperate to Regulate Muscle Relaxation via Atp2a1. *Nature Communications* 2014; 5:3793
- Kim J, Badaloni A, Willert T, Zimmer-Strobl U, Kühn R, Wurst W, Kieslinger M. An RNAi-based approach to down-regulate a gene family in vivo. *PLoS ONE* 2013; 8(11): e80312.
- Park YJ, Kim SC, Kim J, Anakk S, Lee JM, Tseng HT, Yechoor V, Park J, Choi JS, Jang HC, Lee KU, Novak CM, Moore DD, Lee YK. Dissociation of diabetes and obesity in mice lacking orphan nuclear receptor small heterodimer partner. *Journal of Lipid Research* 2011; 52(12): 2234-44.

Patent

- Kim JH, Kim HY, Kim HM. 2008. Human Mesenchymal Stem Cells Established from Human Umbilical Cord Blood and Method for establishing them. Korean Patent #10-2008-0077575, issued August 7, 2008

Participations & Presentations

- ISSCR (International Society for Stem Cell Research) Conference, Vancouver, Canada 2014
- NichHem (Research society for hematopoietic niches) Meeting, Heidelberg, Germany 2014
- SELMET (German national consortium of the skeletal metastases), Dresden, Germany 2014